RIJKSWATERSTAAT
COMMUNICATIONS

No. 16

NAVIGATION LOCKS FOR PUSH TOWS

BY

IR. C. KOOMAN

Chief Engineer, Rijkswaterstaat

1973

RIJKSWATERSTAAT COMMUNICATIONS

NAVIGATION LOCKS FOR PUSH TOWS

by

Ir. C. KOOMAN

Chief Engineer, Rijkswaterstaat

Government Publishing Office – The Hague 1973

Any correspondence should be addressed to

RIJKSWATERSTAAT

DIRECTIE WATERHUISHOUDING EN WATERBEWEGING

THE HAGUE — NETHERLANDS

The views in this article are the author's own.

Contents

Photograph 1. Push tow in the lockapproach of the Hartel Lock

I General Outline

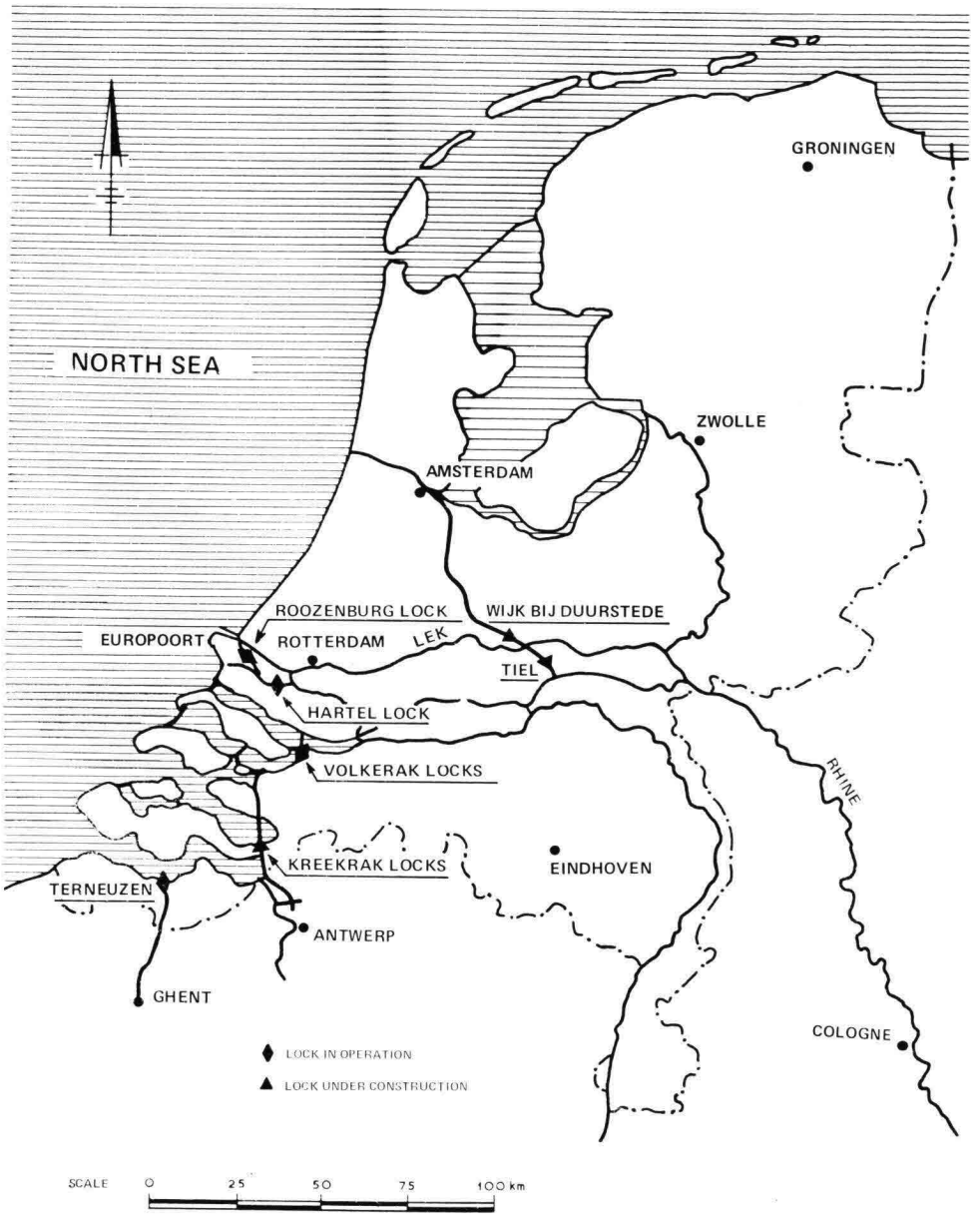

Figure 1. Navigation locks for push tows in the Dutch waterways

1. Introduction and Summary

1.1. Introduction

Pushtow navigation emerged in Western Europe in the late 1950's. In 1957 the first tug specially designed for the purpose was put into service on the river Rhine. Today, push tows make up a large portion of bulk goods transport between Rotterdam and Germany.

Push tows operating between Rotterdam and the Ruhr-area are usually composed of a pusher tug and four barges. Under present regulations, these formations are bound to maximum dimensions. For both up and downstream shipping the 2 × 2 formation (two pairs of barges in a row) must be used, with a maximum length of 185 m. and a width of 22.80 m. A different arrangement, the so-called dove-tail formation, is allowed for downstream shipping only. In 'dove-tail' formation, the pusher tug has two barges in front and one on either side. This makes the 'dove-tail' wider, but considerably shorter than the 2 × 2 formation. The 'dove-tail' is now gradually falling into disuse.

Pushtow navigation on the Rhine is mainly to and from the Rotterdam harbour area, as shipping routes to Amsterdam and Antwerp are not suited to accomodate this form of transport. To make these two ports accessible to push tows from the Rhine, planning started in the early 1960's for the enlargement of the Amsterdam-Rhine Canal and the construction of the Scheldt-Rhine Canal. The Hartel Canal, a new canal designed to serve the western extension of the Rotterdam harbour area, will also offer facilities for pushtow navigation.

A detailed description of the plans to construct or enlarge canals for pushtow shipping is given in Ref. [1].

As part of the overall plan to adapt Dutch waterways to the requirements of pushtow navigation a comprehensive program was set up for the construction of special push-tow navigation locks. These locks are to have a standard width of 24 m. to handle pushtow formations of up to 22.80 m. width. The locations of the locks are given on the map in figure 1.

To work out the proper design criteria a good insight is required into the problems arising from the passage of push tows through locks. As experience in this field was lacking, it was decided to carry out a program of systematic research. An important part of this program proved the model tests carried out at the Delft Hydraulics Laboratory in the years 1964-1966. Part of the test results have been chequed in prototype measurements performed in the Volkerak locks in 1967 and the Hartel lock, in 1968. Further test were carried out in collaboration with the Institute for Perception

RVO-TNO to study the effect of optical guidance on push tows entering locks.
Finally, to get acquainted with experience abroad, a study tour was made of the canalized Moselle in France, in 1966.
The results from the various parts of the investigation are given in twelve sub-reports, listed in Ref. [5] to [16].
It is on the base of these sub-reports that this publication was prepared. It includes three sections:

I General review; a summary of the investigation and its most important results.
II Guiding structures and guiding-light systems.
III Behaviour of push tows on entering and leaving locks, and the relevant hydraulic phenomena.

1.2. Summary

All model tests were performed on a scale of 1 : 25. The model ships were self-propelled.
For the prototype tests a push tow was used, consisting of a pusher-tug and four barges, with an overall length of about 185 m. and a width of 22.40 m. Wherever possible, the results were checked with those of parallel model tests.

An important part of the investigation concerns the shaping of the guiding structures leading towards the lock entrance. These structures are to ensure a smooth and safe lock entry and exit of push tows as well as conventional shipping. One of the main problems of lock-entry navigation is that of push tows getting stuck in the lock-entrance owing to the narrow clearance between the barge-formation and the lock-chamber. On leaving the lock, push tows are unable to manoevre until the whole barge-formation is outside the lock-chamber.
During the study of lock entry of push tows a distinction was made between the mechanical and optical functions of the guiding structures. Likewise a distinction is made between the lock entry and exit regarding the design criteria for the shaping of the guiding structures.
The various aspects of mechanical guidance were studied, and model tests were carried out to investigate the optical properties of variously shaped guiding structures as well as other features, such as side-wind protection to shipping. Guiding-light systems were tried out for their role in facilitating lock-maneuvering.
From the outcome of this study, and from parallel prototype tests, specifications were drawn up for the design of navigation locks to be used by pushtow shipping.
It was found that guiding-light systems do not improve lock-entry maneuvering to any statistically relevant degree.

The second phase of the investigation dealt with the hydraulic phenomena arising

from lock entry and exit of push tows. During entry, a translatory wave is generated which runs into the lock-chamber ahead of the ship and, in turn, upsets the regularity of the ship's progress into the lock. This interference is most marked in low waterdepths. The investigation also showed that, from a depth of 5.50 m. upward, entry times of large, loaded push tows increase steeply with decreasing waterdepths. High sills on the lock floor were found to have a retarding effect on entry.
Considerable fluctuations in waterlevel may occur in the lock-chamber as a result of translatory waves. These fluctuations are most intensive at the closed gate where the reflecting wave doubles its height. The tests revealed a clear relationship between the wave height on the one hand, and the speed of entry, the area of the wetted midship section of the barge formation and the area of the wetted cross-section of the lock-chamber on the other. These factors were composed into dimensionless parameters, to determine the height of the translatory wave for boundary conditions other than those applied to the model. These parameters were then used to compare the recorded wave-heights in the Hartel and Volkerak locks with those in the model.
In the model, the longitudinal forces that are exerted by translatory waves on ships moored in the lock-chamber, were gauged. The longitudinal force is mainly caused by the inclination of the water level during the passage of the wave and is the horizontal component of the ship's weight. The longitudinal force sets the ship in motion so that forces arise in the mooring-hawsers. During the model tests, ample attention was paid to this 'dynamic' effect. From the results it appears that the hawser forcers are a multiple of the longitudinal forces resulting from some slack in the hawsers due to the average 0.25 m. freedom of movement in the longitudinal direction.
The tests results show that the safety of moored ships is endangered when the longitudinal force reaches a value equal to 0.05 to 0.06% of the ship's weight. This situation already arises with fully loaded push tows entering at low speed. For this reason it is not advisable to allow push tows to enter the lock-chamber when there are other ships present.
For the safety of ships lying behind the push tow in the lock-chamber, great care should be taken in using the propellers. Special caution must be observed when revving up the propellers.
With regard to the exit times it was found that these too, progressively increase as the waterdepth decreases from about 5.50 m. for a large, fully loaded push tow.

During lock entry, currents occur above the lock apron. Close to the lock entrance the return current prevails. At a greater distance the current from the propellers predominates, but only in the neighbourhood of the extended center line of the lock. Current-velocities are highest around the corners of the lock entrance.

From numerous results it is clear that a waterdepth of 1.6 to 1.7 times the draft can be considered optimal for flat-floored locks used by large push tows. In a lock with sills the waterdepth over the sill should be roughly 1.5 to 1.6 times the draft.

2. Ships used

2.1. Model

For the model tests self-propelled model ships were used, built to a scale of 1 : 25. Most tests were carried out with push tows consisting of one pusher tug and four 'large' or 'small' barges. For some tests, six large barges were used. A number of navigation tests were made with a motor vessel of the Rhine-Herne Canal type. For most tests this vessel was made to represent a moored ship in the lock chamber. A small lighter with a displacement of 500 m^3, was used exclusively for this purpose.

N.S.M.B. propeller No.	2,926
diameter (D)	1,950 mm.
number of blades	3
pitch at 0.7 R (H)	1,620 mm.
pitch ratio at 0.7 R (H/D)	0.831
developed-area ratio (F_a/F)[1]	0.536
type of blade	Kaplan
direction of rotation	inward
number of propellers	2
power (per propeller)	750 S.H.P.
propeller speed	275 r.p.m.
sailing speed[2]	13 km./h.

Table 2.1 Propeller data of the pusher tug (Prototype dimensions)

[1] Developed area of one blade: F_a
Area of the propeller circle: F

[2] At an unlimited waterwidth, a waterdepth of 5.00 m. and for a 2 × 2 formation of small barges with a draft of 3.00 m.

Illustrations of the shapes of the ships, the main dimensions and the composition of push tows are shown in figures 2 to 6.
The pusher tug and the motor vessel were constructed in the Netherlands Ship Model Basin (N.S.M.B.) and were fitted with propelling and steering equipment in the Delft Hydraulics Laboratory.
The pusher tug was driven by two propellers operating independently of each other. The two main rudders and the backing and flanking rudders, which were placed in

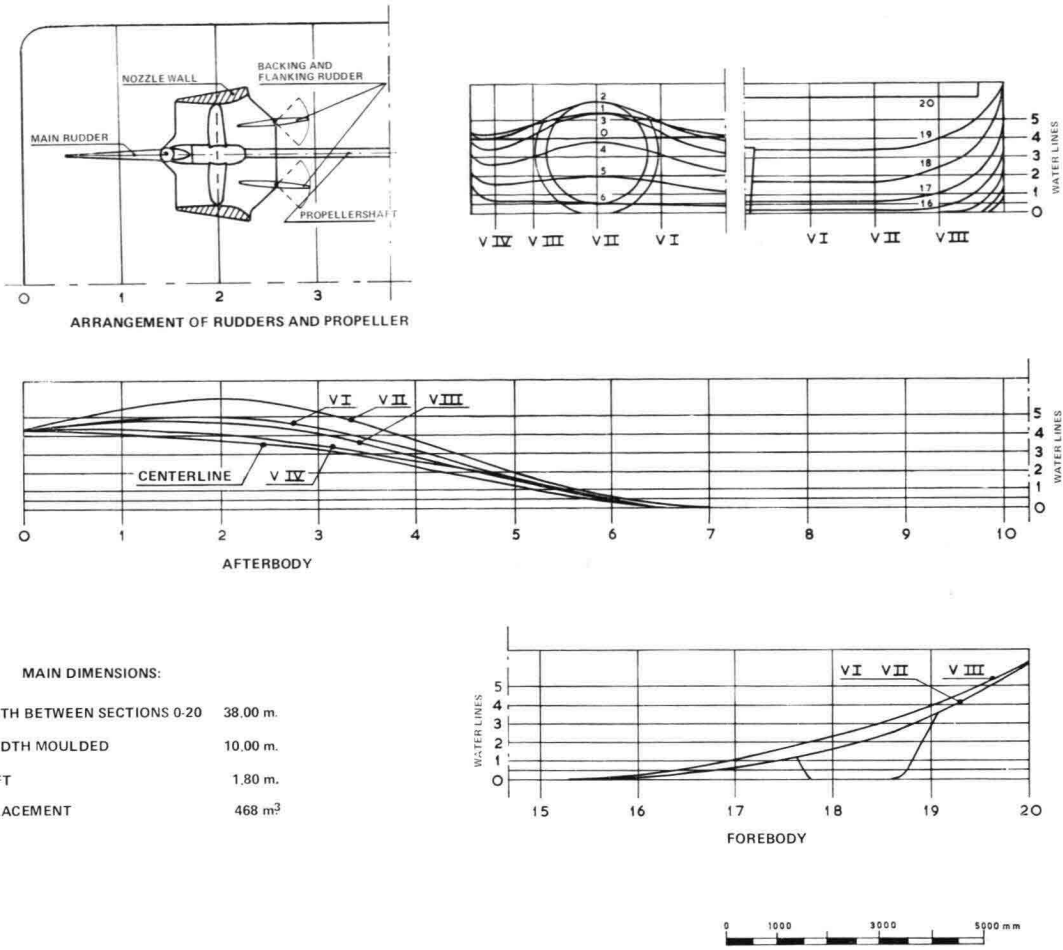

Figure 2. Body plan of twin screw pusher tug

pairs, could also be operated independently. The propeller data are given in table 2.1. The framing of propeller and rudders is shown in figure 2. The rudder angles and propeller revolutions per minute could be read from an instrument-panel.
The loaded ships were powered by batteries placed on board. The batteries for the unloaded ships were installed on the embankment and were connected to the ship by flexible wires.

2.2. Prototype

For the prototype tests a push tow from the Mannesmann Shipping Co. was used.

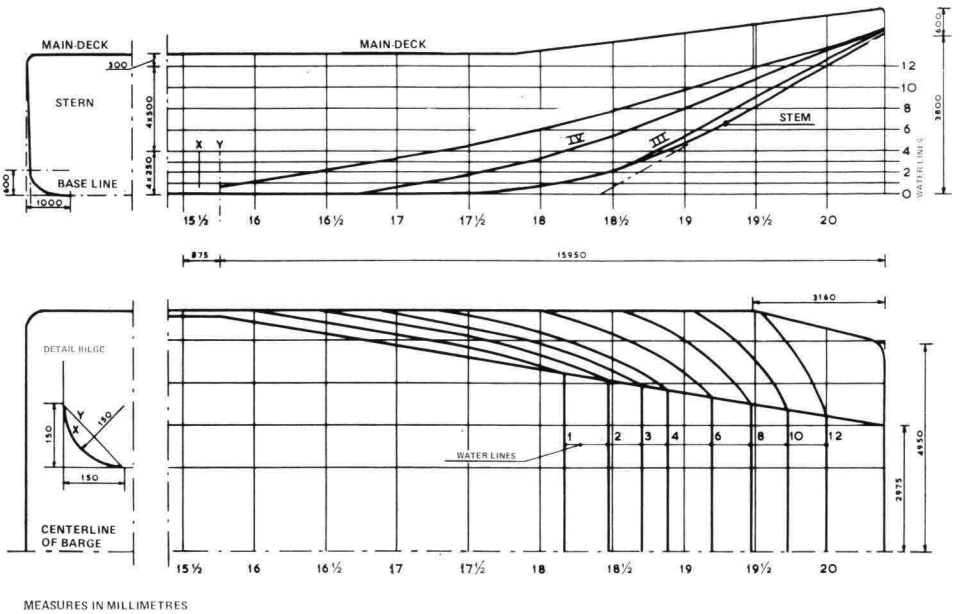

MAIN DIMENSIONS:

LENGTH OVER ALL	76.50	m.
LENGTH BETWEEN SECTIONS 0-15½	59.675	m.
BREADTH MOULDED	11.33	m.
DEPTH OF HULL	3.30	m.
DRAFT (MAX.)	3.30	m.
DISPLACEMENT (MAX.)	± 2700	m^3

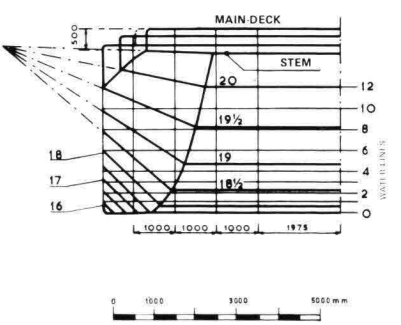

Figure 4. Body plan of the 'large' push barge

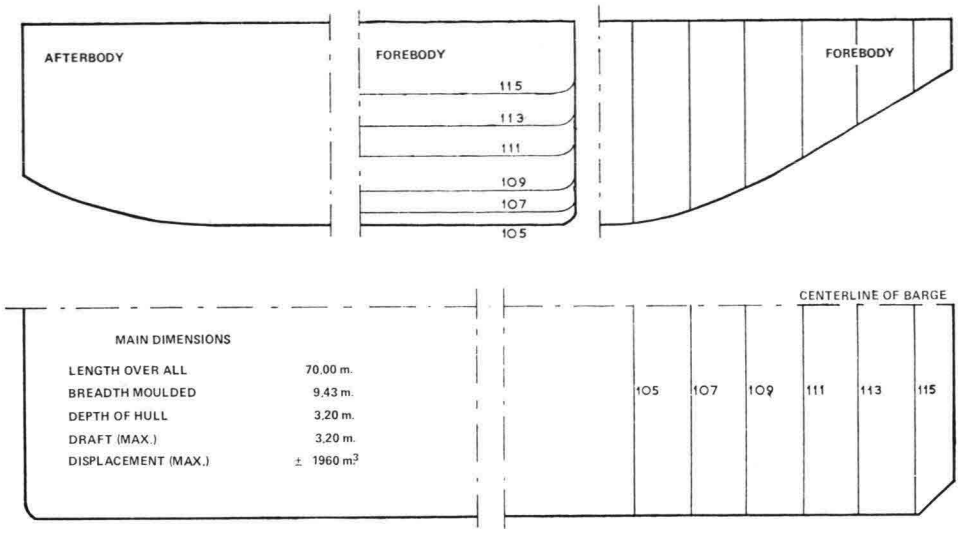

Figure 3. Body plan of the 'small' push barge Scale 1 : 125

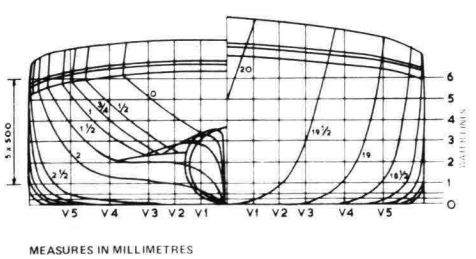

MAIN DIMENSIONS:

LENGTH OVER ALL	79.95 m.
LENGTH BETWEEN PERPENDICULARS	76.92 m.
LENGTH BETWEEN SECTIONS 0-20	77.42 m.
DISTANCE BETWEEN SECTIONS	3.87 m.
BREADTH MOULDED	9.45 m.
DEPTH OF HULL	2.50 m.
DRAFT (MAX.)	2.50 m.
DISPLACEMENT (MAX.)	1598 m³

Figure 5. Section forms motor-vessel of Rhine-Herne canal type

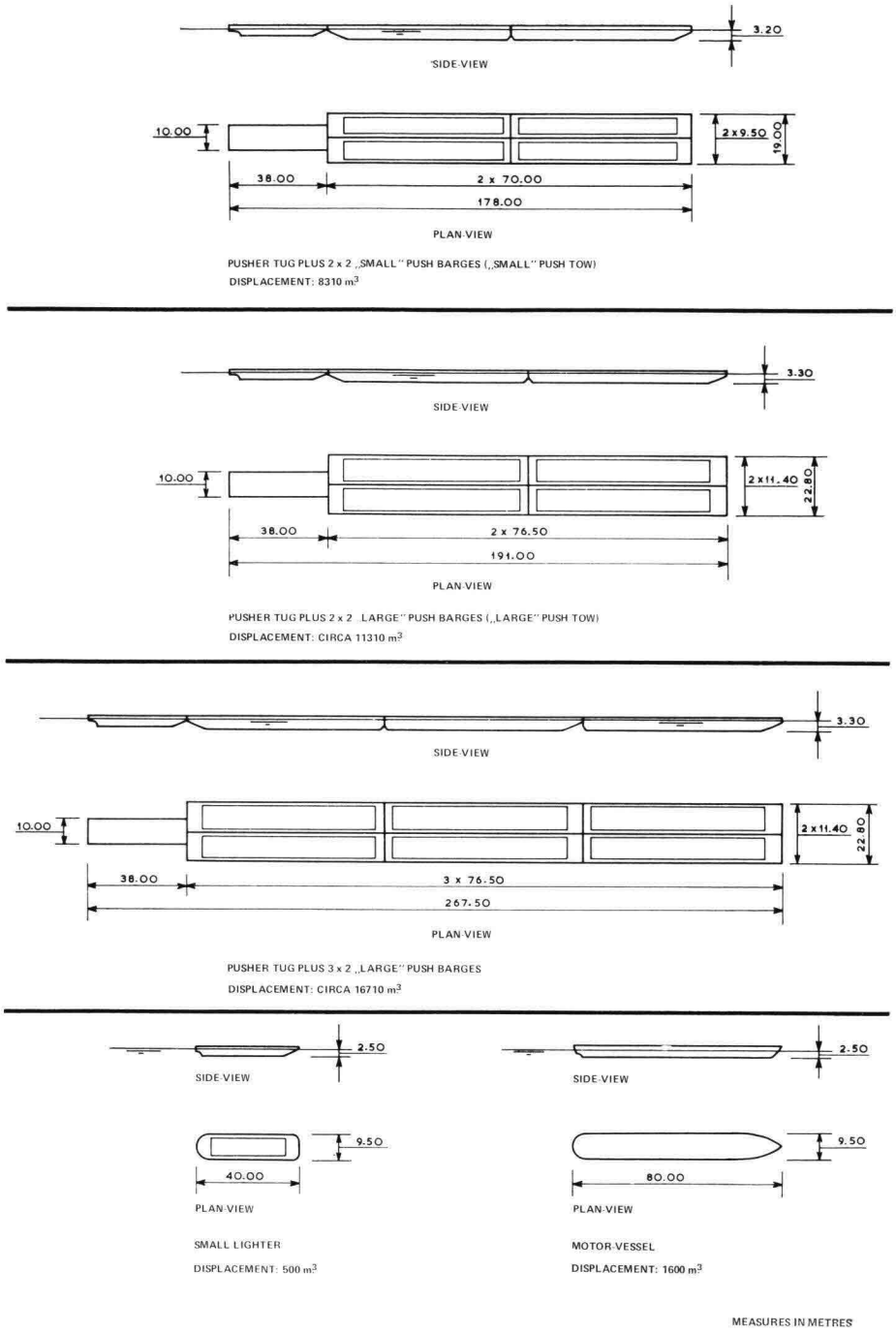

Figure 6. Main dimensions model ships

It was composed of the twin propellered pusher tug Mannesmann II and four push barges. The main dimensions are given in table 2.2.1. The most important propeller data can be found in table 2.2.2.
The underwater shapes of the push boat and the push barges are similar to those of the models, shown in figures 2 and 4 respectively.
Both propellers can be operated independently as can the main rudders and the backing and flanking rudders. Propeller speeds and rudder angles can be observed in the wheel-house.

quantity		pusher tug	push barge	push tow
length over all	(m.)	36.00	74.40	184.80
beam	(m.)	9.50	11.20	22.40
depth of hull	(m.)	2.52	3.30	3.30
maximum draft	(m.)	1.75	3.20	3.20
loading capacity at maximum draft	(ton)	–	2,100	8,400

Table 2.2.1. Main dimensions

diameter (D)	1,950 mm.
number of blades	3
pitch (H)	2,130 mm.
H/D	1.092
number of propellers	2
direction of rotation	oppostie to one another
power per propeller	900 HP
number of revolutions (max.)	241 r.p.m.

Table 2.2.2. Propeller data of pusher tug Mannesmann II

3. Model

3.1. Scales

The model tests were carried out on a scale of 1 : 25. According to Froude's scale rule the velocity scale then becomes 1 : 5. The derived scale factors are given in table 3.1.

quantity	scale
length	1 : 25
height	1 : 25
speed or velocity	1 : 5
time	1 : 5
propeller speed	5 : 1
discharge	1 : 3,125
mass and force	1 : 15,625
power	1 : 78,125

Table 3.1. Scales

Scale 1 : 25 was chosen on the following grounds:

a. At a scale of 1 : 25 the dimensions of the model of the push tow allow the model's helmsman to sit in the rear pair of barges. In this way reality in the navigation tests is most closely approached. As the weight of an average-sized helmsman is only 10 to 11% of that of the model ship, his presence on board has no adverse effect on the model's weight distribution.
b. Scale investigations to prepare for the model tests as described in Ref. [2], carried out in the Netherlands Ship Model Basin, have shown that no unacceptable scale effects occurs at a scale of 1 : 25. A scale effect in the rudder force was not evident. Compensation for the scale effect in the frictional resistance can be made by using a propeller speed roughly 10% higher than indicated by scale rules.
c. At this particular scale, the dimensions of the lock model remain within economically acceptable limits.

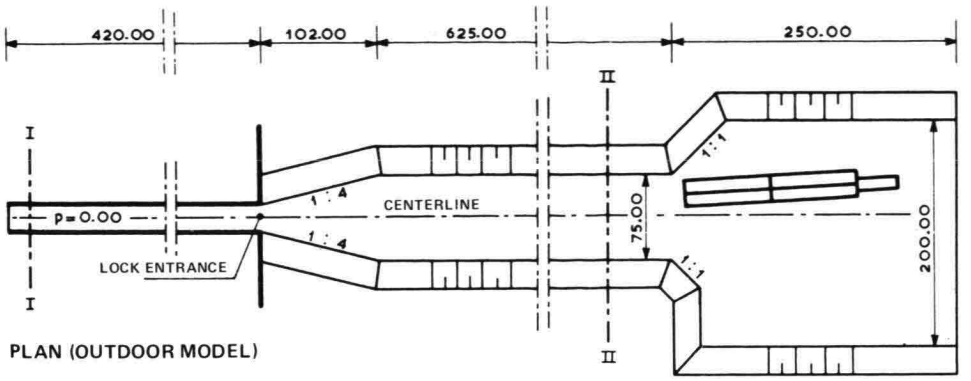

PLAN (OUTDOOR MODEL)

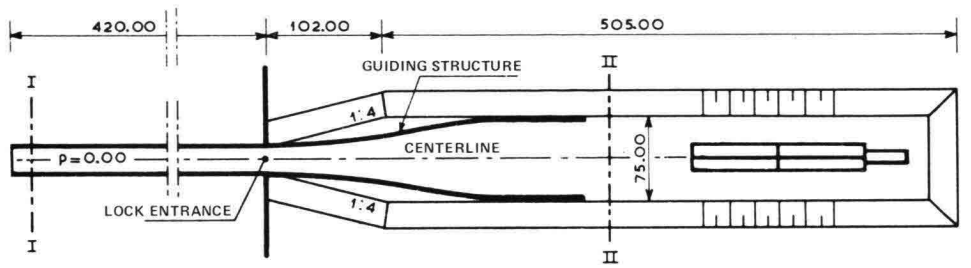

PLAN (INDOOR MODEL)

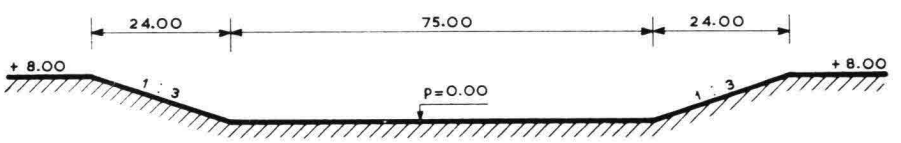

CROSS-SECTION II-II

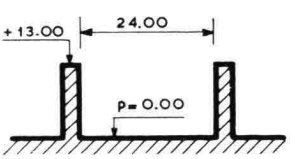

CROSS-SECTION I-I

MEASURES IN METRES (FULL SCALE)
p = 0.00 is DATUM LEVEL

Figure 7. Plans and cross-sections of the lock models

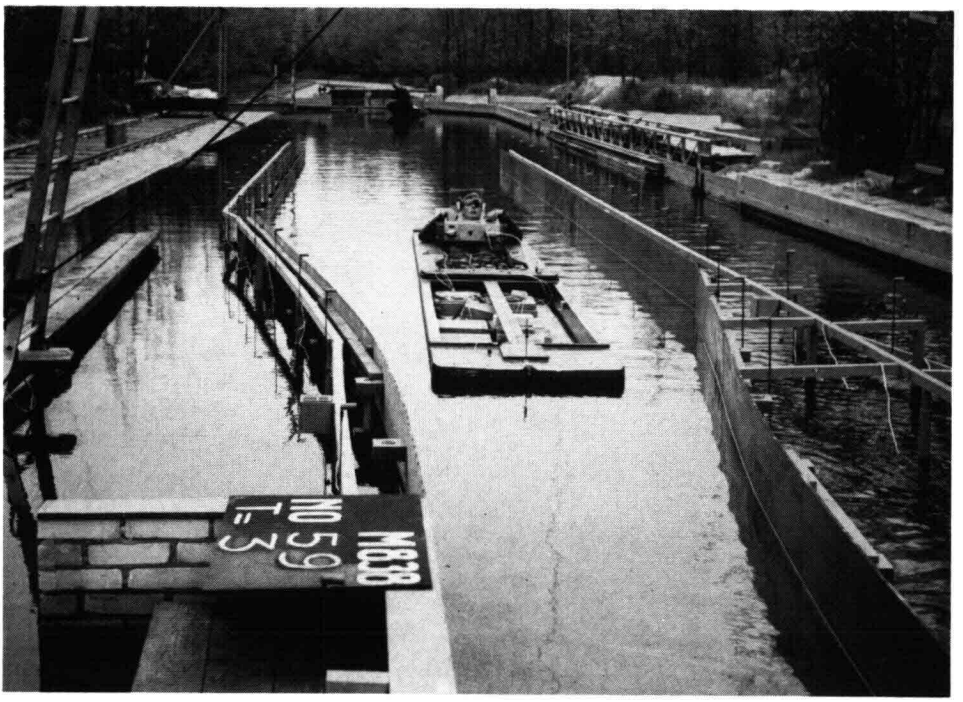

Photograph 2. Southern lockapproach of the Volkerak Locks in model and prototype

3.2. Construction and arrangement

The investigation began in a model situated in the open. After a short period, a new model was built in a shed in order to exclude weather influences and to improve the efficiency and the accuracy of measurement. Drawings of both models are shown in figure 7.
For the investigation of optical guidance requirements for the Volkerak locks, a new model was built in the open, which resembled the prototype as closely as possible. An impression is given in photograph 2.
Part of the research on the protection offered by the guiding structures against side-wind took place in one of the wind tunnels of the Hydraulics Laboratory.
In all lock models, the lock approach as well as the lock chamber were of flat bottom construction. Wherever necessary, replaceable locks sills were used. There were no gate-recesses in the chamber walls.
In front of the lock entrance, there was an apron of loosely dumped stones with a diameter equivalent to about 0.20 m.
The shape of the lock approach was changed only during the investigation of currents over the apron (figure 75, paragraph 16.1) and during a detailed investigation concerning optical guidance (figure 27, paragraph 7.4.).
The bottom of the guiding structure was 1.25 m. below water level.
Further details are given under the relevant subject headings.

3.3. Performance of the investigation

A distinction is made between the tests concerning approach and entry of the lock and the tests examining the variations in sailing speed during entry and exit of the lock and the accompanying hydraulic phenomena.
In the latter case, ships were guided along a cable running in the lock centerline above the model ship. The rudders were fixed in middle position. The propeller speed was changed, if necessary, from the bank. Further details of these tests and the methods used are described in part III.
During the manoeuvre tests with the large deep loaded push tow, the rudders and propellers were operated by a helmsman from the rear pair of barges, as shown in photograph 2. The tests were carried out with a constant propeller speed. The rudder angles were continuously recorded on a magnetic tape.
During the manoeuvre tests with an unloaded push tow, the steering was effected from the bank, the helmsman choosing the position most favourable for observation of the course to be taken. The control panel was connected with the pusher tug by means of an electric cable in such a way as to exert only a negligible force on the ship.
Further details and registration methods used are described in part II.

4. Prototype tests

4.1. Pushtow navigation tests in the Volkerak locks

The approach and entry manoeuvres were carried out with a push tow in the southern lock-chamber and from the lock approach on the Hollands Diep side. The push tow was partly loaded. The draft was only 2.50 m.
A sketch of the locks and the position of the measuring and observation posts is given in figure 8. The measurement methods used are only described briefly in this report.
The quantities measured and the methods used will be dealt with in separate paragraphs.

1. Determination of the position of the push tow.
   The successive positions of the push tow in the lock approach were determined with the help of two theodolites at post A and sextants at posts B, C en D. The interval between observations was 30 seconds.
   In the lock-chamber the position was determined by registering the time at every 10 meters travel and with the help of a plane-table from post E.
   From the successive positions the course of the sailing speed can be deduced.
2. The water level variations in the lock-chamber.
   The rise and fall of the water level was gauged at stations (51) up to and including (64) with the help of stepwise electrical depth gauges with 0.05 m. per unit of depth. Each gauge had a panel with lamps, one per unit of depth, which was photographed every two seconds.
3. The current velocities above the lock bottom near the lock entrance.
   The current velocities were measured at posts x, y and z, at 0.40 m. above the lock bottom, with turbulence meters. The signals were recorded continuously. The flow direction was not measured.
4. Rudder angles and propeller speed.
   Observations of the rudder angles and the propeller speed were made in the wheelhouse of the pusher tug.
5. The vertical tide.
   The change of the water level with time was observed visually on the depth gauge in the lock approach.
6. Wind velocity and direction.
   The wind velocity was measured with a hand-anemometer, and the direction of the wind with a weather-vane.
7. The velocity and direction of the tide-run in the lock approach.

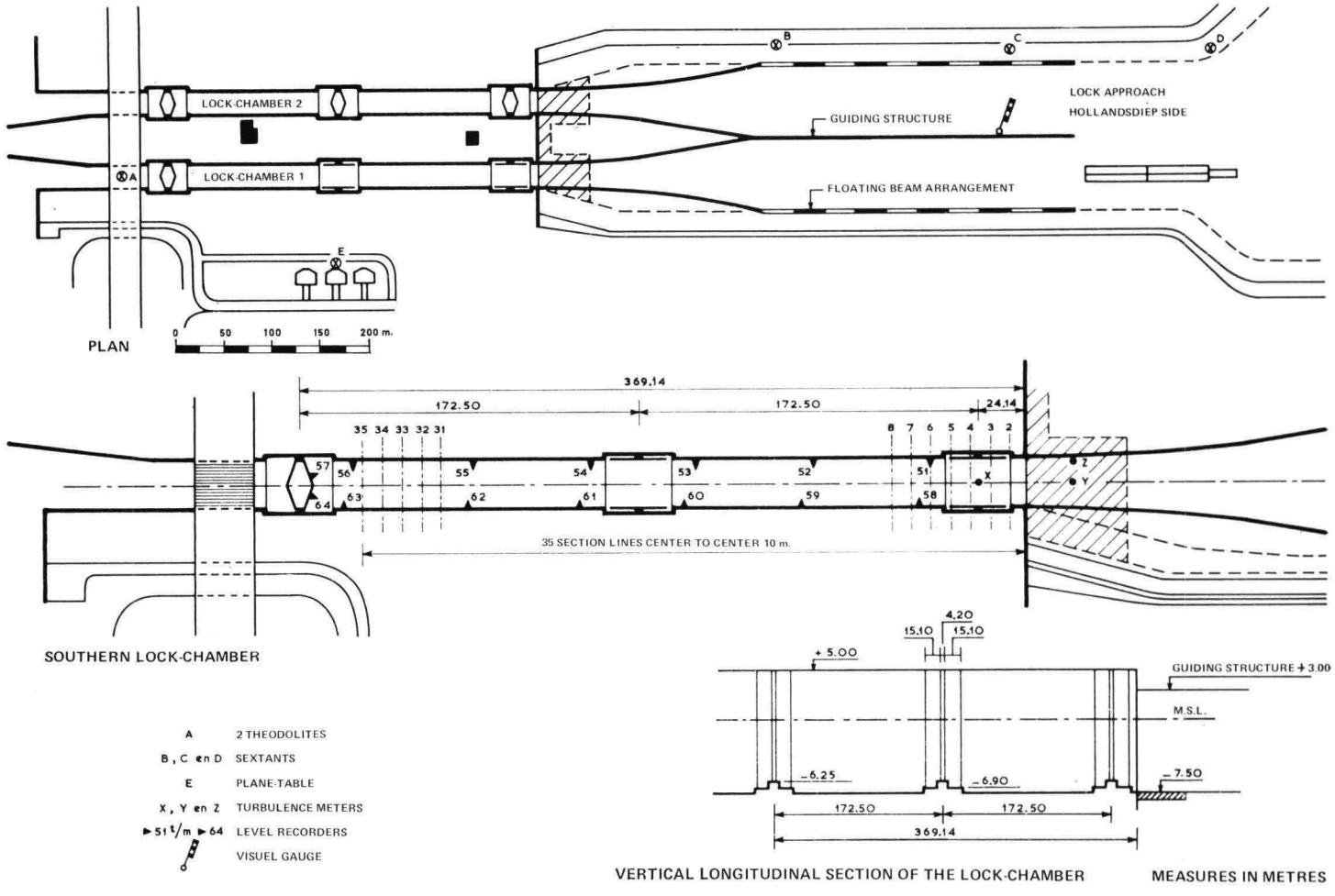

Figure 8. Volkerak Locks

The latter quantities hardly affect judgment of the test results.
A total of 9 entry runs were carried out. For the fifth run the push tow started from the lay-by south of the locks and sailed along the guiding structure to the lock-chamber. The starting point of the other entry runs was halfway down the southern part of the lock approach, some 800 m. from the lock entrance. All manoeuvres were carried out by daylight.
The influence of the wind on the behaviour of the push tow during the test runs may be neglected. It was therefore disregarded in judging the results.
Owing to the great waterdepths and the reduced draft of the barges, the hydraulic phenomena during the lock entry were less marked than expected.
The prototype test results will be discussed together with the model test results under the subject headings. If necessary, testing procedures will be further explained for better understanding and judgment.
The measurements were organised by and carried out under the supervision of the Hydraulic Department of the Deltadienst of Rijkswaterstaat.

4.2. Pushtow navigation tests in the Hartel lock

The entry manoeuvres were carried out in the lock approach at the Old Meuse side, with a deep loaded push tow. The draft was 3.20 m. A sketch of the situation and the position of the measuring and observation posts is given in figure 9. The measurement methods used are only briefly described in this report. They will be dealt with point by point.

1. Determination of the push tow's position.
   The successive positions of the push tow in the lock approach were recorded by two synchronised cameras. These were placed on board the push tow and photographed marks on the guiding structures. This part of the measuring was done by the Measurement Department of the Rijkswaterstaat.
   Just outside the lock entrance and in the lock-chamber, the passing of the section lines was recorded. The distance from the push tow to point R.L. was, moreover, measured with a radiolog on board of a gauging vessel. The 'shore station' was situated on the push tow.
2. The water level variations in the lock-chamber.
   The variation of the water level was recorded at various observation points. The visual gauges III and VI were photographed at intervals of 2 seconds. In point II, IV and V float gauges were used, the recording of which also took place photographically.
3. The current velocities above the apron.
   The current velocities, occurring during the entering manoeuvre were measured in point Z by an 'Ott' current velocity meter, which was placed 15 m. from the lock entrance under the southern guide, at 0.50 m. above the apron.

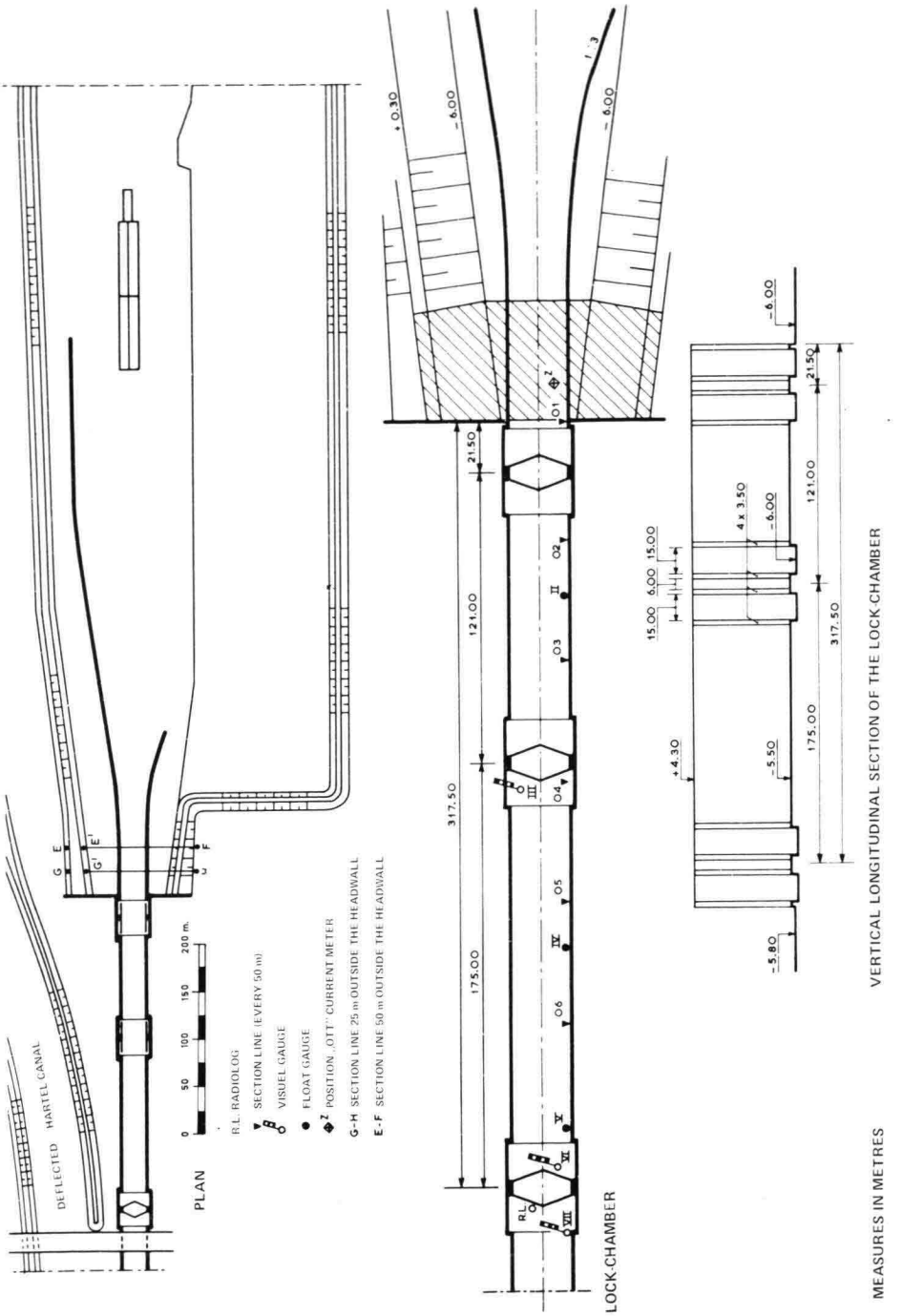

Figure 9. Hartel Lock

4, 5 and 6. These points are identical with the corresponding points in paragraph 4.1. In total, 5 entry runs were carried out. The starting point of each run was halfway down the lock approach, about 800 m. from the lock entrance. All manoeuvres were carried out by day light.
The influence of the wind is negligible and will therefore be disregarded from now on. The treatment of the testresults is the same as that of the tests results in the Volkerak lock. (paragraph 4.1.).
The measurements were organised by and carried out under the supervision of the Public Works Department of Rotterdam.

II Guiding structures and guiding-light systems

5. Introduction

5.1. Functions of guiding structures

Guiding structures are used in lock approaches to promote smooth and safe entry and exit manoeuvering. Design criteria for guiding structures therefore incorporate several requirements for safety and locking capacity.
Although navigation locks for push tows will in general have to deal with both push-tow navigation and conventional shipping, the push tows are considered to be the deciding factor for reasons of safety, because of their great mass and dimensions and the special shape of the forebody of the push-barges.
The narrow clearance between the lock-chamber and the barge formation is particularly striking, as illustrated by photograph 3.
As for safety, the following possibilities must be taken into account for the shaping of guiding structures:

a. Getting stuck in the lock entrance,
b. Collisions with opened mitre gates (in the chamber),
c. Collisions with the guiding structures,
d. Collisions with the headwalls,
e. The safety of waiting ships during the lock exit.

As for locking capacity, the following points should be taken into consideration:

a. Speed of the ships when entering and leaving the lock,
b. Accommodation for waiting ships to take up starting positions,
c. Manoeuvering space for ships entering and leaving the lock chamber,
d. Standardization.

The above-mentioned aspects concerning safety and capacity will be discussed in more detail in the following paragraphs.

5.2. Purpose, starting-points and scope of the investigation

The purpose of the investigation was to develop design rules for the shaping of the guiding structures for navigation locks for push tows. The following subdivision is used:

a. The structure's shape (considered in plan view) in relation to the center line of the lock,
b. The height of the structure above and below waterlevel,

Photograph 3. Push tow in chamber of Hartel Lock

c. The length,
d. Facilities to link the lay-by to the lock-entrance guiding structure. (In the lay-by ships wait for their turn to be locked).

The investigation originally centered on locks operating in two directions, with separate research procedures for entry and exit requirements. Only at a later stage, when plans for the addition of a third chamber to the Volkerak locks became final, the possibility of one-way locking was taken into account. We will touch upon this technique later in the report.
The investigation was sub-divided as follows:

- A general study of the functions of guiding structures.
- Model tests on mechanical and optical guidance.
- Model tests on lock exit manoeuvering of unloaded push tows with special regard to side-wind effects.
- Parallel prototype tests.

Both the model and prototype tests were performed with formations consisting of large barges (two pairs of barges in a row). The requirements of conventional shipping were considered as part of the general study.

6. Shape of the guiding structures as seen in plan view

6.1. General

To avoid collision with the head walls, especially of large push tows, guiding structures are necessary on either side of the lock approach.
The guiding structures always have a mechanical function and sometimes, as in the case of push tows, an optical function as well. The mechanical function is the guiding of a ship through physical contact with the construction. The optical function is provided by the sort of shaping that is conducive to visual orientation.
Evidently the entrance guides are to act as a funnel receiving vessels and guiding them into the lock. The shape of the funnel and the width of its mouth determine the length of the guiding structure. A width of about 40 m. is necessary to allow for a push tow, or for two big conventional ships sailing side by side and approaching the lock-chamber under unfavourable conditions.
There should be adequate space to enable ships to manoeuvre as soon as possible after leaving the lock. In this connection an unloaded push tow influenced by side-wind is determining. Therefore the guiding structure should diverge as much as possible. This is also important for the position of the lay-by which should be situated as close as possible to the lock-chamber in order to optimize the locking capacity for push tows as well as conventional vessels.
Preferably, the lay-by should be linked to the funnel by means of an uninterrupted structure with a guiding function. In the absence of such a transition guide, delays are likely to occur during entry manoeuvres. The angle between the guiding structure and the lock center line must be as wide as possible, without reducing the structures' guiding function for entering vessels. In practice, good results have been obtained with a guide angle of 1 : 6 to the lock center line.

6.2. Mechanical guiding

6.2.1. Entering at an angle to the lock center line

Photograph 4 shows that large (2 × 2) push tows with only a narrow clearance from the lock-chamber can easily get stuck when entering at an angle to the lock center line. Stagnation and damage to locks and ships can be the result. Open mitre gates are especially vulnerable in this respect.

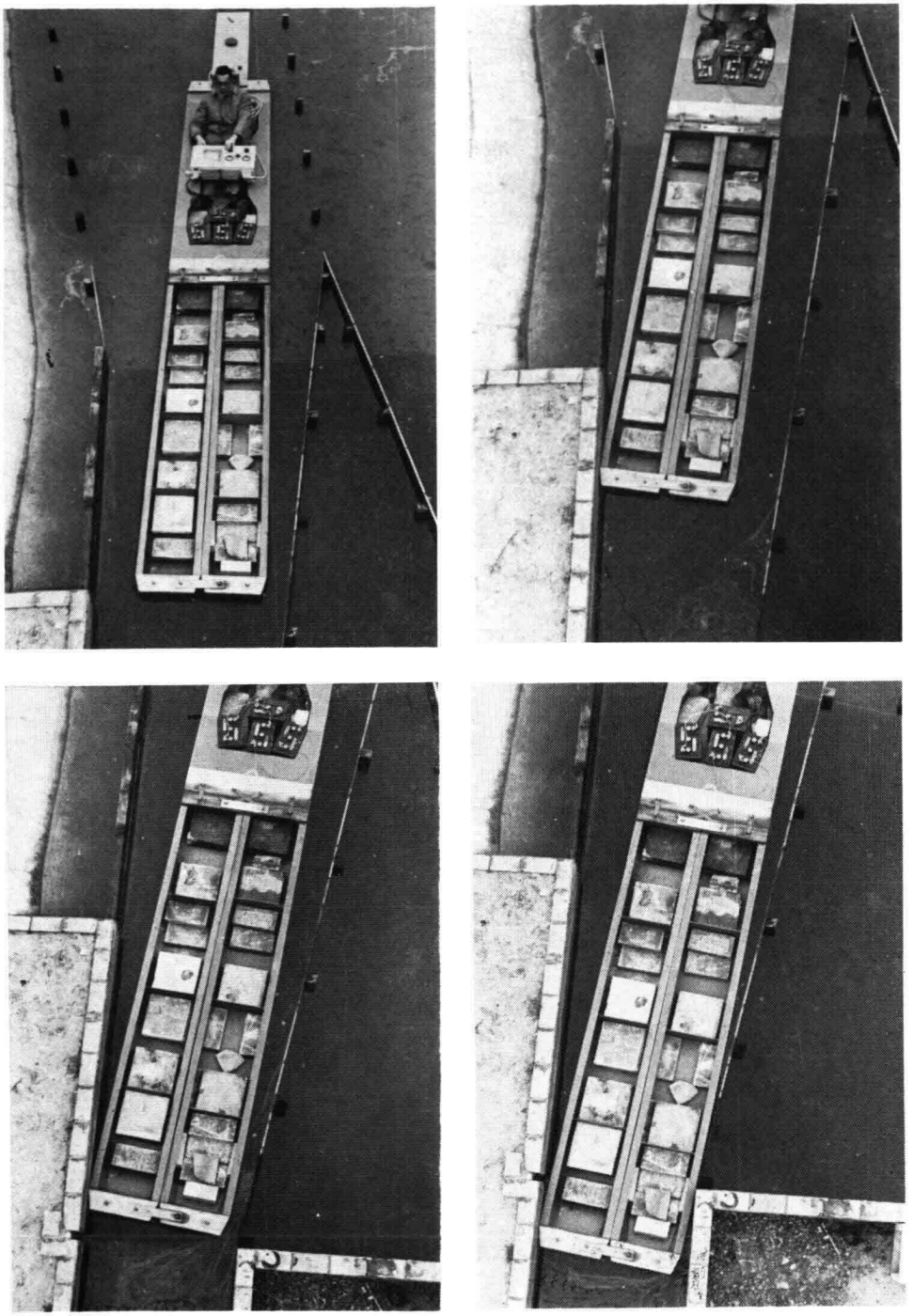

Photograph 4. Push tow getting stuck in the lock-entrance

A push tow on entering at an angle, hits the lock at points A and B as indicated in figure 10. The reaction of the impacts and the friction in these points cause a moment M_p which tends to swing the push tow round, and a moment M_n opposing the swing tendency. The forward speed will, moreover, be abruptly reduced. The force of the impacts depends on the sailing speed during entry, the characteristics of the push tow, the angle of entry (α) and the friction coefficient.

The influence of α on the progress of entry was studied with tests in the model. The large 2 × 2 push tow was used. The tests were carried out with a constant approach speed and a constant propeller speed. The rudders remained in neutral position. The push tow sailed along a straight guiding structure, whose angle to the lock center line was varied systematically.

The influence of α on the progress of entry is manifest in the loss of forward speed. Average speed on the first 50 m. inside the chamber was chosen as parameter.

The influence of the friction coefficient was investigated by using different materials (steel, brass, and hard plastic) for the bow of the barges.

The measurement results are given in figure 11, the visual observations in table 6.2.1.

tan α	behaviour of the push tow	
	loaded	unloaded
1 : 8	the p.t. got stuck	the p.t. got stuck
1 : 10	the p.t. swung round. V_s decreased to zero	as 1 : 8
1 : 12	as 1 : 10	as 1 : 8
1 : 16	border-line case; V_s decreased in some cases to zero	border-line case; V_s decreases to zero; in some cases the p.t. swung round
1 : 20	V_s decreased, but not to zero; the p.t. entered grazing the lock wall	the p.t. entered grazing the lock wall

Table 6.2.1. Observed behaviour of the push tow at various entry-angles (p.t. = push tow; V_s = forward speed)

Roughly, the measuring results show that the entry into the model lock is smoother if tan α is less than 1 : 20. The use of different materials appeared to have only a slight influence.

Although any translation of model test results into full scale is liable to distortion by scale-effects, it may be concluded that it is advisable to shape the guiding structures in such a way as to allow push tows to enter the lock at a narrow angle to the lock centre line.

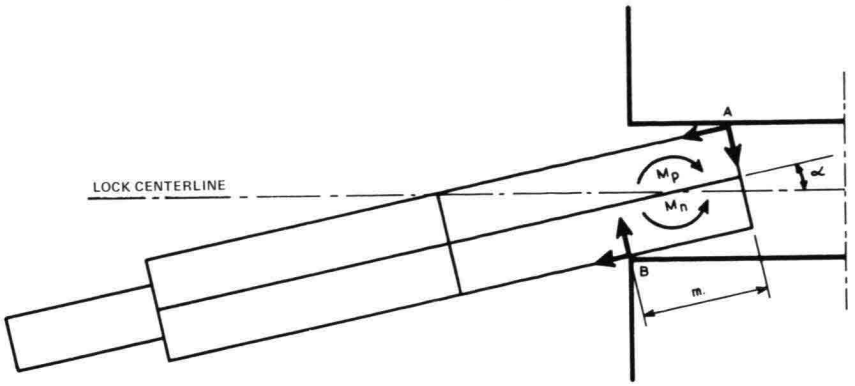

Figure 10. Outline of the position of a push tow which has got stuck

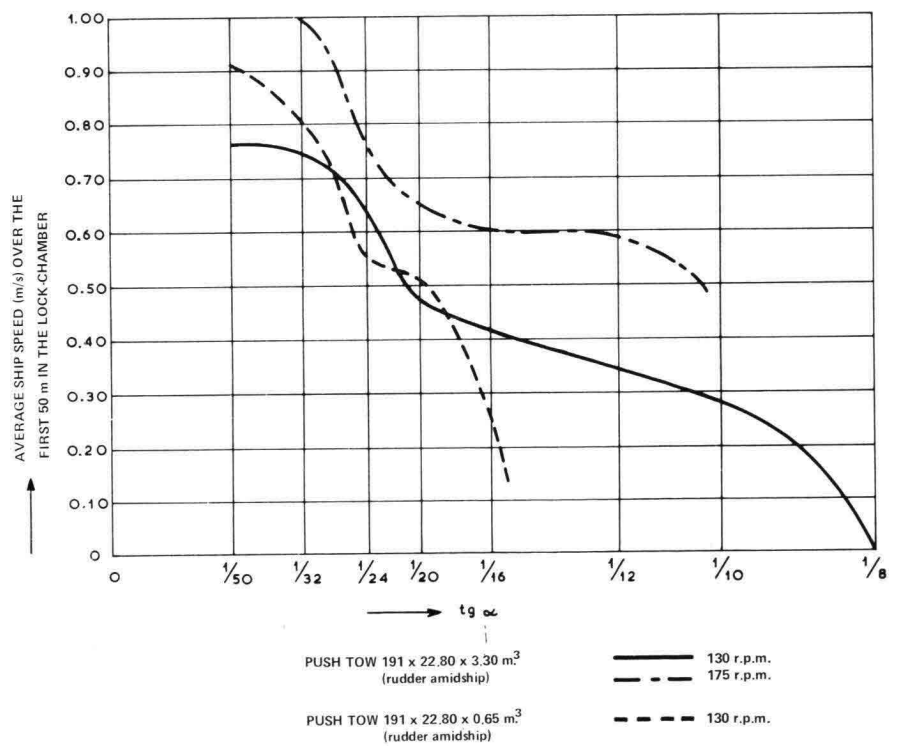

Figure 11. Speed characteristics of ship entering lock-chamber at various angles to lock-centerline

6.2.2. *Comparison between a straight and a curved guiding structure*

The alternative to a straight guiding structure with a constant angle to the lock center line, is a curved structure passing flush into the line of the chamber wall. The differences between both shapes are demonstrated in figure 12. Parabola $y = x^2 / 1250$ [m.] was chosen for the curved shape.

a. The transition of the straight guide into the line of the chamber wall is angular. This is not the case with the curved shape.
b. The angle of the curved guide to the lock center line near the lock-entrance is narrow, as shown in table 6.2.2.1.

x (m.)	0	10	20	30	40
tan α	1 : $\sim$	1 : 62.5	1 : 31.2	1 : 20.8	1 : 15.6

Table 6.2.2.1. Angle of the parabolic guide at various distances from the lock-entrance

Small angles are favourable for the position of the push tow during entry. Moreover the effect of a collision with the guiding structure is slight, owing to the narrow angle of approach.

c. The arm length of the impact-moment (m) at the time of getting stuck is a measure for the effectiveness of the mechanical guidance (see figure 12). The parabola is more favourable in this respect than a straight guide, as shown in table 6.2.2.2.

tan entry-angle	length moment-arm (m)	
	straight guide	$y = x^2/1250$ [m]
1 : 20	24.0	39.0
1 : 24	29.0	41.5
1 : 28	33.5	44.5

Table 6.2.2.2. Length moment arm by figure 12

d. The transition from the lay-by to the lock entrance guide is a smooth, continuous line. The transition structure itself may be straight. This cannot be effected when using a straight guiding structure with a slight angle to the lock center line, because in that case the lay-by would be too far away from the lock.
e. A curved guiding structure diverges more drastically than a straight one with a

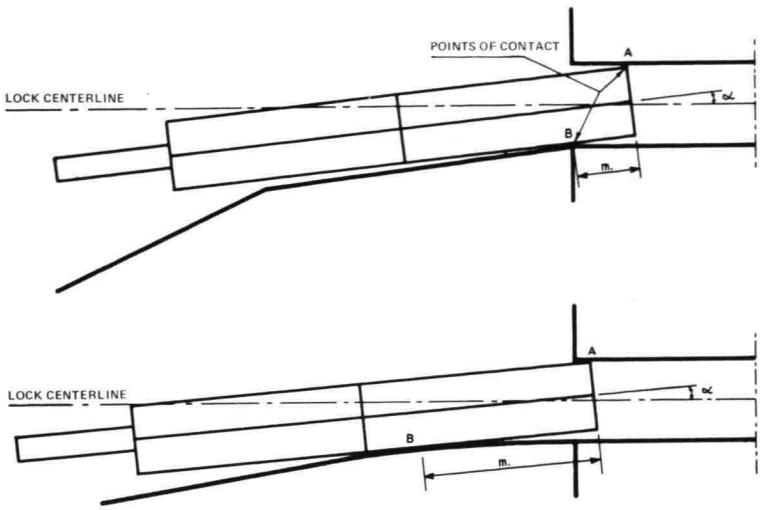

Figure 12. Comparison between a straight and a curved guiding stucture

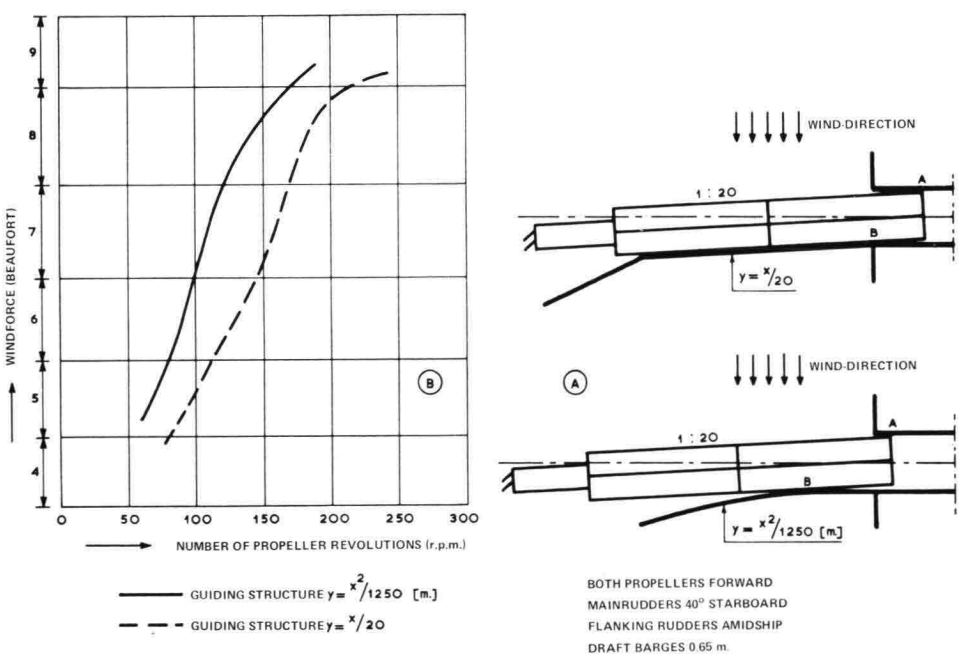

Figure 13. Minimum number of revolutions required to enter the lock with various wind-velocities in case of a straight and of a parabolic shaped guiding structure

small angle. This is especially important for ships leaving the lock. A comparison between various symmetrical guiding structures follows in table 6.2.2.3.

guiding structure	straight shape 1 : 16	straight shape 1 : 20	parabola $x^2/1250$ [m]	circle $R = 600$ m
x (m)	128	160	100	97.6

Table 6.2.2.3. Distance (x) from the lock-entrance to the point where the width of the funnel is 40 m.

f. The difference in guiding quality was visualized in the model by means of entry tests with an unloaded push tow under the influence of side-wind. The starting position and the testing conditions are indicated in figure 13a. The minimum propeller-speed required for the straight guide is considerably higher than for the parabola.

6.3. Optical guiding

6.3.1. Purpose and set-up of the investigation

In view of the narrow clearance between push tow and lock-chamber it is important that the helmsman can take his bearings when approaching the lock. The entry accuracy and thereby the safety, are improved in this way. A guiding structure with good optical guidance characteristics may moreover have a favourable effect on the locking capacity, because it encourages higher entry speeds.
Because the guiding structures form an important part of the optical layout, model tests were designed to determine the characteristics of a guide providing good optical guidance.
Four different layouts were tested. They are shown in figure 14 and are indicated by the numbers (I) to (IV). The height of the guiding structures above water level was 1.75 m. in all cases.

6.3.2. Execution of the tests

For the entry test runs eight well-trained laboratory workers were employed as helmsmen. The helmsman had to sit down in the two rear barges of the push tow model, in addition to which had been tried to achieve optimum reality on scale basis (eye-

level, position of the head, etc.). One eye of the helmsman was covered to reduce his capacity of estimating distances, in order to bring testing conditions up to reality (photograph 2, paragraph 3).
The push tow was started at about 550 m. from the lock-entrance. The navigation speed was 5 km./h. while the propeller speed was kept constant.
The helmsman was instructed to follow the lock center line as well as he could, and to enter the lock without hitting the guiding structure. Each entry test was considered to be finished once the bow of the push tow has passed the lock-entrance.
A total of 96 entry runs were carried out, each helmsman performing three entries in each of the four layouts. The order in which the helsman had to enter the various layouts, was varied in such a way as to eliminate learning and sequence effects.
The following quantities were recorded:

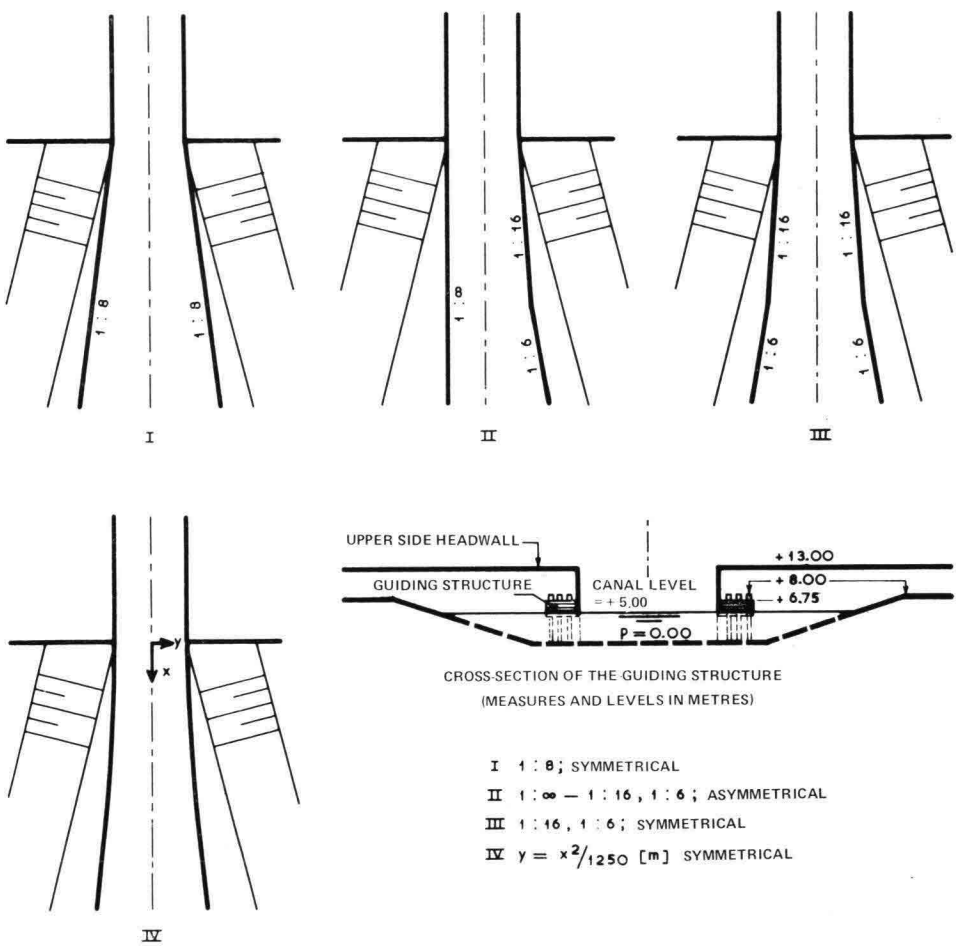

Figure 14. Shaping of the tested guiding structures

a. The rudder-angle, which was continuously recorded throughout the runs,
b. The position of the push tow, which was photographically established over the last 90 m. from the lock-entrance (at 4 to 5 positions),
c. The place of any collisions with the guiding structure,
d. The preference of the various helmsmen.

6.3.3. *The analysis of the measurement results*

a. The rudder angle.
From the rudder angle recordings, the standard deviation for each run was calculated.

b. The position of the push tow.
The position of the push tow is represented by the items X_i, Y_i and α_i, as indicated in figure 15.
The index i gives the number of the position, n being the total number of recorded positions.
With the help of the above-mentioned quantities each of the entries was given a quality-mark ($Cy\alpha$), which was calculated using the following equation:

$$Cy\alpha = \frac{1}{n} \sum_{i=1}^{n} \frac{|Y_i| + 50\,|\tan\alpha_i| + \frac{Y_i \tan\alpha_i}{|Y_i \tan\alpha_i|}\sqrt{|Y_i\, 50 \tan\alpha_i|}}{0.01\,(X_i + 25)}$$

The lower the value of the $Cy\alpha$ the better the entry. When drawing up the equation the following considerations were taken as a starting point.
1. The position of the ship is termed worse as it has more difficulty in moving back to the lock center line as indicated in figure 16.
2. A deviation from the right position is counted heavier as the distance to the lock entrance decreases (X in the denominator).
3. The angle (α) to the lock center line and the distance perpendicular to the center line (Y) were weighed against each other to the effect that $\tan\alpha = 1/8$ was counted just as heavy as a value of Y equal to about a quarter of the lock width.
4. $Cy\alpha$ is an average value.

c. Collisions with the guiding structure.
Each run was evaluated in points
2 points for an open entry (no collision)
1 point for a collision for $0 < X \leqslant 2.5$ m.
0 points for a collision for $X > 2.5$ m.

d. Preference.
The preference of the test persons is indicated by points 1 to 4 (decreasing order of preference).

The optical guiding qualities of the various guiding structures were compared with the help of the four above-mentioned parameters.

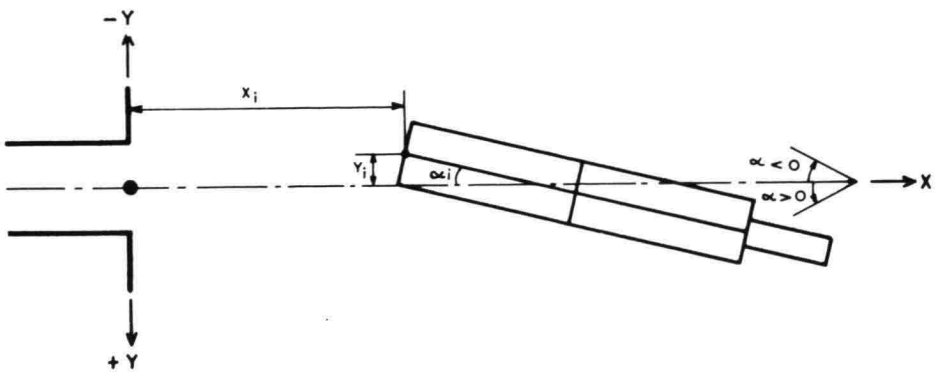

Figure 15. Position of the push tow

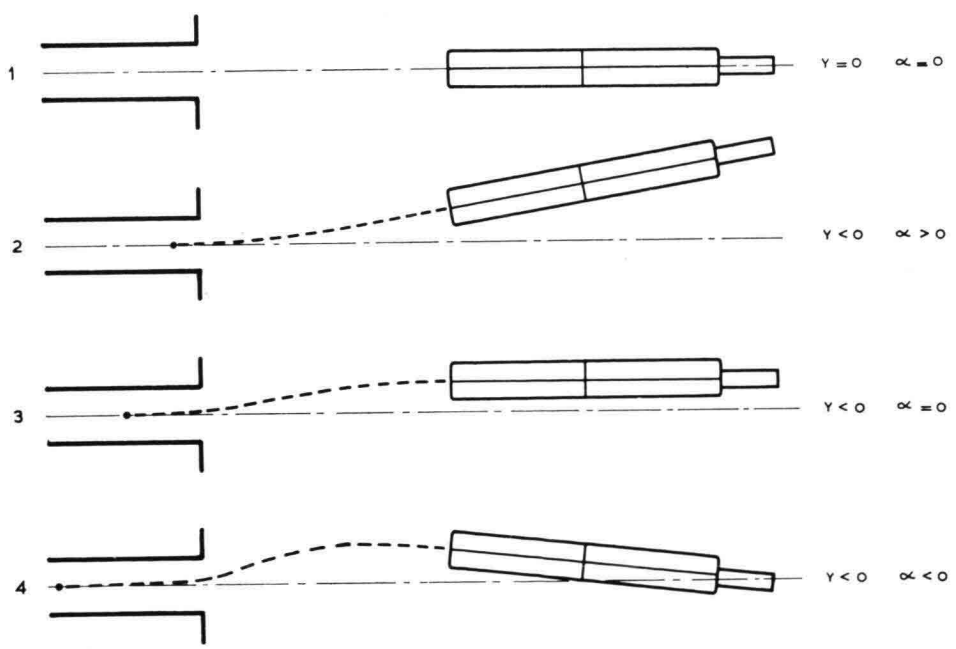

Figure 16. Positions of push tow getting unfavourable from 1 to 4 in view of entering the lock

6.3.4. *Results*

An analysis of variance was applied to all measurement results in order to judge the occuring differences between the guiding structures are statistically significant.
The analysis of variance will not be discussed in detail. Only the results will be dealt with.

a. Standard deviation of the rudder angle.
There were no indications for significant differences between the four shapes of the guiding structures. A possible cause may be that the standard deviation was determined over the whole run, including the start during which comparatively very large rudder angles are used.

b. Quality mark.
The average $Cy\alpha$ values for the various test persons are indicated in table 6.3.4.1. From this an impression can be obtained about the spreading in the measurement results. From the analysis of variance it appears that the guiding structures have a significant influence on the $Cy\alpha$ values. The differences between the guiding structures themselves are indicated in table 6.3.4.2. and figure 17a.

c. Collision scores.
The average number of marks for each test person is indicated in table 6.3.4.1. With regard to the collision scores there is also a significant difference between the guiding structures. A comparison is given in table 6.3.4.2. and figure 17b.

No. testperson	$Cy\alpha$				collision scores			
	I	II	III	IV	I	II	III	IV
1	3.28	3.68	1.85	1.41	1	0	1	2
2	2.90	1.41	1.73	2.72	3	2	3	2
3	1.20	1.46	1.58	1.45	5	2	5	3
4	4.55	2.82	1.80	2.26	0	1	4	4
5	1.63	1.97	1.76	1.54	4	3	4	4
6	2.29	2.94	1.26	1.14	1	2	4	4
7	2.72	1.57	1.34	2.46	4	3	5	2
8	2.89	1.43	1.43	0.98	3	4	4	4
Sum	21.46	17.28	12.75	13.96	21	17	30	25

Table 6.3.4.1. Performance of the test persons in the various situations (a low $Cy\alpha$ value and a high collision score are favourable)

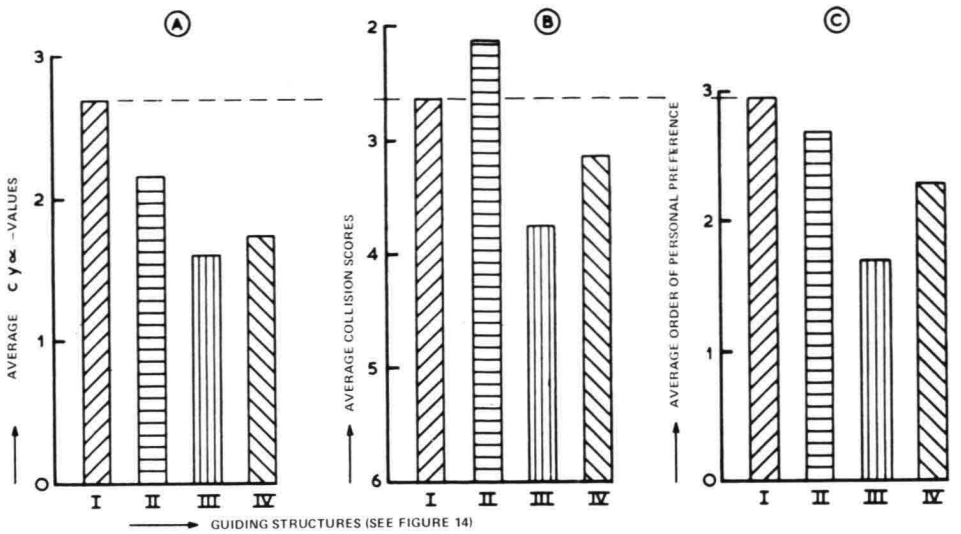

Figure 17. Comparison of the guiding structures based on Cyα-values, collision scores, and personal preference of the test-persons

Cyα values	level of significance	collision score	level of significance
III > I	0.01	III > I	0.05
IV > I	0.01	III > II	0.01
(II, III, IV) > I	0.05	III > (I, II, IV)	0.05
(III, IV) > (I, II)	0.05	(III, IV) > (I, II)	0.05
(III, IV) > I	0.01		

Table 6.3.4.2. Significant differences between the guiding structures (> is better than)

d. Preference of the test-persons.
The average preference is given in figure 17c.

6.3.5. Notes and conclusions

First, it should be pointed out that measurement results only have a comparative value. If in the model a certain shape proves better than another, the same may be expected of the prototype. There is no certainty about the value of the measurement results for the prototype in the absolute sense.

A comparison of the guiding structures shows, that on the basis of the $Cy\alpha$ values shape II is better than shape I, but that on the basis of the collision scores it is the other way round. The reason is that II is considerably narrower than I. Shape IV too is quite narrow near the lock entrance, which explains the comparatively great number of collisions. The collision score in case of shape I, is also remarkable, because it offers most space to the entering ship.
The following conclusions can be drawn from the comparisons in table 6.3.4.2 and figure 17:

1. Narrow guiding structures offer better optical guidance than wide ones,
2. A combination of narrow and symmetrical is better than either narrow or symmetrical,
3. The favourable results of shape IV have revealed that the funnel should be narrow, especially near the lock entrance,
4. The measurement results agree quite well with the personal preferences of the test-persons,
5. If an optically well-shaped guiding structure is required, it is advisable to apply types III or IV.

6.4. Conclusions

Based on the model tests and the considerations, the following demands should be made with regard to the shaping of the guiding structures of navigation locks for push tows, locking in two directions:

1. Mechanical guidance.
   a. The maximum possible angle at which a push tow enters the lock should be small,
   b. A great distance between the points of contact when 'getting stuck',
   c. A guiding structure without acute bends is to be preferred.
   Advisable are: (1 : $\sim$ – 1 : 20, 1 : 6; asymmetrical) and (curved; symmetrical).

2. Optical guidance.
   a. A funnel-shaped guiding structure which is narrow near the lock entrance
   b. A symmetrical shape.
   Advisable are: (1 : 16, 1 : 6; symmetrical) and (curved, symmetrical).

3. Shape requirements for lock-exit.
   A divergence which is as drastic as possible.
   Advisable are: (1 : 8; symmetrical) and (curved; symmetrical),

4. Position of lay-by (waiting accomodation).

The lay-by should be situated as close to the lock entrance as possible. A transition construction, with a guiding function, must connect the lay-by with the funnel part of the guiding structure.

Advisable are: Both symmetrical and asymmetrical shapes such as e.g. (1 : ∼ − 1 : 8; asymmetrical), (1 : 8, symmetrical), (1 : ∼ − curved; asymmetrical) and (curved; symmetrical).

The asymmetrical shapes are only suitable for single waiting accomodations on one side of the lock centre line.

In conclusion, it can be said that a curved symmetrical guide has most advantages and is therefore preferable. The curved shape can be realized as a parabola, e.g. $x^2/1250$ [m] or $x^2/1000$ [m] or as a circle with a radius $R = 600$ or 500 m.

The curved shape may pass into a straight one at an angle α to the center line when $\tan \alpha = 1/6$. The straight section links the curved part of the guiding structure with the lay-by.

Other standards may apply to the guiding structures of a lock with exclusively one-way traffic. Further research on this subject is required.

7. Height of the guiding structures

7.1. General description

An important consideration when determining the height of the structures above waterlevel is their mechanical guiding function for high-riding, unloaded push barges. The structures' reach below water level should meet the mechanical guiding requirements of deep-seated, fully loaded ships.
A factor co-determining the height of the structures is their function as side-wind guards for shipping.
Yet another question is the optical effect of guiding structures of unequal height left and right of the lock center line.
These factors have been investigated and will be discussed in the following paragraphs.

7.2. Mechanical guiding

7.2.1. Height above water level

An unloaded push barge, running into a comparatively low guiding structure, will stand out over the structure for some considerable length, depending on the angle of approach. This creates several problems. For one thing, the barge's forebody may tear off parts of the guide's superstructure. Another danger is that of the barge's slanting stem forcing itself up on to the guiding structure, transferring part of its weight to it.
While this paper is being prepared (1970) a push barge is under construction whose specifications may serve as a standard for our calculations.
The forebody-plan of this barge is shown in fiugre 18. This plan was used to calculate the distance (*a*) by which the unloaded barge stands out over guiding structures of various heights. A standard draft was assumed of 0.50 m. In practice, this would be between 0.50 an 0.65 m.
The results of the calculations are given in figure 19, from which it may be concluded that a minimum height of circa 3 m. above waterlevel will be sufficient. Only extremely wide approach angles, which are unlikely to occur in practice and which are not even possible in view of available manoeuvering space might still give dangerous situations.
The above mentioned height also applies to the guiding construction in the lay-by, which is occasionally used by mooring push tows.

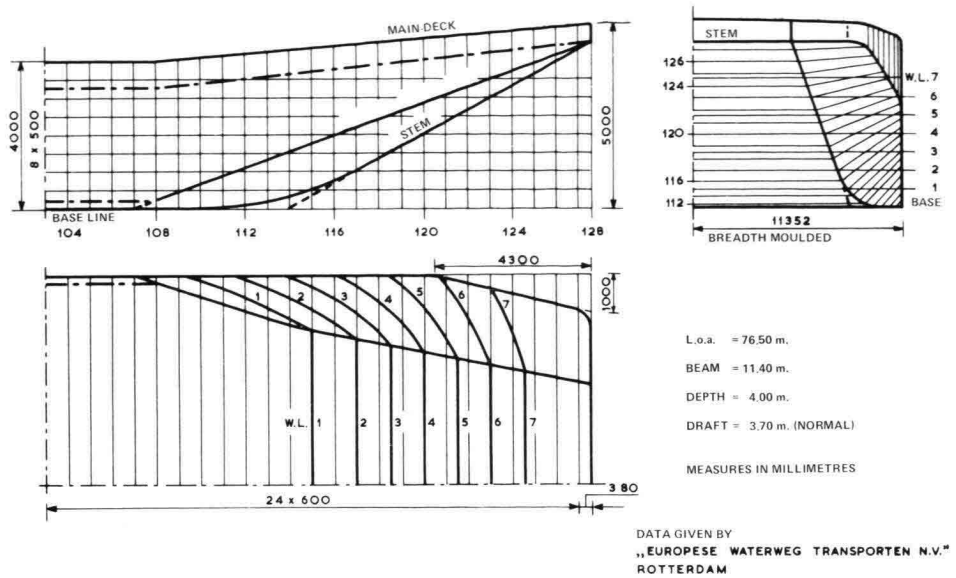

Figure 18. Plan of the forebody of the push barge 'Europe IIA'

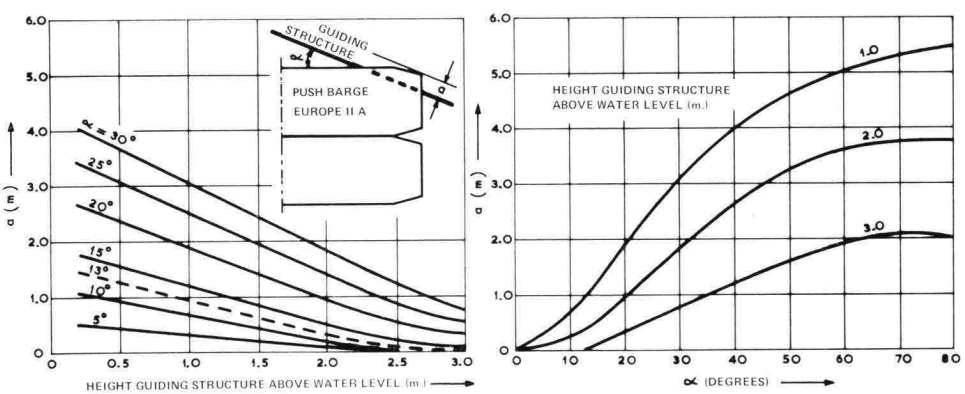

Figure 19. Distance (a) over which the push barge 'Europe IIA' sticks out over the guiding structure

7.2.2. *Reach below waterlevel*

A guide which is 'open' under water, is preferred to a completely closed wall, in connection with suction phenomena. At all times, a symmetrical solution should be striven after in the sense that the degree of perforation is about equal on either side.

The reach of the guide below waterlevel ought to have a certain value to prevent heavily loaded ships from getting stuck under the construction. Taking possible water level variations caused by long waves, into account, a minimum reach of 0.7 m. below water level will be safe enough.

7.3. Protection against side-wind

7.3.1. General description

Loaded push tows are generally insensitive to side wind. Unloaded push tows, however, combining a large lateral dry area with a minor draft, are very sensitive to wind. If the guiding structure adequately fulfils its mechanical function the entry into the lock will in general give no great problems.
Lock exit, however, may not be as easy. Owing to the fact that to resist side-wind pressure, ships have to sail obliquely in the wind. The ship then makes an angle with its steering course, the equilibrium drift angle, the size of which among other things depends on the wind-velocity and the sailing speed. When leaving the lock, however, a large push tow is forced to sail straight owing to its narrow clearance from the lock-sides. Moreover, its speed will be rather low. Model tests have shown that an unloaded push tow leaving the lock while exposed to side-wind with a force of 5 Beaufort may already get into trouble.
A push tow which is 'blown away' during the exit ends up on the lee shore, where often ships will be present on the lay-by.
A solution to the problem may be found in providing a wind-protected transition, in which the push tow can gain sufficient speed. This is also important for conventional shipping. By improving lock exit conditions, locking capacity can be substantially increased.
Obviously it is the guiding structures which have to provide the side-wind protection for the transition zone. Model tests were used to try to establish height requirements in this connection.

7.3.2. Model tests

In a wind flume of the Delft Hydraulics Laboratory, a section of which is given in figure 20, tests were carried out in order to determine the wind pattern between the entrance guides. Part of the guide, as marked in figure 21, was imitated on a scale of 1 : 25. In cross-sections I and II wind-velocity distributions were measured with the help of a screw anemometer.
The fetch for the guide was 50 m. (1250 m. prototype), which is sufficient to develop a

good velocity profile. The selected wind velocity was 15 m./s. and the direction was perpendicular to the lock centerline.
The velocity distribution is determined by the relatively sharp upper side of the otherwise closed guide, where the air stream separates. It may therefore be expected that the velocity distributions are similar for other wind velocities.
The measurement results for guide heights of 3 and 5 m. are indicated in figure 22. From this it appears that the influence of wind on ships leaving the lock is reduced considerably.
In the model of the navigation lock for push tows, navigation tests were carried out with an unloaded push tow, the dimensions of which are given in figure 23. After extensive tests with the help of electric fans, a wind pattern was generated agreeing reasonably well with the measurement results from figure 22.
The positions of the push tow leaving the lock were photographed. Propeller-speed was kept constant during the tests.
A view of the test arrangement and of the measured wind-velocity distributions between the guides is given in figures 24 and 25.
Some photographed tracks of the push tow leaving the lock are given in figure 26. With propellers running half speed and a wind with a force of 8 Beaufort, a push tow will be blown off-course while leaving the protected transition area.
The navigation tests only have a relative value. The measuring route was very short. The steering of the ship, which was done by remote control, was not conform reality and the man at the wheel knew the situation quite well.
The investigation as a whole leads to the following rough conclusions:

1. A guide with a height of 3 to 3.5 m. offers a good protection against side wind,
2. A protected transition area of a length of between 100 and 125 m. will in general be sufficient to allow an unloaded push tow of 2 × 2 barges to leave the lock safely during strong side-wind activity.

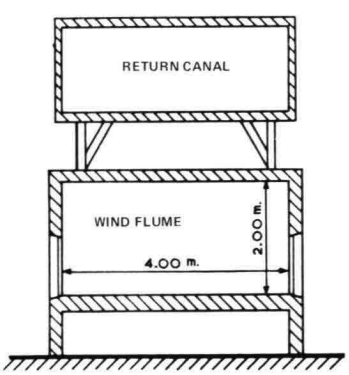

Figure 20. Cross-section of the wind flume

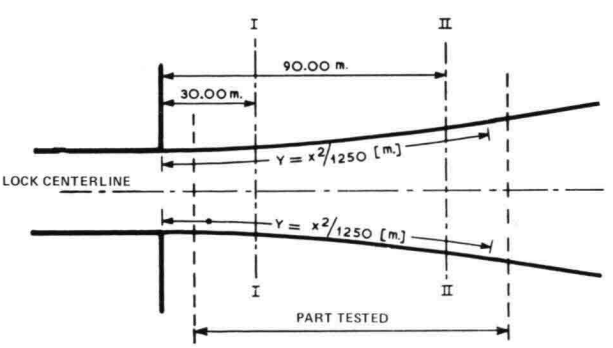

Figure 21. Plan of the guiding structure tested in wind flume

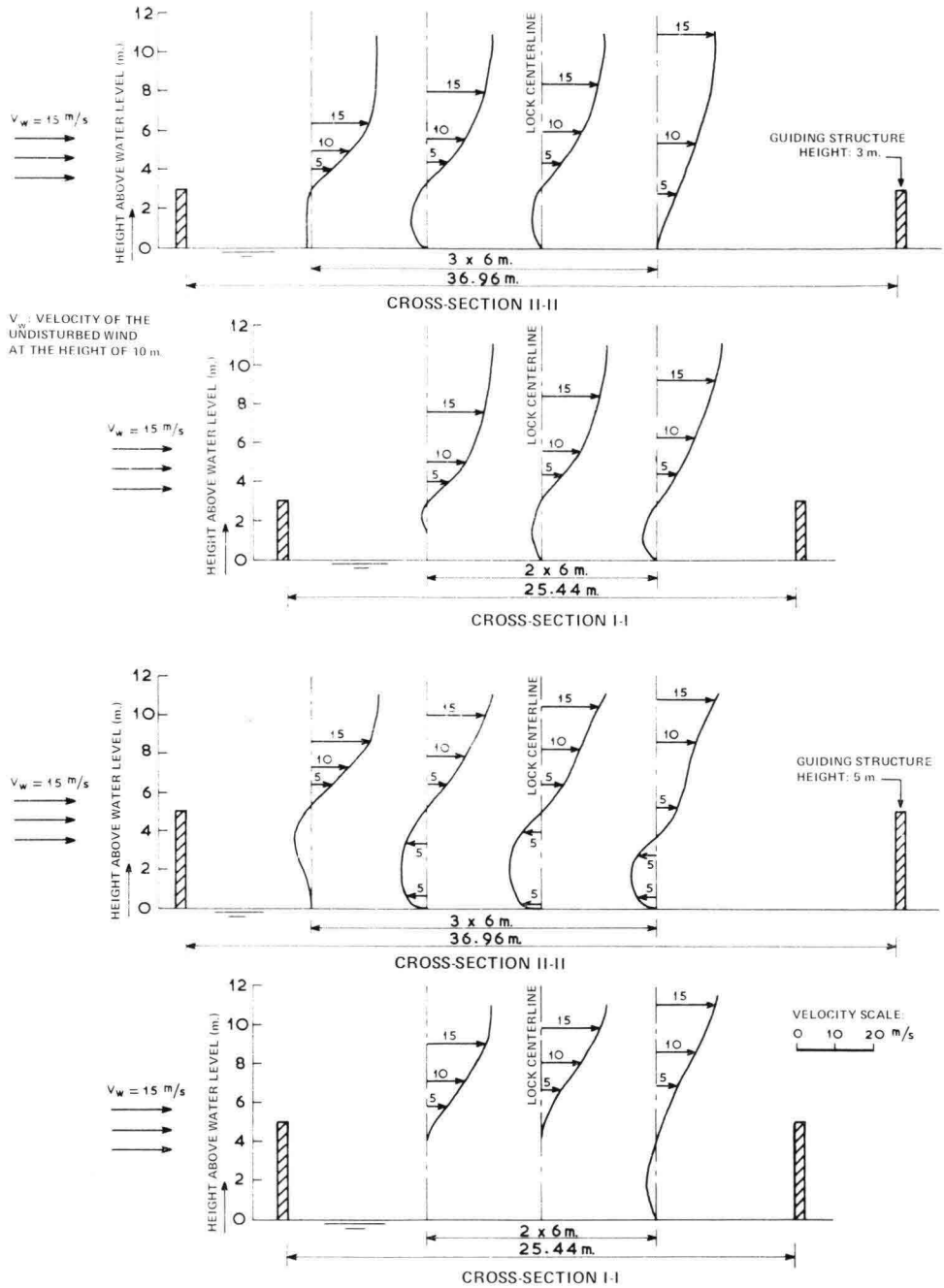

Figure 22. Wind velocity distribution between the guiding structures (wind flume tests)

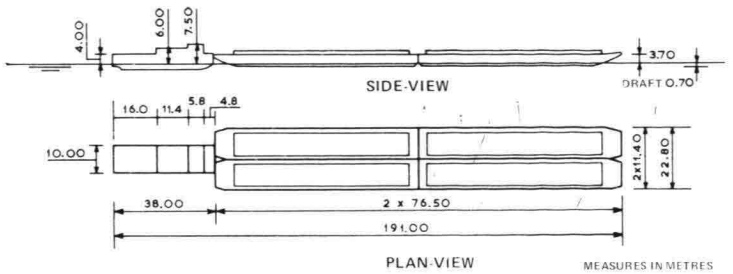

Figure 23. Unloaded push tow

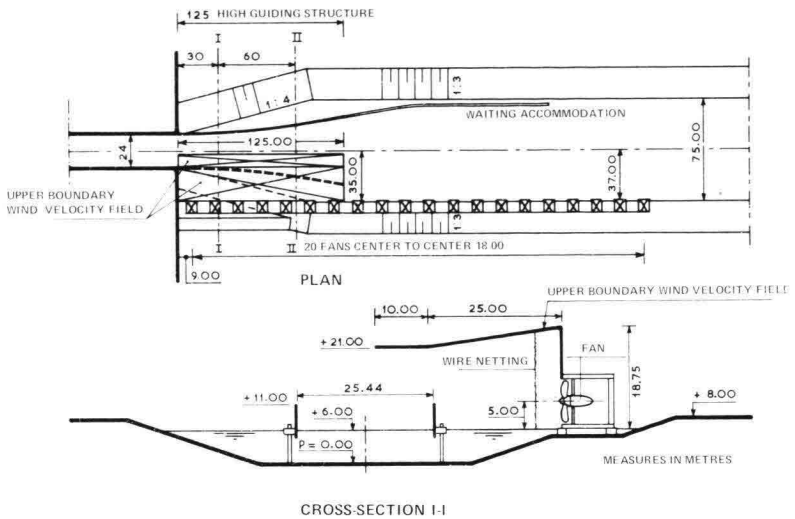

Figure 24. Test set-up in lock model

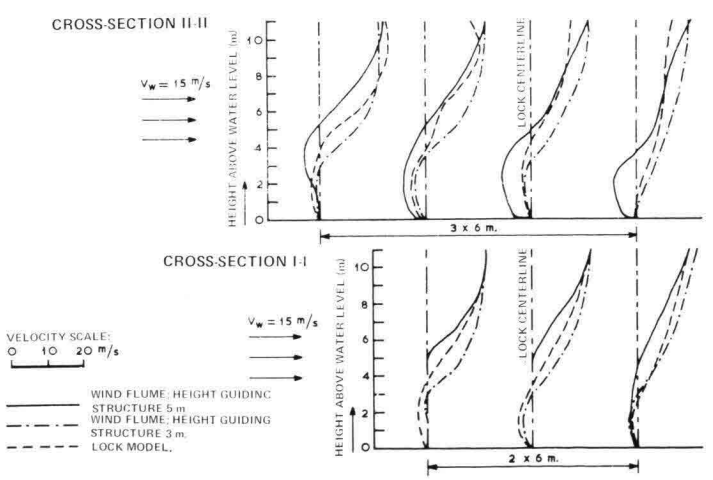

Figure 25. Comparison between wind velocity distribution in wind flume and lock model

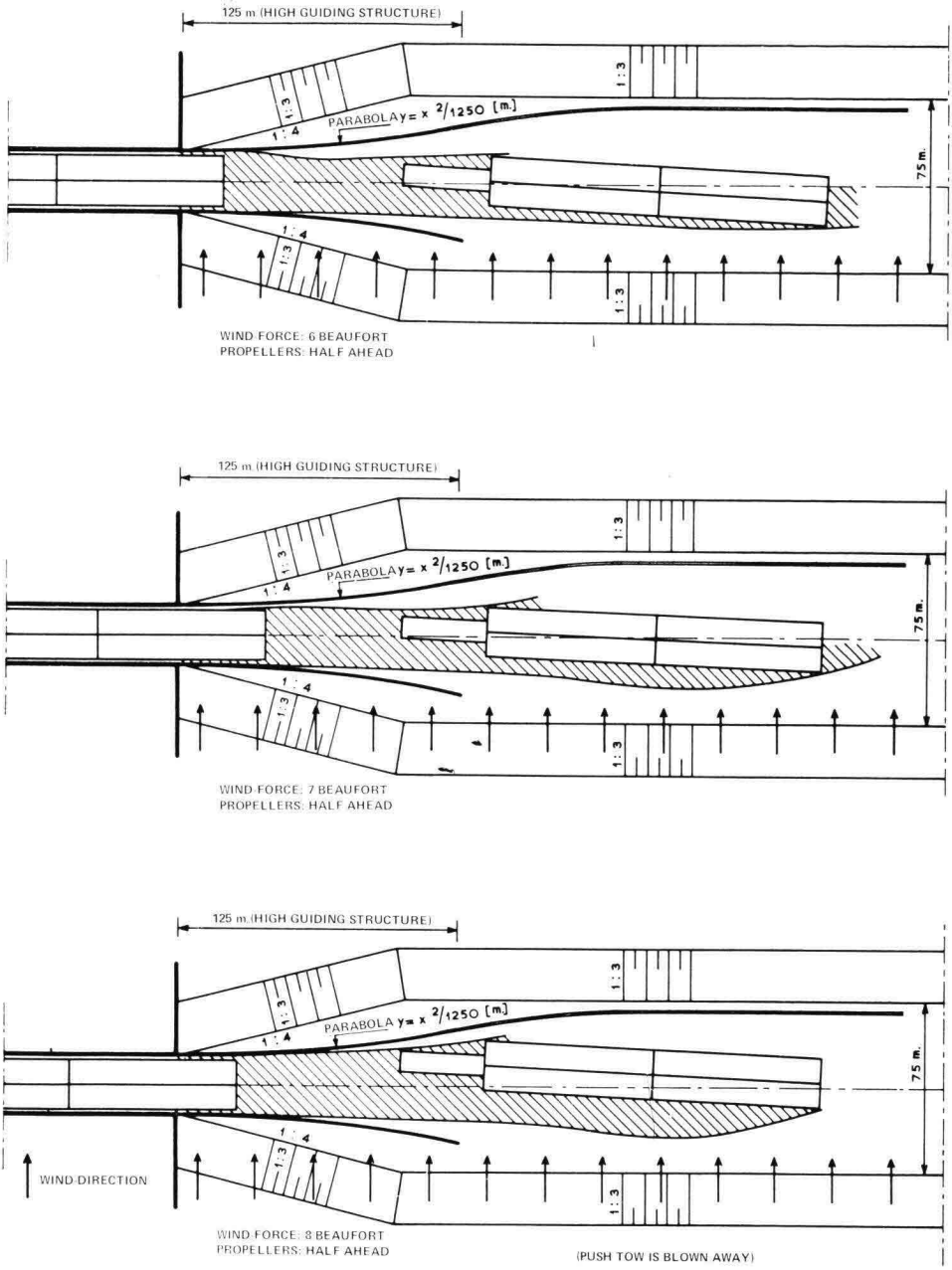

Figure 26. Width of lanes when an unloaded push tow leaves the lock exposed to side-wind

7.4. Optical guiding

7.4.1. Purpose and set-up of the investigation

In connection with the situation on the south side of the Volkerak locks (photograph 2, par. 3) the question was asked whether a slight asymmetry in the basic shape of the guiding funnel would be acceptable for optical reasons. Two circular guides were thought of, with a radius of 600 m., facing each other obliquely with a 55 m. shift between centres along the lock centre line. To find out if this asymmetrical situation and the symmetrical basic form as indicated in figure 27, would lead to a significant difference in navigational behaviour, a number of navigation tests were carried out with essentially the same set-up as the one described in paragraph 6.3.
Mistakenly, a low guide was used at the start. The basic form and the cross-sections of the symmetrical arrangement are given in figure 27. Later on the tests were repeated with a guide, which top was at level with the lock walls, so that it is possible to compare the two symmetrical arrangements, each having a different height. The low guide shows an asymmetrical shape in a vertical sense, owing to the high head wall, jutting forward.

7.4.2. Measurement results

Only a comparison between the guides indicated in figure 27 will come up for discussion here. The performances of the test persons in the two situations are compared, by taking into account the frequency of the collisions of the push tow with the guide. An entry is marked 'open' if no collission took place in the area before the foremost headwall.
In the situation with the low guide 24 entries were carried out by 8 test persons. The number of enterings was doubled for the high guide. The number of open entries and the number of collisions, specified for the starboard and portside, are given in table 7.4.2. The differences between the two guides are statistically significant.

guide	low		high	
	number	perc.	number	perc.
starboard collisions	3	12.5	10	20.8
open entries	6	25.0	28	48.4
port collisions	15	62.5	10	20.8

Table 7.4.2. Number of collisions with the guide

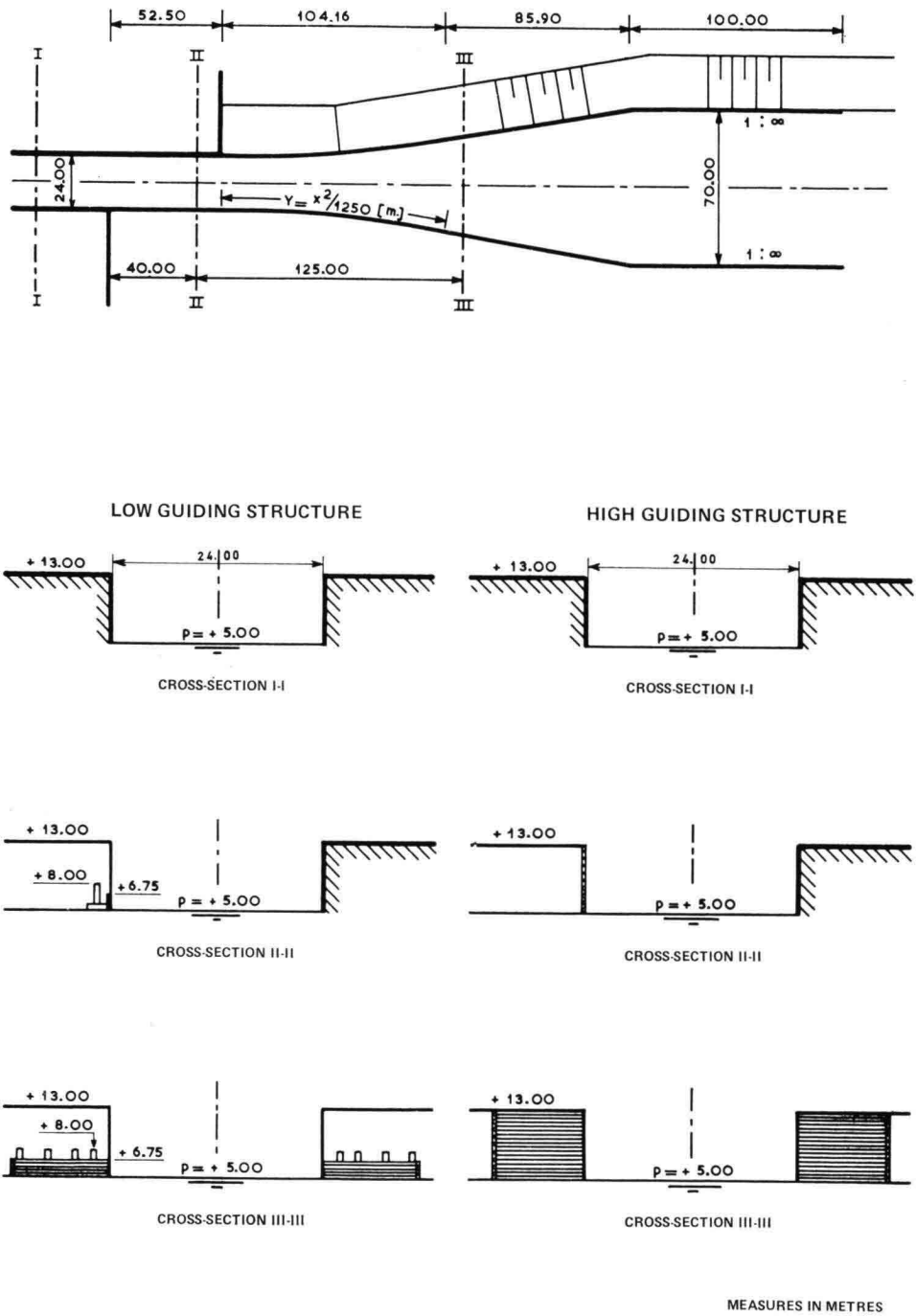

Figure 27. Plan and cross-sections of the symmeritcal guiding structures

The number of open entries is remarkebly low for the low guide, and most collisions take place on the port-side. The high guide shows a great number of open entries while the number of collisions is equally divided over both sides. From this it can be concluded that, after the elimination of the differences in height, the effect of 'wall fear' had disappeared and that optically, the guides' shape had significantly improved.

7.5. Conclusions

The conclusions as to the height of the guiding structure are summed up point by point as follows:

1. A guide height of about 3 m. above the waterlevel can, in view of safety, be considered sufficient in the case of a collision with an unloaded barge of the determining type 'Europa IIA' (figure 18),
2. It is desirable to have a minimum reach of 0.7 m. below water level. The possibility of getting stuck under the guide may be prevented in this way,
3. The establishing of a transition area, protected against side-wind, for the benefit of unloaded push tows leaving the lock, is desirable. The progress of entry and exit of conventional shipping, under bad weather conditions, can also be influenced favourably in this way,
4. Guides with a height of 3 to 3.5 m. above the waterlevel and a funnel length of 100 to 125 m. are sufficient to bring about the transition area mentioned in 3,
5. Great differences in height between the guides on both sides of the lock axis ought to be avoided, in connection with the bad optical conditions.

8. Optical guiding with the help of guiding lights

8.1. Survey

During the investigation into the shaping of the guides (paragraph 6.3.) the question was asked, wether entry manoeuvering could be improved by using a guiding system. In this connection a comparative investigation was made first, which is further indicated by its year, 1964. At a later stage, a special leading or guiding light system was tested for the south side of the Volkerak locks, where the set-up for the guiding structures is asymmetrical. This investigation is indicated 1966.

In 1964 three situations were compared:
N: no lights,
R_1: two lights in the lock centerline,
R_3: lock centerline indication with more lights.
The three situations are further indicated in figure 28. The investigation was carried out with straight guides under 1 : 8 with the lock centerline. (Paragraph 6.6.3; figure 14-1).

In 1966 too, three situations were compared:
M: no lights,
S: the two middle lights of the system being vertically above each other (one point of the lock centerline),
S_3: complete guiding light system. Its operation follows from figure 29.
The situation of the guides can be seen on photographs 2 (paragraph 3.2.) and 5 and in figure 30. This guiding system was developed by the Institute for Perception (RVO-TNO). Photograph 6 shows the configuration of the lights above the left lock chamber of the Volkerak locks, of which this Institute had a made model on a scale of 1 : 200.

8.2. Execution of the experiments

Both investigations were carried out with the help of 6 well trained test persons acting as helmsmen. In each situation each helsman sailed three times both in day time and at night. In the latter case the lock and guide were lighted (photograph 5). The 1964 tests were performed in the same way as the test regarding into the 'optical' shaping of the guides (paragraph 6.3.2.). The set-up and execution of the tests by night were,

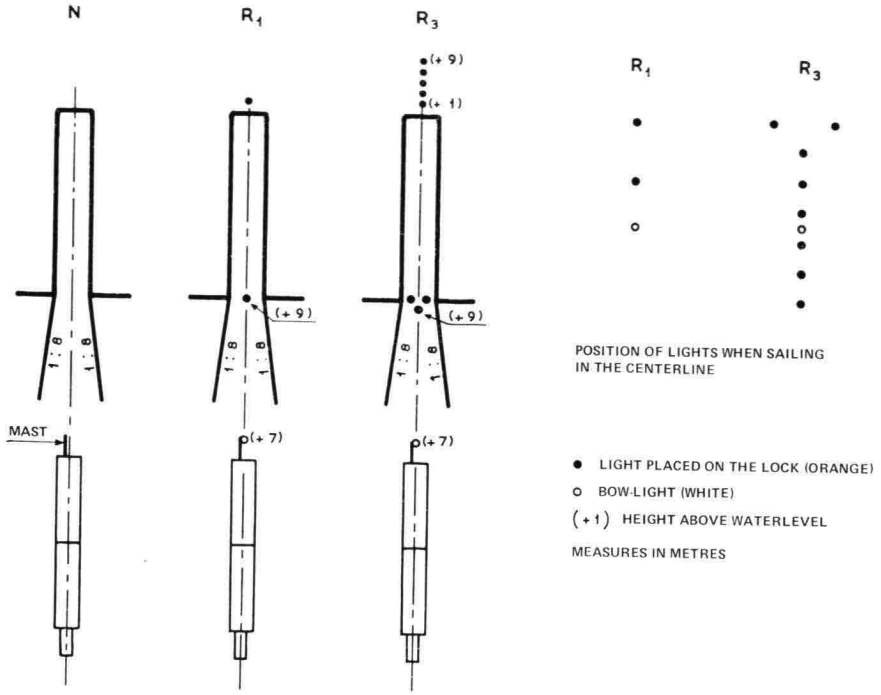

Figure 28. Position and shape of the guiding light system (1964)

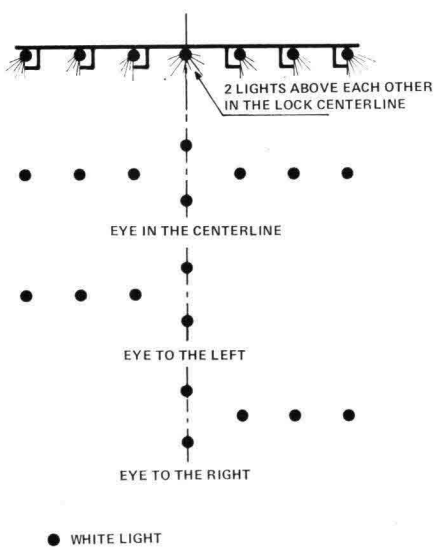

Figure 29. Construction and operation of the guiding light system (1966)

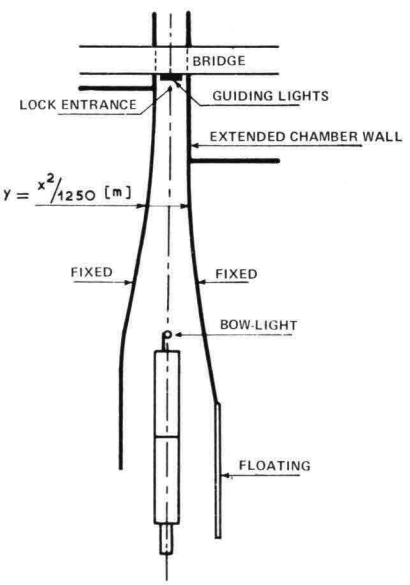

Figure 30. South-side Volkerak lock. Set-up guiding light system (1966)

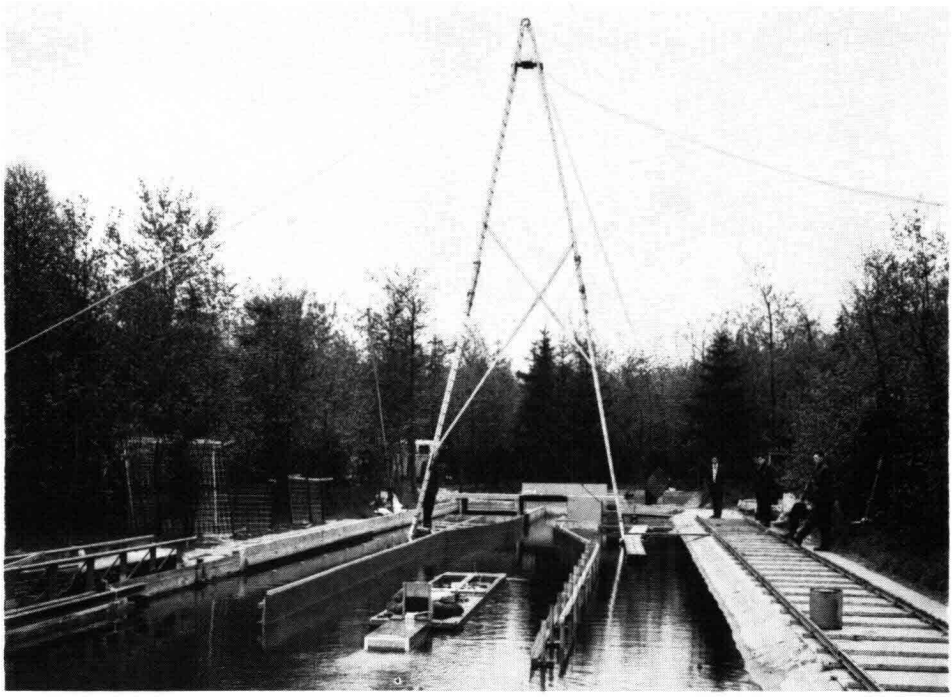

Photograph 5. Optical guidance by using a guiding light system in the Volkerak Lock model (1:25 m)

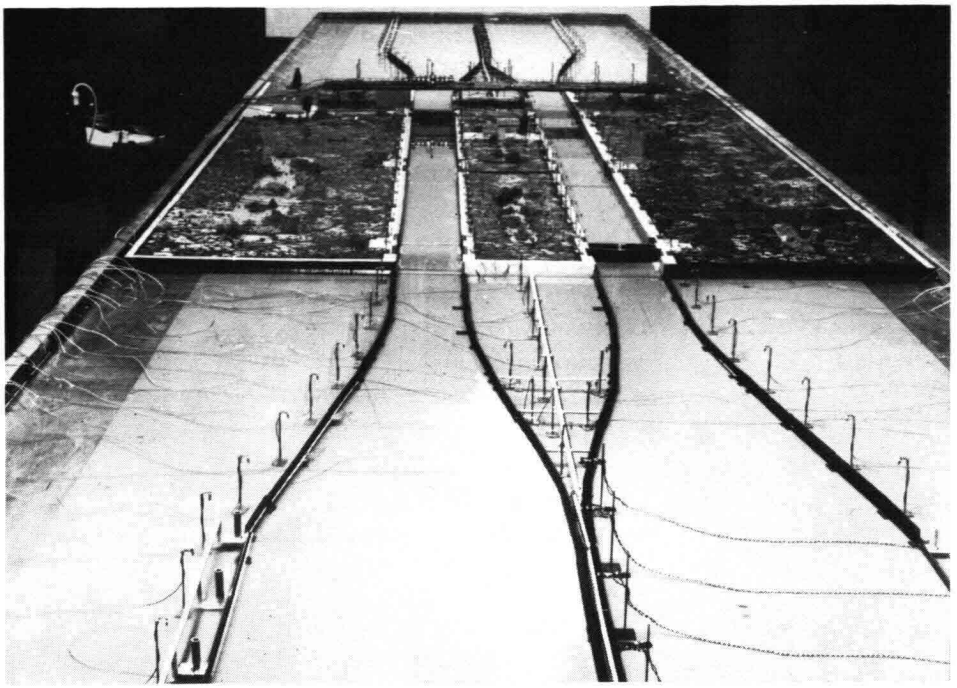

Photograph 6. Guiding light system in a model (1 : 200) of the Volkerak Locks

however, far from satisfactory. Therefore various changes were introduced for the 1966 investigation:

a. The rudder angle was continuously recorded over the latter half of the test run. The starting point was about 1000 m. from the lock entrance,
b. The position of the push tow was photographed 8 to 9 times over the last 200 m. before the lock entrance,
c. and d. are the same as in 1964.

In 1964 the bow light in situation *N* was also put out, so that the steering of the push tow took place in the dark under very unfavourable conditions. Immediately after the start the helmsman was entirely disorientated and the distance to sail was too short to restore the bad position of the push tow completely. In 1966 the bow light was lit in situation *M*, as in reality. Lock and guides were moreover better illuminated than in 1964.

For both experiments a tests scheme was used which made it possible to check the sequence and learning effects.

8.3. Processing of the test results

The results of the 1964 tests were processed in the same way as those of the guides (paragraph 6.3.3.). But the collisions with the guide were evaluated differently, for statistical reasons:

a. Open entry: 2 points,
collision $X < 1.25$ m.: 1 point,
collision $X > 1.25$ m.: 0 points.

The results of the 1966 tests were processed along the same lines as those of the 1964 tests. Some minor changes were introduced:

b. The denominator of the equation for the calculation of the qualitymark ($Cy\alpha$) for an entry, was changed to 0.01 ($\frac{1}{2}X_i + 25$), to give more weight to the positions of the push tow at greater distances from the lock,

c. The collisions are evaluated as follows:
open entry and collision at $X \leqslant 25$ m.: 2 points,
collision at 25 m. $< X \leqslant 50$ m.: 1 point,
collision at $X > 50$ m.: 0 points.

The way of scoring was different from that of 1964 owing to the much narrower 'funnel' in 1966, which causes the collisions to take place at a greater distance from the lock entrance,

d. The test persons' personal opinion was not expressed in points.

For a proper understanding of the test-results it should be borne in mind that a low $Cy\alpha$ value and a high collision score are favourable.

8.4. Results

An analysis of variance was applied to all measurement results in order to ascertain whether the various optical situations exercise a statistically significant influence on the sailing achievements. As in paragraph 6.3.4 there will be no further discussion of the analysis of variance itself.

1. 1964

In connection with the imperfections in set-up and execution, the results of the entries by night will be left out of consideration. The results of the daytime entries will now be discussed more in detail.

a. Standard deviation of the rudder angle.
The standard deviation of the rudder angle is no significant source of variance. There is however a tendency to apply somewhat greater rudder deviations in the case of guiding lights, as appears from figure 31a.

b. An impression of the differences in average sailing performances of the test-persons in the various situations can be obtained from table 8.4.1. The analysis of variance shows that the influence on $Cy\alpha$-values is yet just significant. Figure 31b shows however that the differences are very small. The practical importance must therefore be considered slight.

c. Collision score.
The avarage number of points for each test-person is indicated on table 8.4.1 for the various situations. Here too, the differences in sailing performances were significantly influenced by the optical conditions. The average values for each situation can be compared in figure 31c.

d. The test-persons appear to have no preference for situations with or without guiding systems.

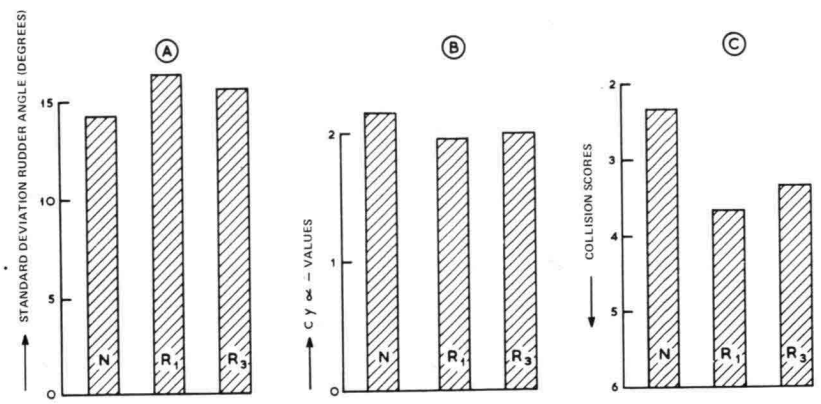

Figure 31. Average results of lock entries in 1964

2. 1966

The analysis of variance has revealed that the three situations analysed, have no singificant influence on the parameters, which were applied. There is however a significant difference between the sailing performances by day and those by night.
The average performances of the test-persons in the various situations are given in tables 8.4.2 and 8.4.3. The average values for each situation are indicated in figure 32. The test-persons had no preference for a particular situation.

8.5. Notes and conclusions

Owing to differences in design and execution, the results of 1966 cannot be directly compared with those of 1964.

No. test-persons	$Cy\alpha$			collision score		
	N	R_1	R_3	N	R_1	R_3
1	1.38	1.73	2.01	3	3	2
2	1.54	2.37	0.57	3	4	5
3	2.42	1.04	0.58	2	4	4
4	1.84	2.22	2.46	0	3	6
5	1.35	2.60	4.26	4	5	2
6	4.39	1.77	2.07	2	3	1

Table 8.4.1. Sailing performances of the test persons in 1964

No. test-persons	day			night		
	M	S	S_3	M	S	S_3
1	2.43	1.81	2.03	2.51	1.51	3.14
2	1.97	1.57	2.46	4.88	3.65	2.88
3	2.33	1.94	1.76	3.12	5.09	4.55
4	1.72	1.76	1.62	1.71	2.21	1.33
5	4.34	4.02	6.67	3.12	6.77	4.64
6	1.68	1.46	1.99	1.99	2.01	1.40

Table 8.4.2. Sailing performances ($Cy\alpha$-values) of the test-persons in 1966

No. test-persons	day			night		
	M	S	S_3	M	S	S_3
1	4	1	1	1	1	1
2	6	6	4	2	2	4
3	5	5	6	2	1	3
4	2	3	3	3	6	3
5	3	4	3	3	2	2
6	3	6	4	2	2	3

Table 8.4.3. Sailing performances (collision scores) of the test-persons in 1966

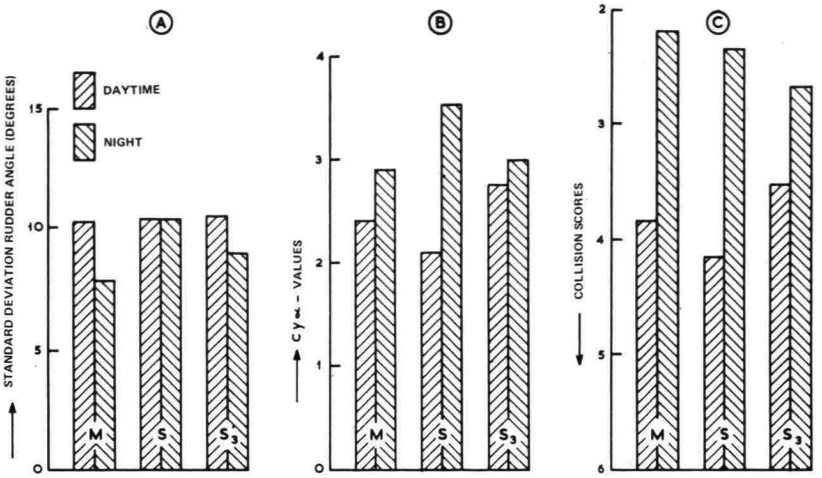

Figure 32. Average results of lock entries in 1966

From the test results of 1964 it would appear that the use of guiding light systems brings a slight improvement on sailing performances. However, the tests were carried out under circumstances in which the guides (paragraph 6.3.3, figure 14-1) should be qualified as optically inadequate. The improvement of sailing performances expressed in $Cy\alpha$-values owing to the use of a guiding light system as compared to that of an optically more favourable guiding structure is shown in figure 33. From this it is clear that the effect of the guiding light system might have been nil if a guiding structure with better optical qualities had been used along with the lights.

The experiment carried out in 1966 led to the conclusion that the sailing performance of a helmsman steering a large pushtow towards the lock entrance is hardly influenced by the use of any, however effective, guiding light system.

In conclusion, it may be said that the use of guiding structures with good optical qualities will render te additional use of guiding light systems rather irrelevant to push tow crews maneuvering towards the lock entrance.

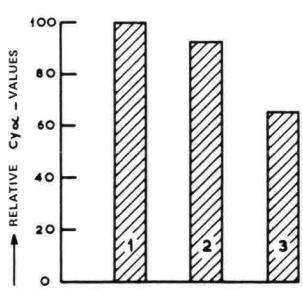

NO	GUIDING STRUCTURE	GUIDING LIGHT SYSTEM
1	I (1 : 8)	NONE
2	I (1 : 8)	R_3
3	PARABOLA	NONE

Figure 33. Improvement of entry results by applying a guiding light system or an optically more favourable guiding structure

9. Experiences from the prototype

9.1. Volkerak locks

The push tow used for the entry tests had a reduced draft (see paragraph 4.2), so that there is little sense in comparing the measurement results with those of the model tests. A total of 8 entries were carried out under favourable weather conditions. In 4 cases there were collisions with the guide before the bow had passed the lock entrance. The influence of bank suction may have played a part here. The angle under which the collision took place was very small in all cases, so that the collisions were rather sliding movements along the guide than clearly perceptible collisions, in spite of the high sailing speed.
During the entries small rudder angles were applied. Only quite close to the lock entrance the deflections became greater.
The applied sailing speeds turned out much higher than was expected at first. Apart from the expert skill and experience of the push tow captain this could point to the crew's confidence in the quality of the shaping and the construction of the guides. In one case – entry No. 5 – the waiting accomodation on the south side was chosen as the starting-point. Occasionally touching the guide, the push tow sailed into the lock without any difficulty.
The entries No. 2 and 5 are represented in figure 34. In table 9.1 a survey is given of the entries.

Run No.	1	2	3	4	5	6	7	8
Waterdepth lock approach (m.)	6.90	6.65	6.50	6.85	7.70	8.65	8.80	8.90
Entry speed (m./s.)	1.40	1.70	1.70	1.90	1.95	2.00	2.05	2.05
Collision with guide	–	port	port	port	–	–	–	star-board

Table 9.1. Free entries of the Volkerak locks

9.2. Hartel lock

Five free entries with a fully loaded push tow were carried out. The captain was the same as the one employed for the Volkerak experiments.

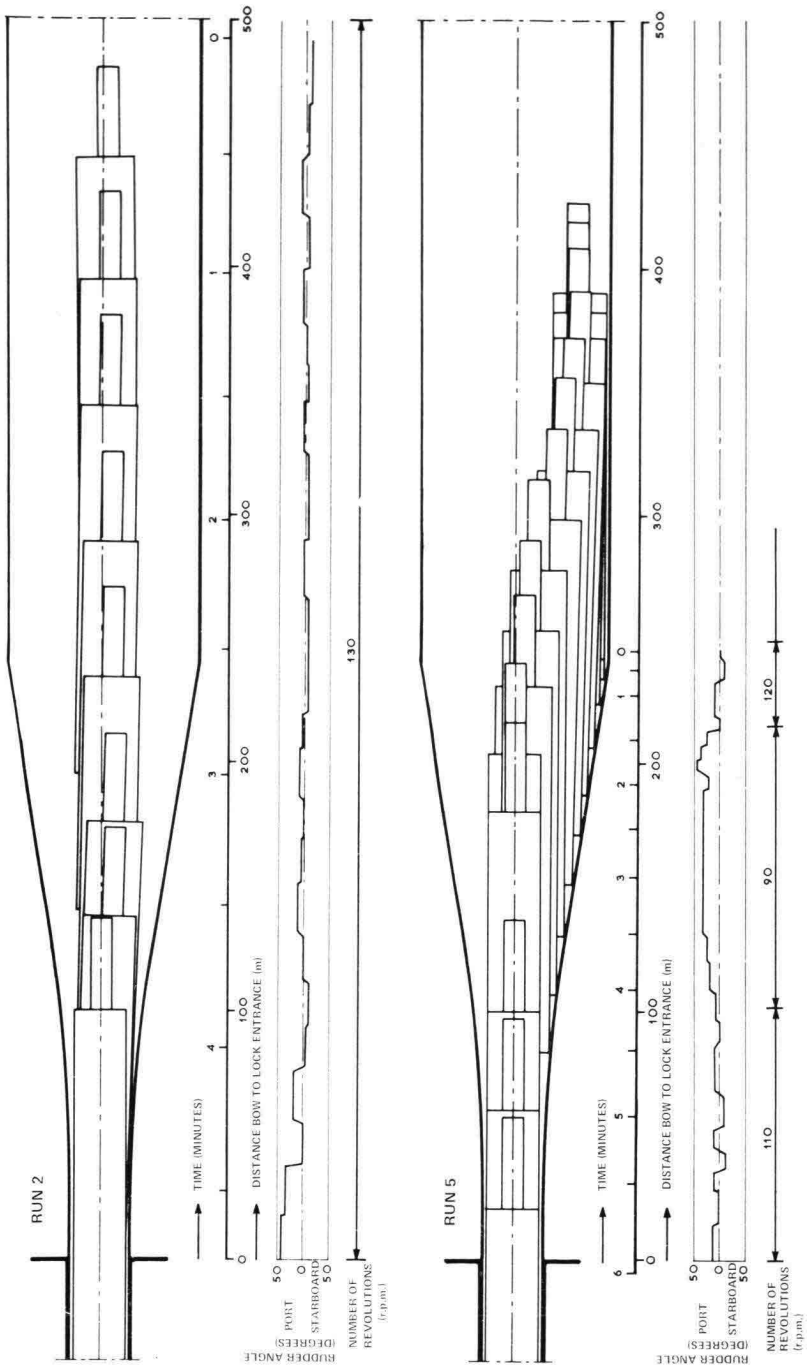

Figure 34. Entry manoeuvres in the lock approach of the Volkerak Locks

Photograph 7. Push tow in the northern lockapproach of the Volkerak Locks

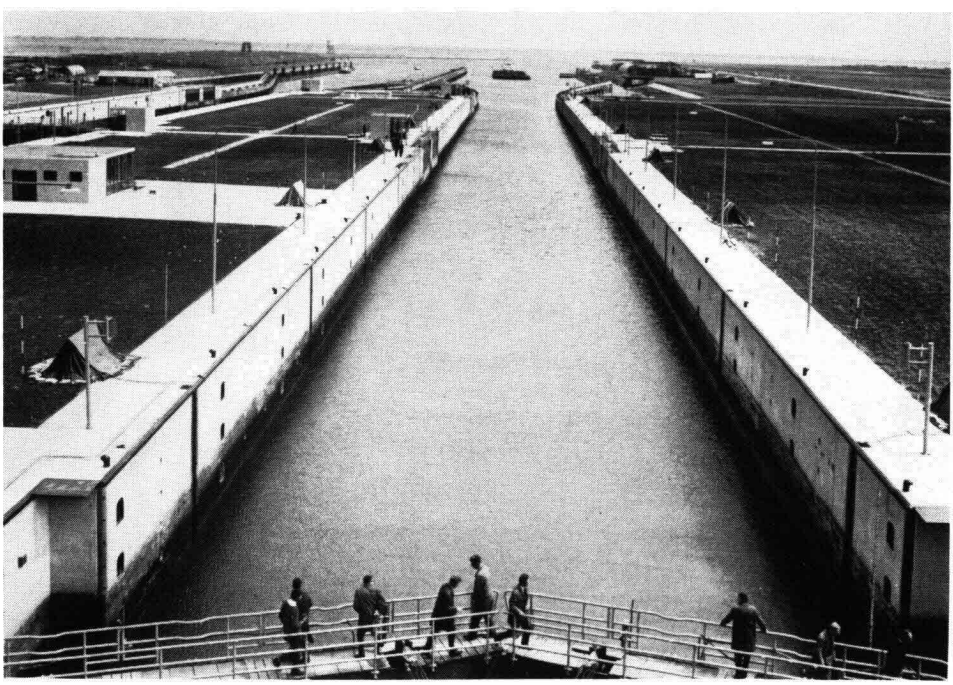

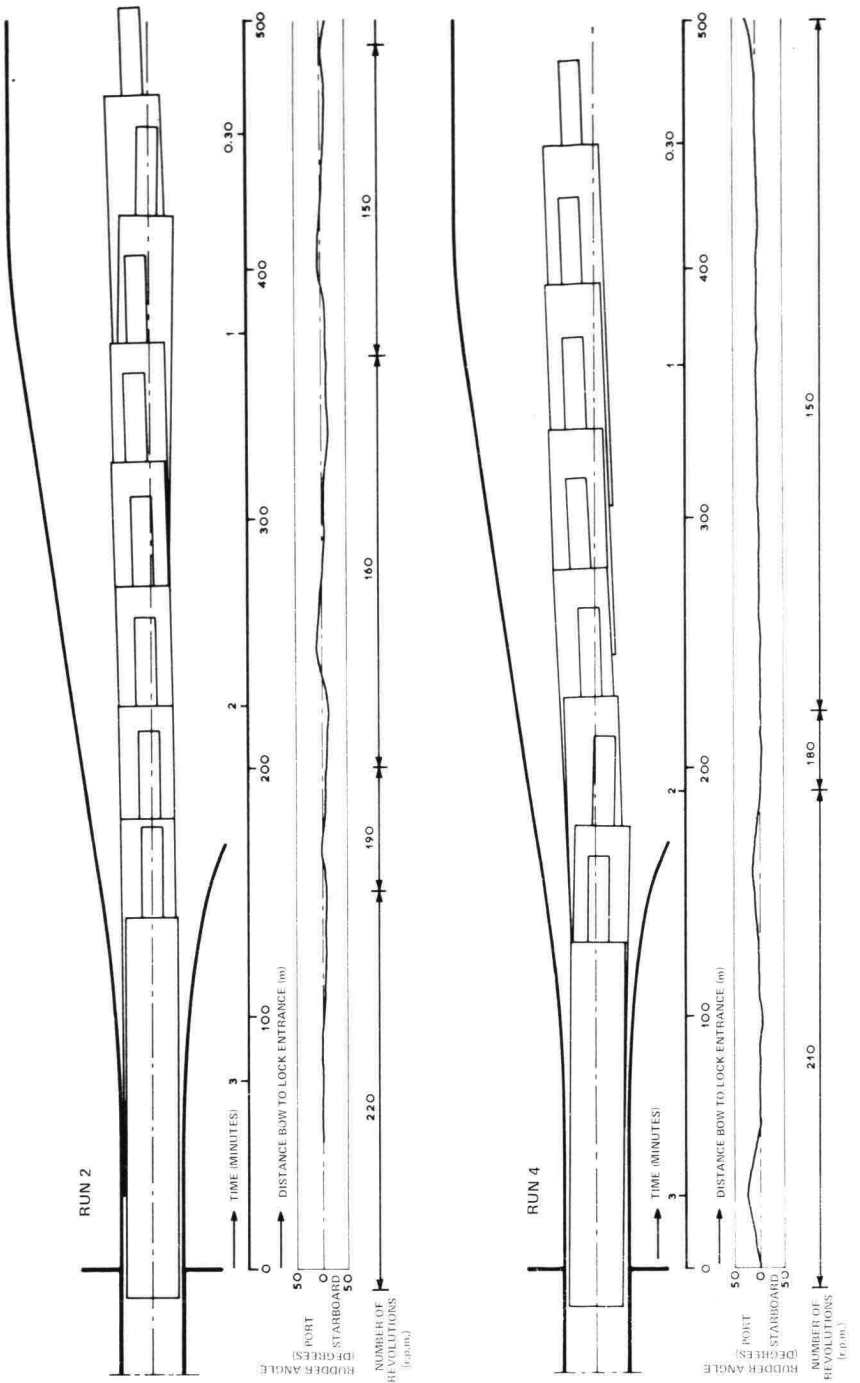

Figure 35. Entry manoeuvres in the lock approach of the Hartel Lock

Here too the entry speed was very high. Still there were no collisions with the guides. For each entry the quality-mark $Cy\alpha$ was computed in accordance with paragraph 6.3. As the entry speed was roughly twice that of the model in the 'optical tests', $Cy\alpha$ was calculated over the last 90 m. (the same distance as that used in the model) and the last 180 m. (about the same sailing time as in the model) towards the lock entrance. But a comparison with the results of the model is only of relative value owing to the difference in test-conditions and persons.
The entries No. 2 and 4 are shown in figure 35. The sailing performances are summed up in table 9.2. The standard deviation of the rudder angle was calculated over a distance of 550 m. towards the lock entrance.

Run No.	1	2	3	4	5	average
Waterdepth lock approach (m.)	5.25	5.05	5.30	5.90	6.35	–
Entry speed (m./s.)	1.80	1.90	2.10	2.30	2.05	2.05
Collision with guides	none	none	none	none	none	none
$Cy\alpha$ (over 90 m.)	0.77	2.00	0.72	2.29	2.65	1.68
$Cy\alpha$ (over 180 m.)	0.79	1.40	1.16	2.57	2.34	1.65
Standard deviation rudder angle (degrees)	8.7	3.8	6.1	7.1	11.4	7.4

Table 9.2. Survey sailing performances entry tests Hartel lock

The sailing performances are of a high level. There are no collisions with the guide, the average quality marks are low and the rudder angles applied are small. A comparison with the results of the model, obtained when testing the optical qualities of guides (paragraph 6.3), only revealed, that in the situations III and IV (figure 14), the performances were on the average quite good. The average $Cy\alpha$ values are 1.59 and 1.74 respectively, which is about the same as the prototype values. But the number of open entries in the model was only 40 to 50% of the total number.

9.3. Moselle locks

The Moselle locks have a width of 12 m. and are among other things used by push tows of 172 × 11.40 × 1.50 m^3. (formation 1 × 1). Both in the upstream and downstream sections a straight guide-wall, lying in a direct line with the chamber wall, was applied. The opposite wall leads away from the lock entrance, under a 1 : 4 angle with the lock axis until a lock approach-width of 30 m. is reached. From this point the wall continues parallel to the lock axis. In the upstream section the height of the guide wall is about 1 m. above the water-level.

Traffic on the river Moselle is not very intensive.
The experiences with the guides can be summed up as follows:

1. A straight wall is quite favourable for the entry of push tows approaching a free lock. The push tow moves into the lock with its bow sliding along the wall. But the entry speed used is rather low.
2. If the lock is not free, the push tow should wait at a distance of about 400 m., from the lock entrance, alongside a row of dolphins in a direct line with the extended lock wall. This great distance might seriously reduce the locking capacity, in case of heavy traffic.
3. If the push tow moors at the waiting accomodation across the straight guide-wall, the entry may take about 20 minutes after the lock has been cleared. During the Volkerak tests an entry from the waiting accomodation took about 10 minutes (entry No. 5).
4. The guiding capacity of the wall under a 1 : 4 angle with the lock axis is insufficient, also for conventional shipping.
5. A loaded push tow leaving the lock has some difficulty in clearing the straight guide-wall. Many push tows stop and reverse to get clear.
6. The height of the guide-wall above waterlevel proves insufficient for unloaded push tows colliding into it at a comparatively wide angle. A height of about 3 m. is considered for future lock guiding walls.

10. Design rules for guides of navigation locks for push tows

General demands can be made on the shaping of guides and beside that specific demands in connection with one-way or two-way traffic.

General requirements

1. For safety reasons, and to allow for higher sailing speeds, a funnel type guide is required for the entry side.
2. To prevent push tows from getting stuck in the lock entrance and to minimize the danger of collisions with the open doors or with the entrance guide itself, the guide should run parallel or near-parallel to the lock axis where it approaches the lock chamber.
3. At a greater distance from the lock entrance the maximum deviation of the entrance guide can be put at about 1 : 6 to the lock center line.
4. The navigable width at the beginning of the guides should be roughly 35 to 40 meters, considering the 'funnel function'. This entails minimum lengths of 70 to 110 m. for the various shapes.
5. The height of the guides above the water should be at least 3 m. in view of the mechanical guiding of unloaded push tows.
6. The height mentioned in point 5 is, at the same time, sufficient to protect unloaded ships against side-wind. For side-wind protection, a length of 100 to 125 m. is required.
7. In connection with suction phenomena, an entrance guide which is 'open' under water is preferred to a closed one. However, a symmetrical solution should be sought in the sense that the degree of 'openess' is about the same on either side of the lock axis. Two closed walls are better than one open and one closed wall opposite each other.
8. Guides ought to reach at least 0.7 m. below the waterlevel in order to avoid vessels getting stuck under the guide.
9. An uninterupted construction with a guiding function, between waiting accommodation and guide, is urgently recommended.
10. Optically effective guiding structures should include the following features:
    a. Symmetrical positioning with respect to the lock axis,
    b. A slight divergence from the lock entrance (e.g. 1 : 16 or less),
    c. A clearly perceptible funnel shape,
    d. Similarity in height on both sides.

Specific requirements for two-way traffic

11. Considering the manoeuvring space required for the ships leaving the lock and the location of the waiting accommodation, diverging guides are necessary.
12. Effective mechanical guidance is ensured by applying a curved shape, passing at one end into the chamber wall without a kink and at the other end passing into a straight line, also without a kink with a 1 : 6 deviation from the lock center line.
13. A straight guide, in a direct line with the chamber wall, will seriously reduce locking capacity.
14. In connection with the push tows entering 'freely' a favourable optical shape is desired.

Specific requirements for one-way traffic

15. The use of a straight guide in a direct line with the chamber wall is possible in principle. But there has as yet not been sufficient evidence of such a shape having a favourable influence on the locking capacity. Objections against this shape are:
    a. A strongly delaying influence on entry and exit manoeuvering in case of incidental two-way traffic,
    b. Disruption of a current trend towards standardisation of guide shapes.

III The behaviour of push tows entering and leaving the lock, and the accompanying hydraulic phenomena

11. Phenomena during the lock entry and exit

11.1. Sailing speed and natural limiting speed

A ship in motion causes a water movement around its hull as the water replaced by the bow moves to the stern to fill up the wake. This water movement, the return current, is attended by a drop in the waterlevel as a result of the loss in the velocity head.
When there is a uniform sailing speed in a prismatic canal, the waterflow is steady with respect to the ship. This waterflow is given, in outline, in figure 36.
The drop in waterlevel and the return current can be roughly calculated with the help of the following equations drawn up by KREY [lit. 3].

$$VF = (V + u)(F - f - B \cdot \Delta h) \qquad \text{(condition for continuity)}$$

$$\frac{V^2}{2g} = \left(\frac{V + u}{2g}\right)^2 - \Delta h \qquad \text{(equation of motion)}$$

The explanation of the symbols used is given in figure 36 and paragraph 17.
From these equations SCHIJF [lit. 4] decuded the existence of the natural limiting speed. This is the sailing speed at which the discharge V.F reaches a maximum value while at the same time, no water is forced upwards by the ship. The limiting speed, V_L, is given in figure 37 as a function of the relation f/F. The equation for the limiting speed is as follows:

$$1 - \frac{f}{F} + \frac{V_L^2}{2gh} - \frac{3}{2}\sqrt[3]{\frac{V_L^2}{gh}} = 0$$

It is not possible for normal inland ships or push tows to break the limiting speed in a prismatic canal. The limiting speed however, may be exceeded for a short period, in the case of a sudden narrowing of the cross-section. This happens for instance if a ship enters a comparatively narrow lock at high speed.
The limiting speeds applying to two types of push tows (paragraph 2.1, figure 6) in the lock approach and the lock-chamber of the lock model (paragraph 3.1, figure 7), are given in figure 38. This also indicates the sailing speeds reached in the given cross-section by the pusher tug 'Vulcaan I' and a four-barge formation, at various propeller speeds.

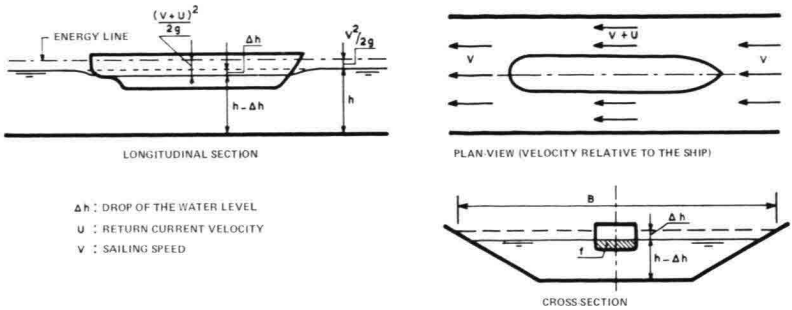

Figure 36. Flow relative to a ship sailing in a canal

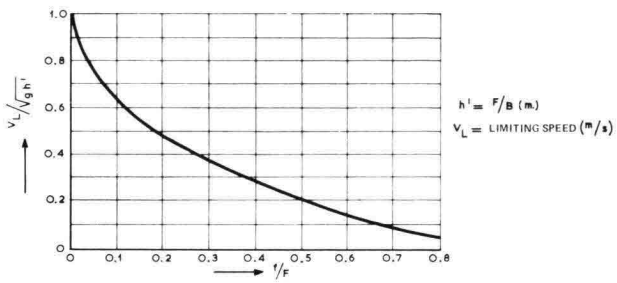

Figure 37. Limiting speed as the function of f/F

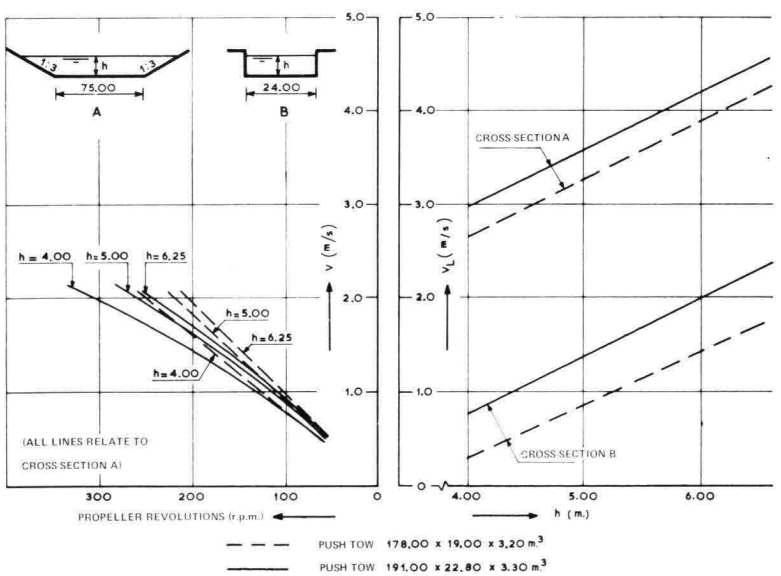

Figure 38. Sailing speed and limiting speed

11.2. Phenomena during entry

The sailing speed of a push tow entering the lock from a comparatively wide lock approach will in many cases be higher than the natural limiting speed in the lock chamber. The maximum possible return current discharge is then smaller than the quantity of water to be removed. The surplus is raised in front of the bow. This has the following consequences:

1. A positive translatory wave is generated, which runs into the lock-chamber ahead of the ship,
2. The return current velocity is temporarily forced up owing to the increased fall,
3. The generated wave delays the ship's entry,
4. The shortage of water flowing back causes a negative translatory wave which enters the lock approach.

The progress of the lock entry is further determined by the ship's resistance which has strongly increased and so retards entry-speed and by the forward and backward motion of the translatory wave owing to which the entry gets an irregular character. If the entry speed is lower than the natural limiting speed, a translatory wave, though a small one, is also raised because the adjustment of the return current to the narrower cross-section of the lock chamber is subject to a certain 'inertia', owing to which a surplus arises in front of the bow.

To evaluate these phenomena a systematical investigation was made. The results are important for the design or the use of navigation locks for push tows. Special attention was paid to the following subjects:

a. The progress and the height of the translatory waves generated,
b. The influence of the translatory waves on the ships moored in the chamber,
c. The progress of the sailing speed in the chamber,
d. The flow velocities over the apron near the lock entrance.

11.3. Phenomena during exit

For a loaded push tow the natural limiting speed in the lock chamber is low, so that lock exit may take quite some time, especially in small water depths. The sailing speed remains low as long as part of the barge-formation is still between the lock walls.
When starting up the push tow in the lock chamber, attention should be paid to the following phenomena, in view of the great engine power of pusher tugs:

1. If the propellers are revved up too quickly a perceptible translatory wave is generated, which can be dangerous for the ships lying in the lock chamber behind the push tow,

2. When applying a high number of revolutions a strong propeller current arises behind the pusher tug. This may trouble other ships, particularly the smaller ones.

A systematic investigation was also made of lock-exit manoeuvering covering the following points:

a. The total exit time of push tows,
b. The influence of the starting of pusher tug's propellers on other ships lying behind it,
c. The propeller flow pattern.

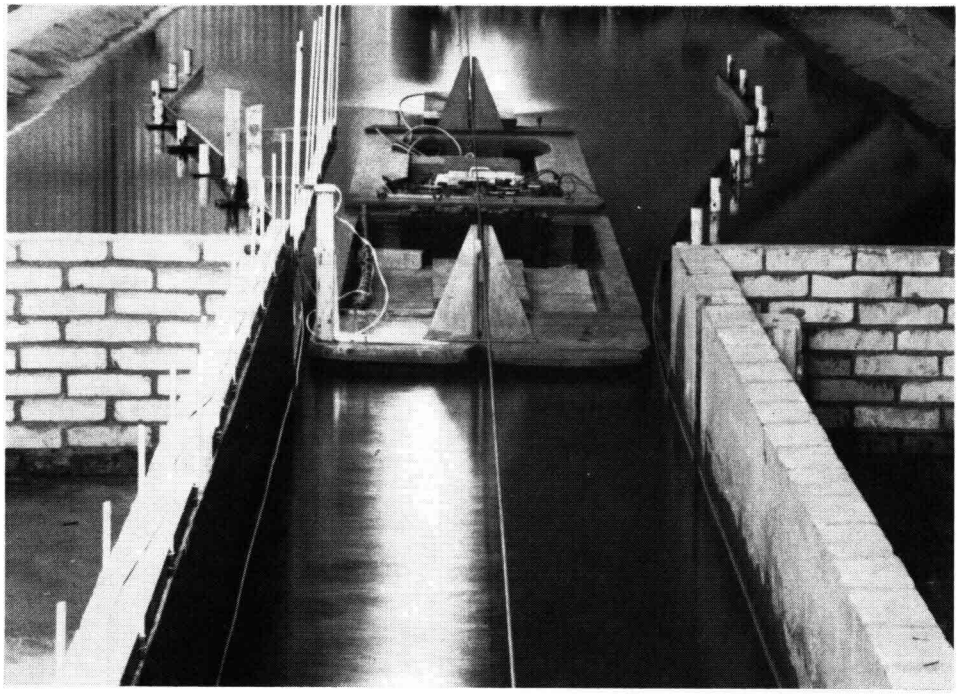

Photograph 8. Guidance of push tows in the indoor model

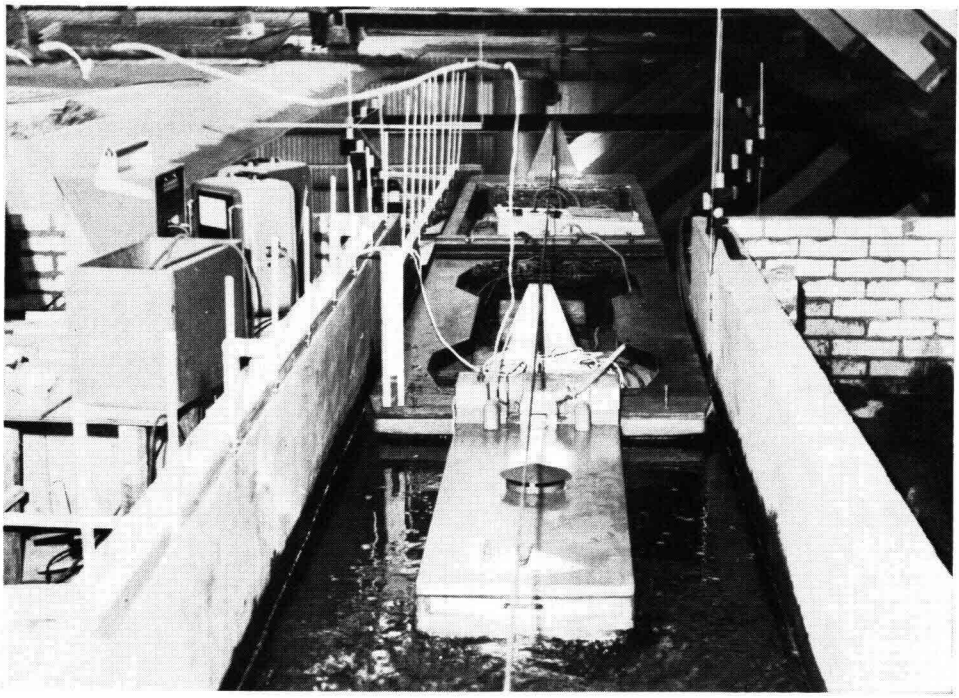

12. Progress of lock entry

12.1. Survey

A ship entering a comparitively narrow lock causes a translatory wave. This not only considerably retards lock-entry, but also makes it irregular, because of continuing backward and forward motions of the wave.
The ship's jerky progress with its sudden retardations and accelerations may trap the ship's crew into faulty reactions.
In order to gain an insight into the progress and the duration of the entry a great number of experiments were made in the lock model. Conditions were varied systematically.
The results of the tests with push tows in the Volkerak locks and the Hartel lock also give a good insight into the nature of the entry as it takes place in practice. On some points a comparison with the results of the model is possible.

12.2. Model tests

12.2.1. Execution of the tests

The tests were carried out in the indoor-model (figure 7). The dimensions of the ships used can be read from table 12.2.1. and figure 6.

ship	main dimensions	f (m^2.)
push tow (large)	191 × 22.80 × 3.30 m^3.	75.0
push tow (small)	178 × 19.00 × 3.20 m^3.	60.8
push tow	267.5 × 22.80 × 3.30 m^3.	75.0
motor vessel	80 × 9.50 × 2.50 m^3.	23.7

Table 12.2.1. Main dimensions model ships used

The longest push tow and the motor vessel were only used incidently.
The waterdepth above the lock floor (h), the length of the lock (L) and the entry speed (V_o) were varied. There were tests on a lock both with and without sills (height of the sill = D).

With only a few exceptions, the number of propeller revolutions was kept constant and the rudders were fixed in middle position. The model ships were conducted along a cable, strung over the model, in the lock axis, as indicated on photograph 8. In this way the ships were kept clear of the chamber wall during entry, to prevent any irregularities in sailing speed.
The progress of the sailing speed was measured every 12.5 m. by means of a time-registration.

12.2.2. Progress of the entry speed

The number of propeller revolutions that had to be established in order to get the uniform sailing speed desired in the lock approach, is indicated in figure 39.
The general nature of a lock entry appears from figure 40. During the first part of the entry the sailing speed strongly decreases owing to the ship's increasing resistance as a result of the narrowing cross-section. An extra delaying force is caused by the generated wave. A further delay occurs when the translatory wave, passes the ship after reflection against the closed gates.
The movement of the ship is accelerated after the positive wave, having been reflected against the open lock entrance, is changed into a negative wave, as a result of which the waterlevel in front of the ship becomes lower than that in its rear. This is why in some cases, a sailing speed is reached, which for a short period, is higher than the natural limiting speed. The influence of the wave-action on the progress of the sailing speed can also be seen in figures 48 and 49 (paragraph 13.1.2).
The progress of the entry speed at various waterdepths for a lock with a flat floor, is given in figure 41.
In figure 42 the entries of various model ships were compared.
Finally in figure 43 the progress of entry at various sill-heights is given. It appears that sills, particularly high ones, have a strongly delaying influence, and are therefore disadvantageous to the locking capacity.

12.2.3. Duration of entry

The time needed by both a large and a small push tow from the moment when the bow passes the lock entrance, to sail into the lock until the stern of the pusher tug has proceeded 25 m. into the lock, is indicated in figure 44 for various conditions. The measurement results show that the duration of entry is hardly, if at all, influenced by a difference in lock length.
The propeller speed was kept constant, during the tests except for one series, where an initial speed of 1.0 m./s. was applied, and where the number of revolutions was increased, at the moment when the front of the reflected wave passed the bow of the

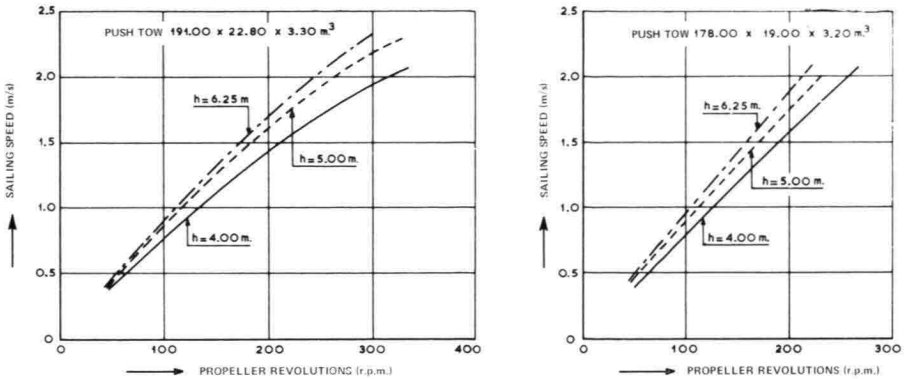

Figure 39. Sailing speed in the lock approach as a function of the number of revolutions

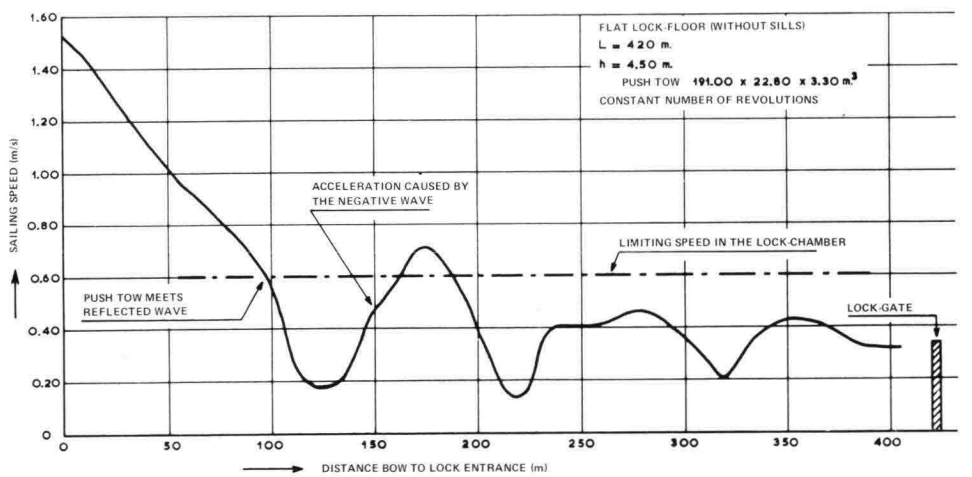

Figure 40. Sailing speed of the push tow in the lock-chamber during entry

barge formation. As a result, the entry took place just as quickly as if an initial speed of 2.0 m./s. had been applied at constant propeller speed.
Table 12.2.3. compares the durations of the entries, as defined above, as measured in locks with sills, to those found for flat-floor locks.

Push tow	h	V_o	Duration of entry (min) for:		
	(m.)	(m./s.)	D = 0 m.	D = 0.50 m.	D = 1.25 m.
191 × 22.80 × 3.30 m³.	4.50	1.5	8.0	9.6	–
191 × 22.80 × 3.30 m³.	5.00	1.5	5.7	–	–
191 × 22.80 × 3.30 m³.	5.50	1.5	4.6	4.9	6.6
191 × 22.80 × 3.30 m³.	6.25	1.5	4.0	–	5.7

Table 12.2.3. Duration of entry for a lock with or without sills at constant propeller speed

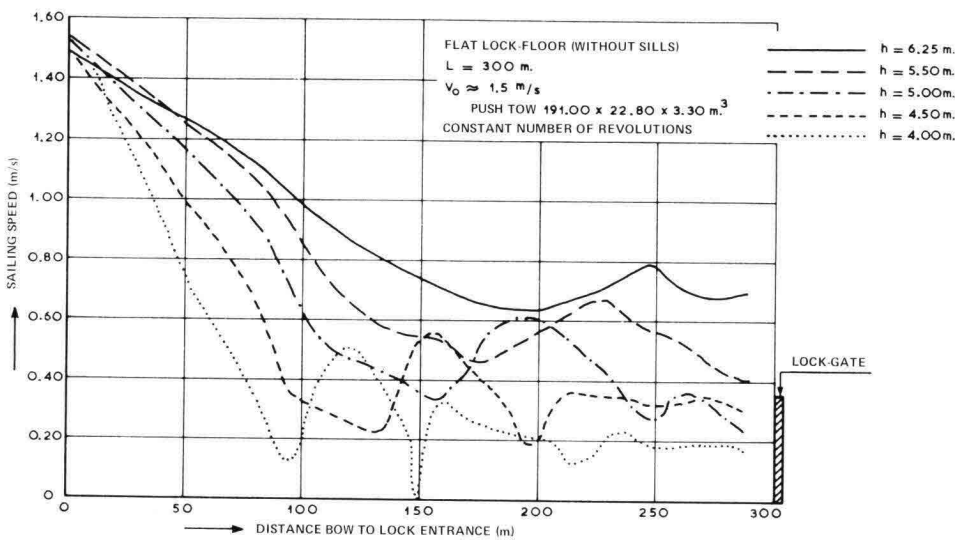

Figure 41. Sailing speed of the push tow in the lock during entry at various waterdepths

12.3. Entries into the Volkerak locks and the Hartel lock

12.3.1. Progress of the sailing speed

The full scale tests were carried out at various waterdepths and different initial speeds (V_o). The number of propeller-revolutions was varied at will by the captain of the push tow. During most entries the formation hit the lock chamber wall at various points, without being perceptibly slowed down.
The progress of two entries into the Volkerak locks and all entries into the Hartel lock are given in figures 45 and 46.

12.3.2. Duration of entry

The duration of entry as defined in paragraph 12.2.3. (see also figure 44), is given in tables 12.3.2.1 and. 12.3.2.2. for the various runs. The times for the Hartel lock are rough as a result of the general set-up of the measurements.

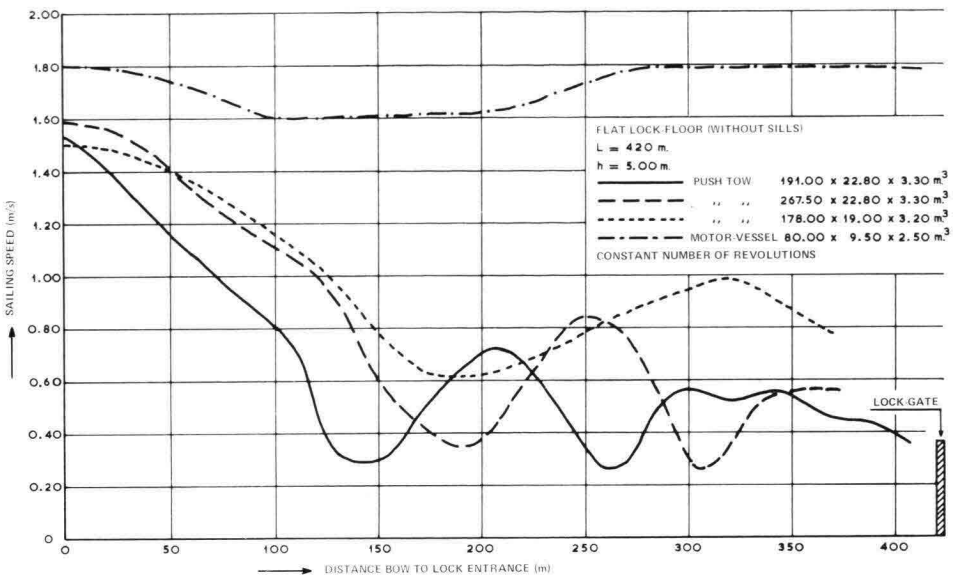

Figure 42. Sailing speed of various ships in the lock-chamber during entry

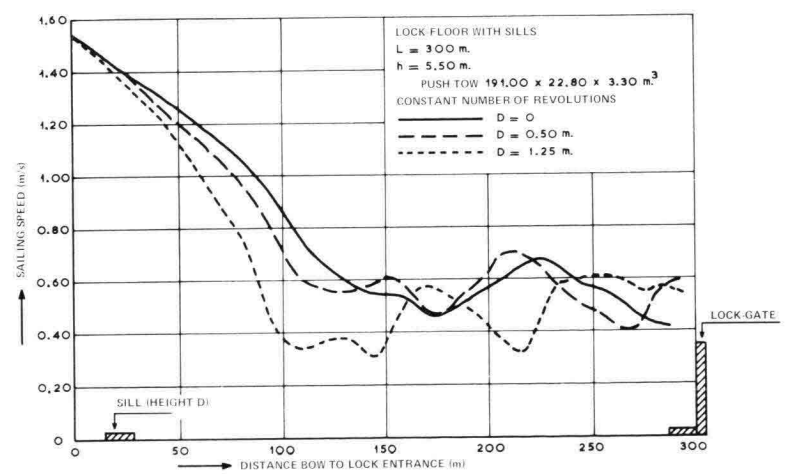

Figure 43. Sailing speed of push tow in lock-chamber with sills, during entry

Run No.	1	2	3	4	5	6	7	8	9
h (m.)	6.91	6.65	6.51	6.83	7.17	7.70	8.63	8.78	8.91
V_o (m./s.)	1.40	1.90	1.75	1.90	1.10	1.95	2.10	2.05	2.05
time (min.)	3.6	3.0	2.7	2.5	3.7	2.5	2.3	2.4	2.6

Table 12.3.2.1. Duration of entries at the Volkerak locks (D = 1.25 m.)

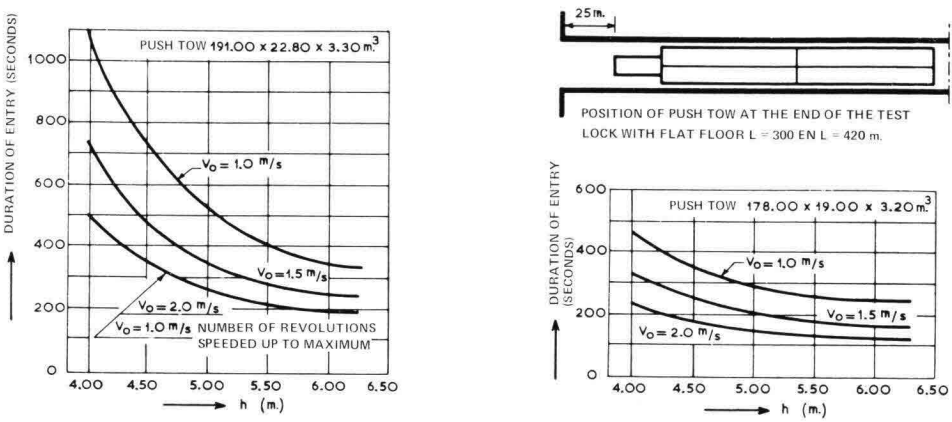

Figure 44. Duration of lock entry

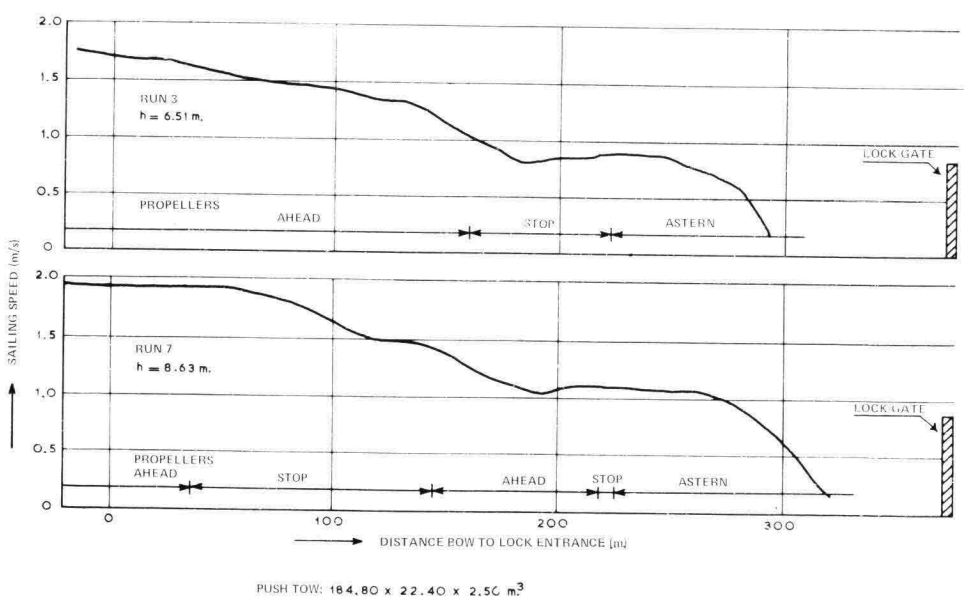

Figure 45. Sailing speed in the chamber of the Volkerak Lock during entry, (D = 1,25 m.)

Run No.	1	2	3	4	5
h (m.)	4.74	4.56	4.82	5.40	5.85
V_o (m./s.)	1.80	1.92	2.10	2.32	2.05
time (min.)	6.0	7.0	5.0	4.0	3.8
(time model) (min.)	(5.7)	(6.2)	(4.5)	(3.2)	(3.2)

Table 12.3.2.2. Duration of entries at the Hartel lock (In brackets the corresponding model values)

12.3.3. Comparison of model with prototype

The prototype test findings at the Volkerak lock cannot very well be compared with the model test findings, because of the difference in draft between the push tows used. A cross-check of the model findings against those at the Hartel lock is only possible in those cases where the circumstances were roughly similar. Only broad comparisons were possible, due to the difference in the use of the propellers.
In figure 47 the progress of run No. 2 is compared with an entry in the model. Over the first 100 m. the correspondence can be called reasonable. After that, the influence of a different use of the propellers becomes noticable. For a more precise comparison between model and prototype the model test would have to be repeated in such a way that the circumstances and the actions in the prototype are reproduced as closely as possible.
In table 12.3.2.2. the entry durations in the model are compared with those of the Hartel lock. The waterdepths and the initial speeds are the same for the entries compared. In the model the number of propeller revolutions was kept constant, resulting in a shorter entry duration than at the Hartel lock.

12.4. Conclusions

1. The entry is especially irregular at small waterdepths.
2. The entry of a conventional motor vessel is hardly delayed, compared to that of a fully loaded push tow.
3. High sills delay the entry. This reduces the locking capacity.
4. The entry speed of push tows in the prototype will in many cases exceed the natural limiting speed in the lock chamber.
5. So far as can be traced the degree of similarity between model and prototype can be called reasonable.

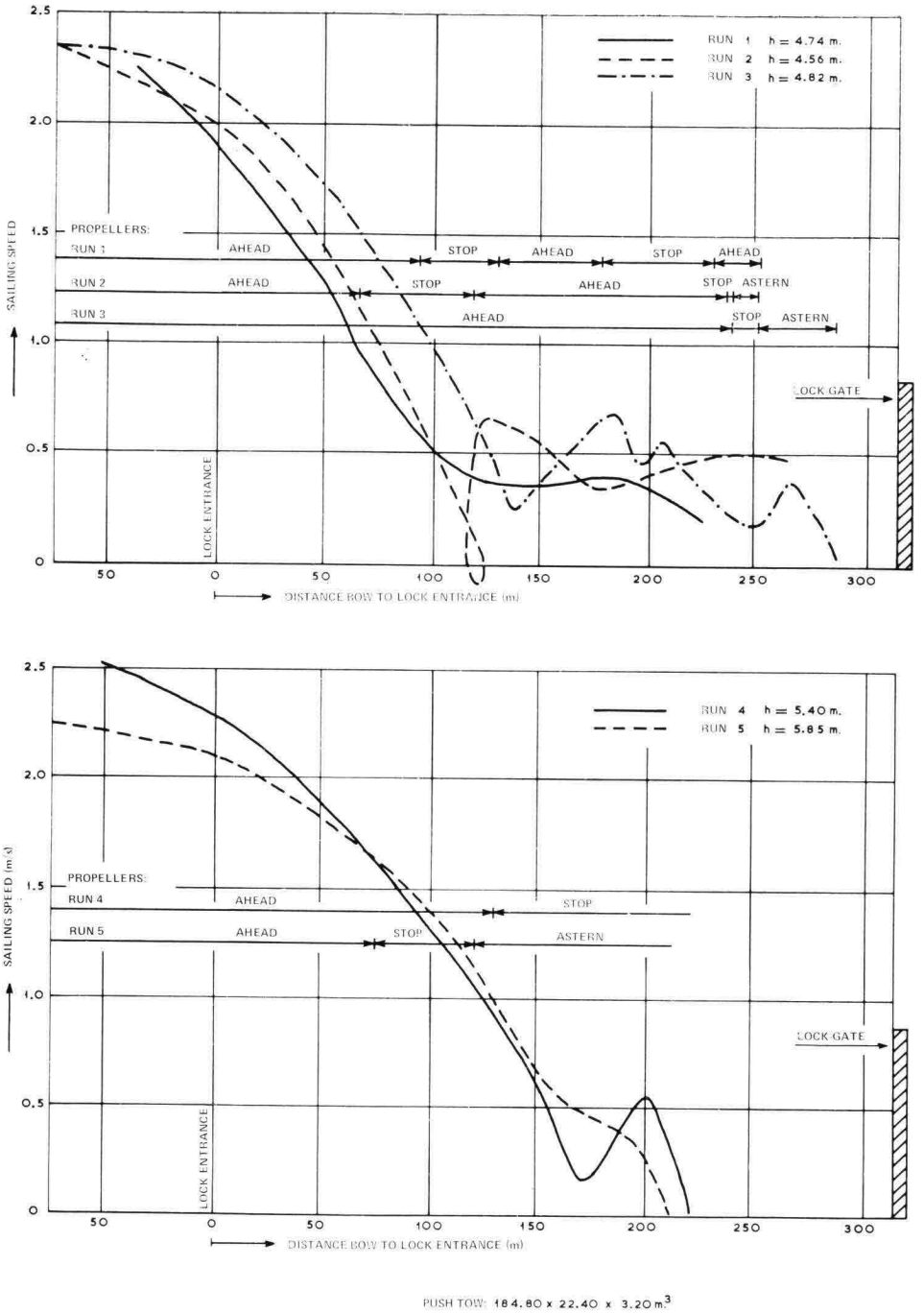

Figure 46. Sailing speed of push tow in chamber of the Hartel Lock during entry

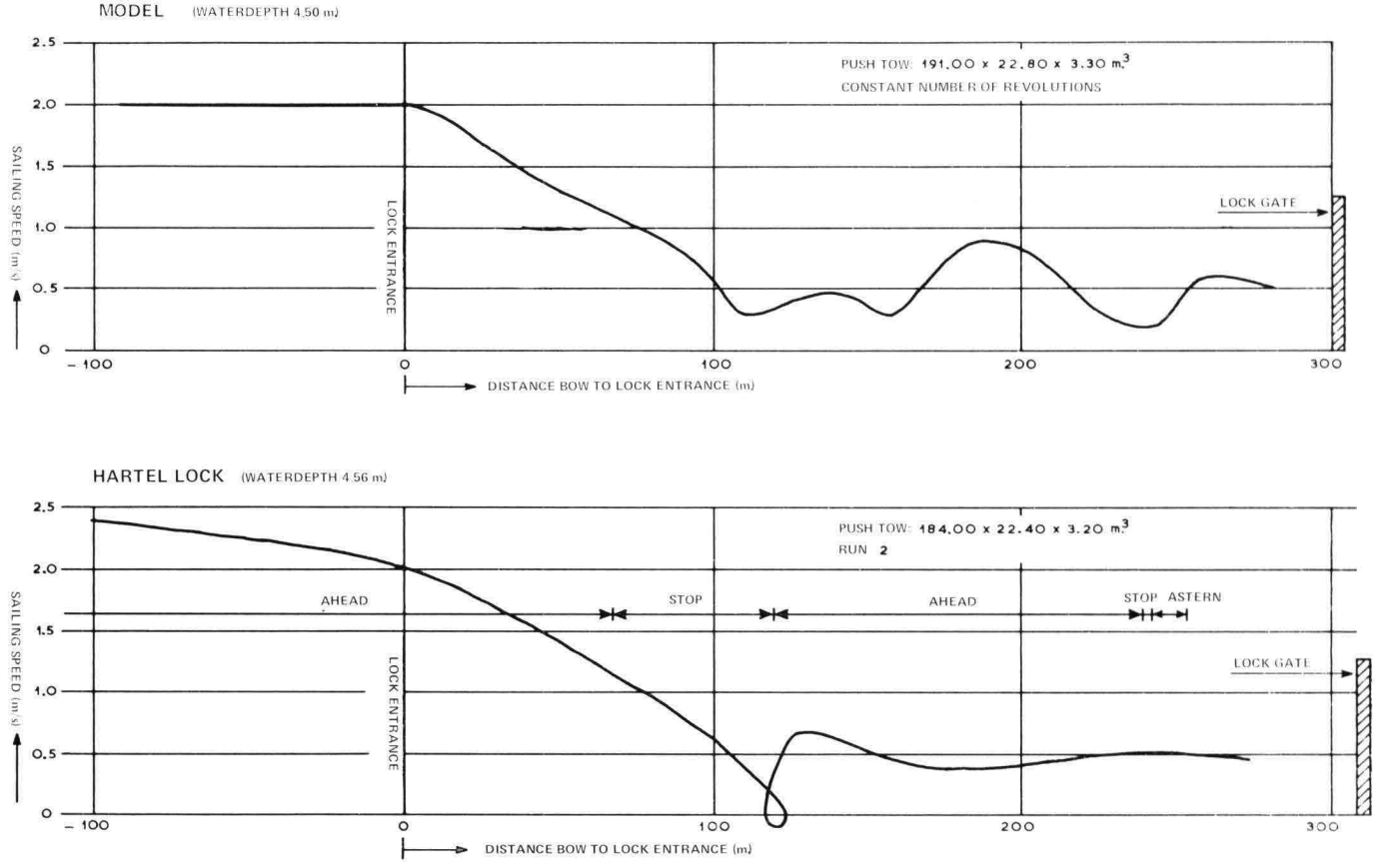

Figure 47. Comparison of an entry into the Hartel Lock and into the lock model

13. Translatory waves in the lock-chamber

13.1. Model investigation

13.1.1. Execution of the tests

The progress of the lock entry and the translatory wave generated during the entry, were measured simultaneously. For the execution of the tests see paragraph 12.2.1. The waterlevel variations were continuously recorded at two stations with the help of resistance wave height recorders (photograph 9). The first station was situated in the lock-chamber at 150 m. from the lock entrance. The second station was situated in the lock-chamber at the closed lock-gate.

13.1.2. Waterlevel variations in the lock-chamber

The shape of the water surface as it presents itself, at a certain point of time, during the entry, between the bow of the push tow and the closed lock-gate was calculated for a great number of different points of time. Use was made here of the water level recordings at the closed lock-gate and of the measured celerity of the translatory wave. The wave motion is imagined as being composed of one wave running forward (Z_1) and one coming back (Z_2). In a particular point the rise of the waterlevel is then equal to $Z_1 + Z_2$. The wave height Z_1 reaches the closed gate after a period t (distance divided by celerity). The wave height Z_2 needs the same time t to travel from the closed gate to the point mentioned above. With the help of two wave heights Z_1 and Z_2 recorded at two points of time at an interval $2t$, it is possible to calculate the resulting wave height $Z_1 + Z_2$ at any point desired. It was possible to check the calculation for the gauging station at 150 m. from the lock entrance.
For two entries, the momentary shape of the water surface, derived at intervals of 25 seconds, is indicated in figures 48 and 49. The progress of the sailing speed and the way it is affected by wave-action is clearly shown in these figures. Figure 48 shows an entry of a large push tow sailing all the way into the lock chamber, up to the closed gate. Finally, figure 49 gives the shape of the water surface, occuring during entry into a lock with sills.

13.1.3. Maximum wave heights

The maximum wave heights occurring at the closed lock-gate have been recorded for

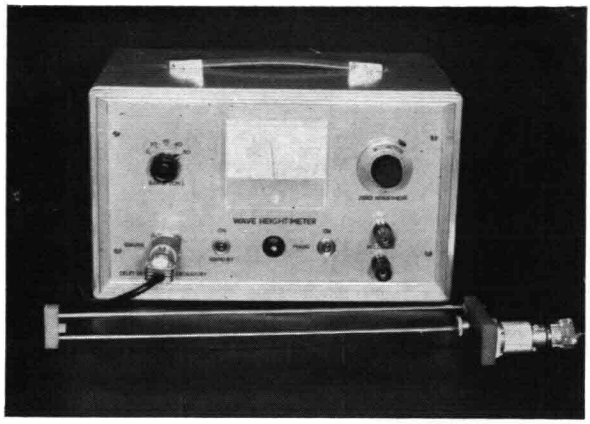

Wave height meter

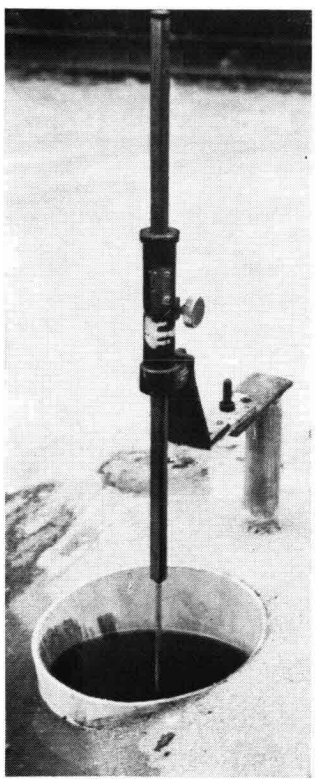

Point gauge

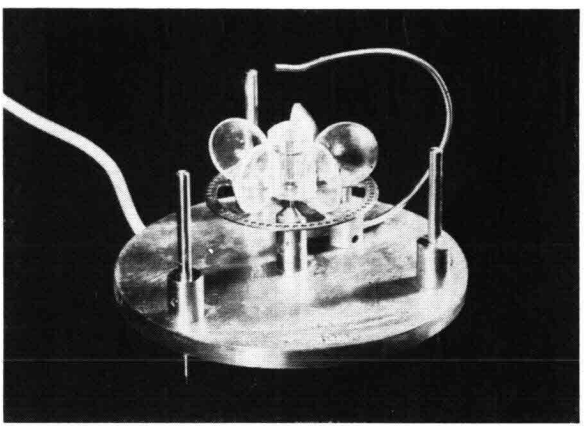

Cup-type current meter

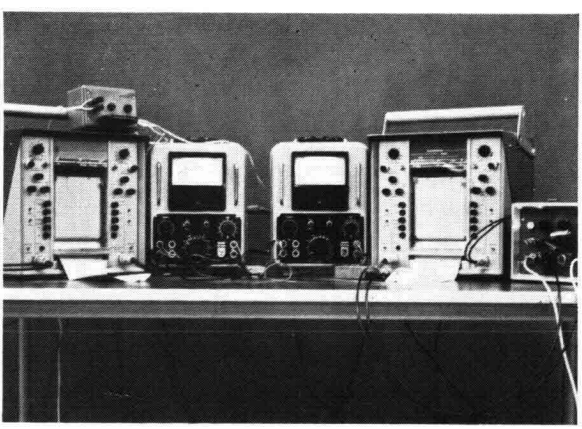

Recorders

Photograph 9. Several used measuring instruments

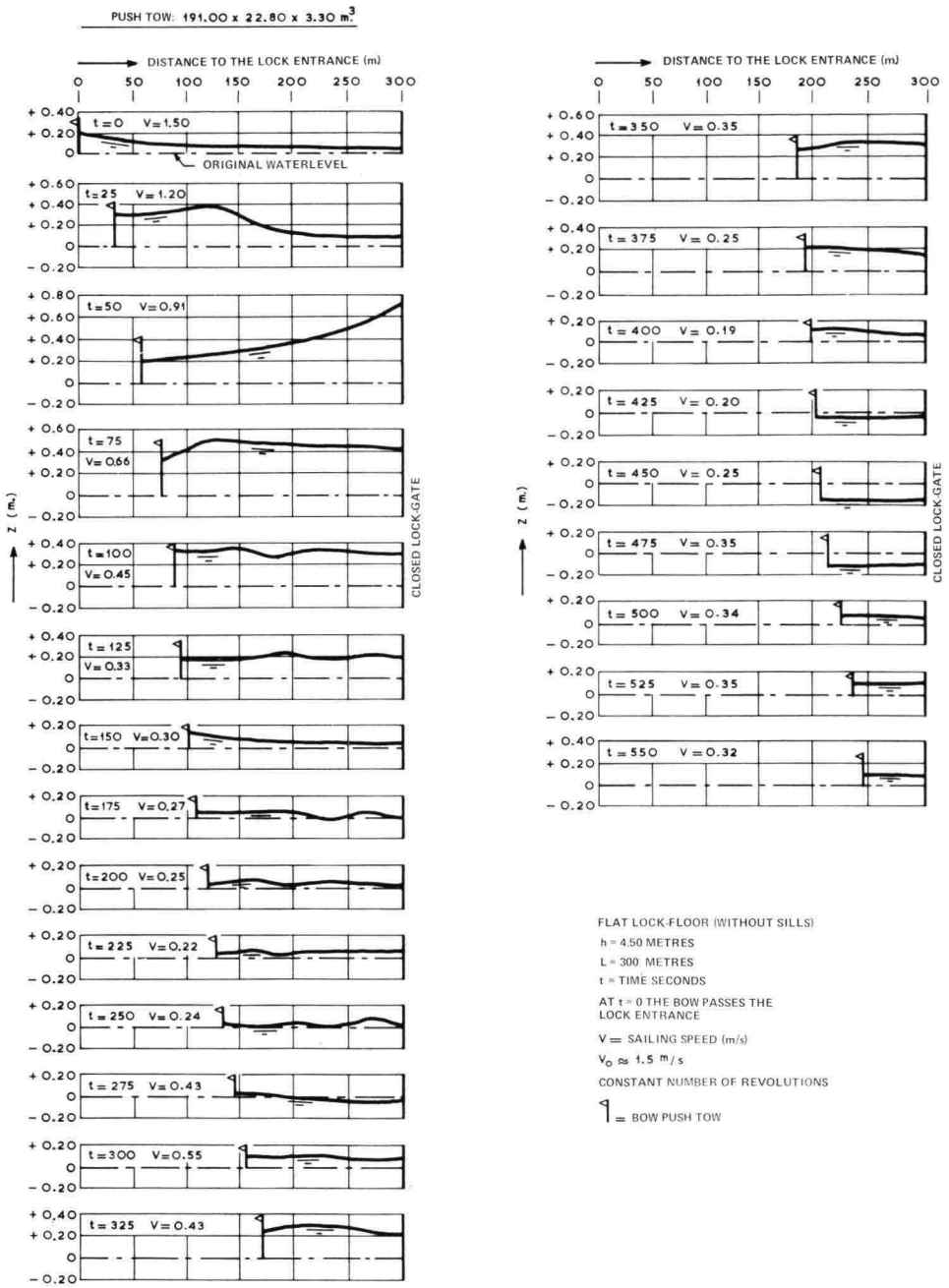

Figure 48. Translatory wave in lock-chamber generated by the entering push tow (flat lock-floor)

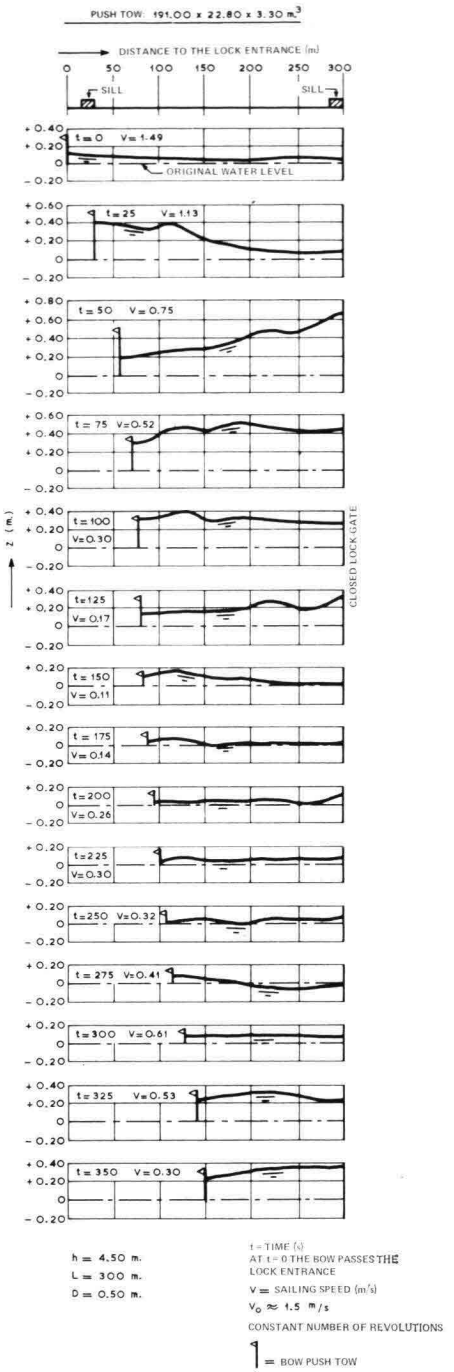

Figure 49. Translatory wave in lock chamber generated by the entering push tow (lock-floor with sills)

a great number of boundary conditions. The spreading in the measurement results was slight. The wave heights reached the same maximum values at lock lengths of 300 and 420 m. The maximum wave heights, at the closed lock-gate, for a large and

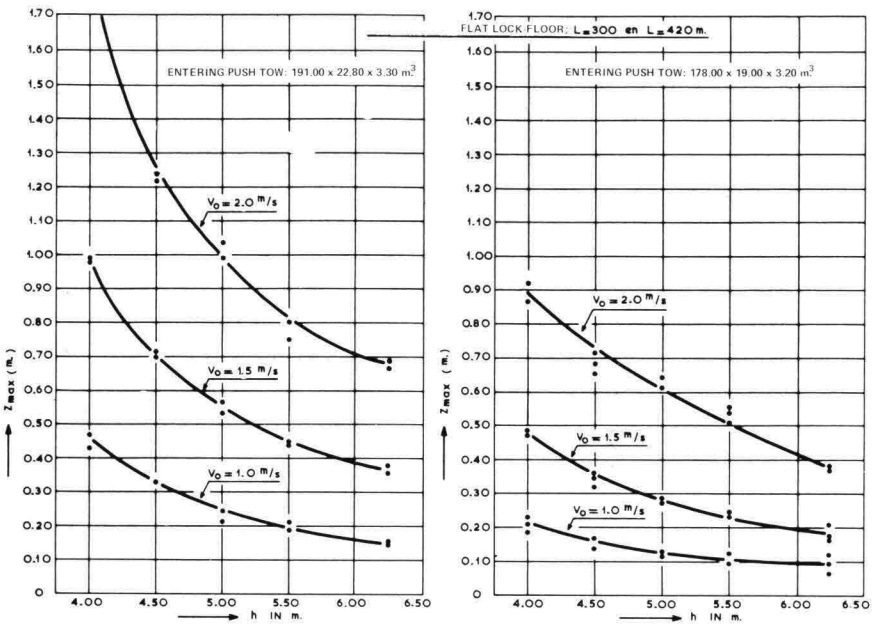

Figure 50. Maximum wave height at closed end of lock-chamber

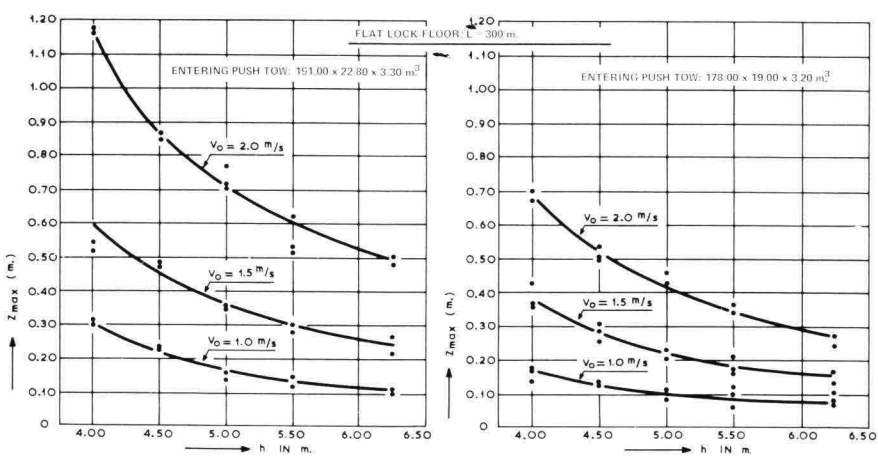

Figure 51. Maximum wave height at 150 m. from the lock entrance

for a small push tow are given in figure 50. In figure 51 the maximum wave heights are given which occur at a distance of 150 m. from the lock entrance. However, the maximum depression of the waterlevel does not depend on the waterdepth but only on the sailing speed, as appears from figure 52.

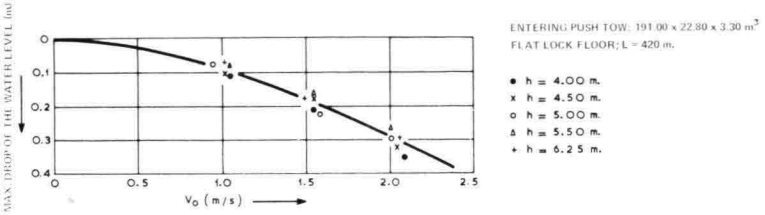

Figure 52. Maximum drop of waterlevel at closed end of lock-chamber

The maximum wave heights, occurring in a lock with sills, are indicated in tabel 13.1.3. A distinction is made here between two wave crests, which can be seen in figure 49.

The use of certain parameters has made it possible to determine a linear relation bewteen Z_{max} on the one hand and V_o, f and F on the other, based on test results. This relation is indicated in figure 53. The parameters are dimensionless, so that it becomes possible to determine Z_{max} foı an arbitrary set of boundary conditions. In this connection the following remarks have to be made:

1. If a lock is equipped with mitre gates the reducing effect, from the local widening (gate-recesses) and the local deepening (floor-recess), if any, must be taken into account when determining Z_{max},
2. In a lock with sills the translatory wave has two crests. The first arises when the bow passes the lock entrance; the second when it crosses the sill. Both crests must be calculated,
3. In the case of a converging lock entrance, for instance when the guides reach to the bottom, for

$$\frac{V_o^2}{gh} \cdot \frac{f/F}{1 - f/F}$$

the maximum value which occurs during entry must be taken. V_o and F are then related to that particular cross-section where this parameter gets its maximum value.
4. Lower wave heights than those indicated in figure 53 will occur when the ships have pointed bows. The opposite is true for bluff-bowed vessels.

h (m.)	V_o (m.)	D (m.)	Z_{max} at the closed lock-gate (m.)		Maximum wave slope ($^0/_{00}$)						Push tow
					Forward running wave measured over the following distances:			Reflected wave measured over the following distances:			
			1st top	2nd top	50 m.	80 m.	100 m.	50 m.	80 m.	100 m.	
4.50	1.0	0.50	0.32	0.35	1.5	1.2	1.0	1.9	1.7	1.5	
5.50	1.0	0.50	0.19	0.20	0.7	0.6	0.5	0.8	0.8	0.7	
5.50	1.0	1.25	0.20	0.24	0.7	0.6	0.5	1.1	1.0	0.9	
6.25	1.0	1.25	0.15	0.19	0.6	0.6	0.5	0.8	0.8	0.7	
											191 × 22.80 × 3.30 m³.
4.50	1.5	0.50	0.70	0.75	4.3	3.2	2.8	5.9	4.8	4.1	
5.50	1.5	0.50	0.45	0.46	2.4	1.8	1.5	2.7	2.3	2.0	
5.50	1.5	1.25	0.45	0.65	2.4	1.8	1.5	4.1	3.1	2.7	
6.25	1.5	1.25	0.35	0.45	1.9	1.5	1.3	2.9	2.2	2.0	
4.50	1.0	0.50	0.20	0.20	0.6	0.5	0.5	0.7	0.7	0.7	
5.50	1.0	0.50	0.13	0.14	0.4	0.4	0.3	0.5	0.4	0.4	
5.50	1.0	1.25	0.13	0.19	0.4	0.4	0.3	0.8	0.6	0.6	
6.25	1.0	1.25	0.10	0.13	0.3	0.3	0.2	0.5	0.5	0.4	
											178 × 19.00 × 3.20 m³.
4.50	1.5	0.50	0.38	0.42	1.7	1.5	1.4	2.7	2.2	1.9	
5.50	1.5	0.50	0.26	0.30	1.0	0.9	0.8	1.2	1.2	1.1	
5.50	1.5	1.25	0.26	0.38	1.0	0.9	0.8	1.9	1.3	1.3	
6.25	1.5	1.25	0.23	0.28	0.9	0.8	0.7	1.0	0.9	0.9	

Table 13.1.3. Maximum heights and slopes of the translatory wave generated during entry in a lock chamber with sills

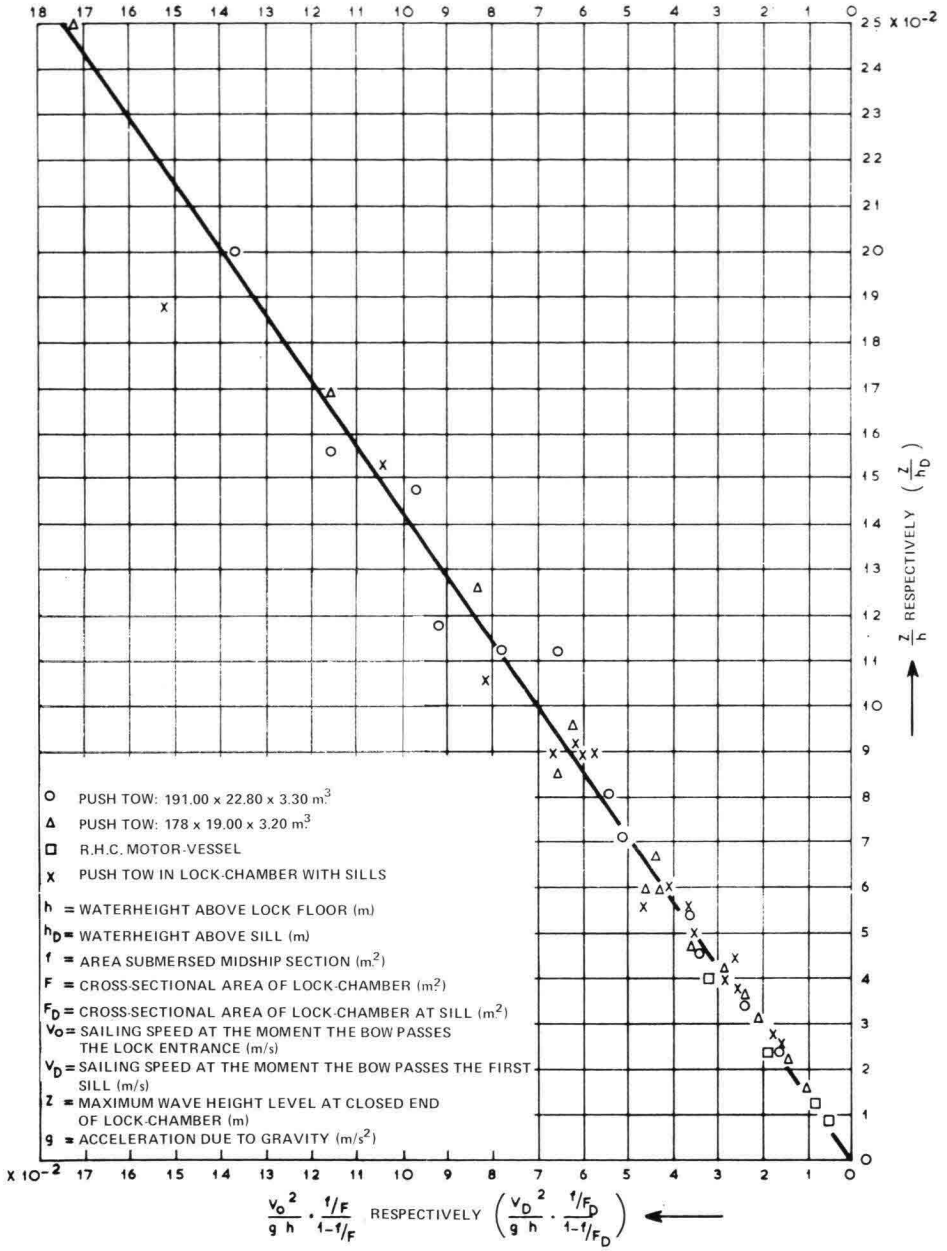

Figure 53. Maximum heights of translatory waves at closed end of lock-chamber caused by entering ships

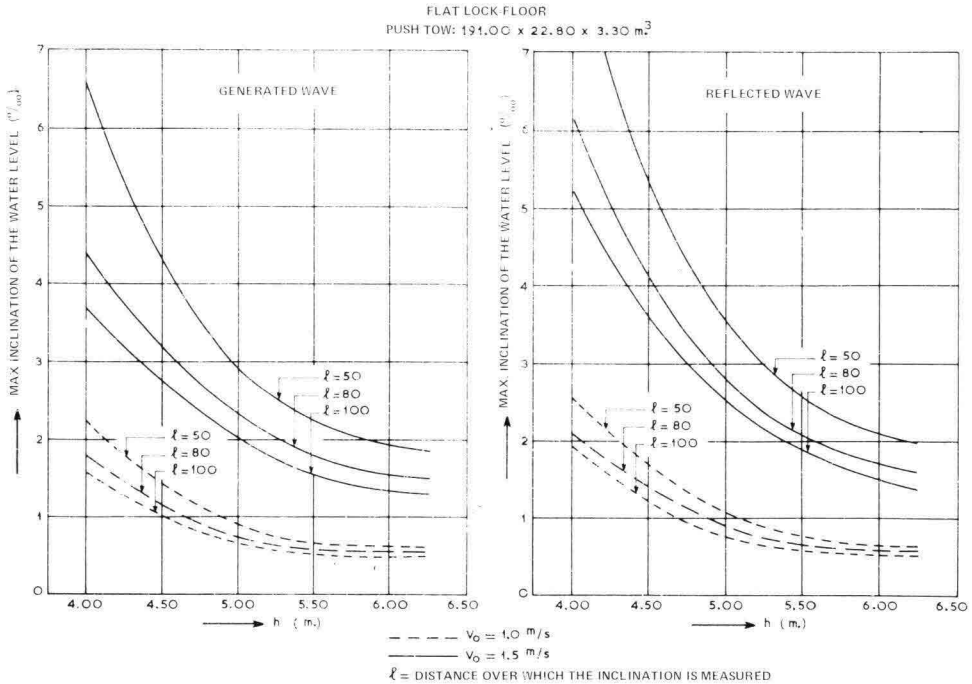

Figure 54. Maximum slope of the translatory wave in the lock-chamber

13.1.4. Slope of the translatory wave

By the slope of the translatory wave we mean the difference in waterlevel, occurring at the same point of time at two stations of the lock axis, divided by the horizontal distance between those stations. This slope is important in view of the safety of the ships moored in the chamber. The translatory wave generates a longitudial force on these ships which is directly proportional to the extent of the wave slope. For various boundary conditions for the large push tow the maximum wave slopes are given in figure 54 and in table 13.1.3. They were measured over distances corresponding with the lengths of frequently occurring ships. The slopes are maximum direct after the fore body of the push tow has passed the lock entrance (forward wave) and after the first reflection from the closed lock-gate.

13.2. Translatory waves in the Volkerak lock and the Hartel lock

13.2.1. Waterlevel variations in the lock-chamber

In the Volkerak locks there were only slight waterlevel variations as a result of the great waterdepth and the reduced draft of the entering push tow. Therefore, only a

few momentary shapes of the water surface of the Hartel lock are given. In figure 55 this is done for run No. 4. The time-interval is 20 seconds. The procedure followed is the same as in paragraph 13.1.2. The calculated shape of the water surface can be checked with the help of the values measured in some intermediate stations.
The influence of the local extension of the wetted cross-section of the lock-chamber at the open lock gates, is clearly perceptible from the pictures of the water surface.

13.2.2. Maximum wave heights

The maximum wave heights at the closed lock gate are stated in table 13.2.2. except for the first 3 entries into the Volkerak lock, the recordings of which are unreliable. The values of the maximum drop of the waterlevel are also listed.

Hartel lock

Run No.		1	2	3	4	5
h	(m.)	4.74	4.56	4.82	5.40	5.85
V_o	(m./s.)	1.75	2.00	2.15	2.30	2.10
Z_{max}	(m.)	0.65	0.85	0.78	0.84	0.51
Max. drop	(m.)	0.25	0.33	0.22	0.38	0.24
Z_{max} (corrected)	(m.)	0.71	0.93	0.85	0.91	0.55

Volkerak lock

Run No.		4	5	6	7	8	9
h	(m.)	6.83	7.17	7.70	8.63	8.78	8.91
h_D	(m.)	5.58	5.92	6.45	7.38	7.53	7.66
V_o	(m./s.)	1.85	1.18	1.95	2.10	2.05	2.05
Z_{max}	(m.)	0.33	0.14	0.28	0.29	0.30	0.21
Max. drop	(m.)	0.23	0.06	0.22	0.22	0.14	0.23
Z_{max} (corrected)	(m.)	0.35	0.15	0.30	0.31	0.32	0.22

Table 13.2.2. Wave heights in the Hartel lock and the Volkerak locks

13.3. Comparison between model and prototype

In figure 56 the shapes of the water surface at different points of time occurring at run No. 2 in the Hartel lock, are compared with the results of a model test, made under,

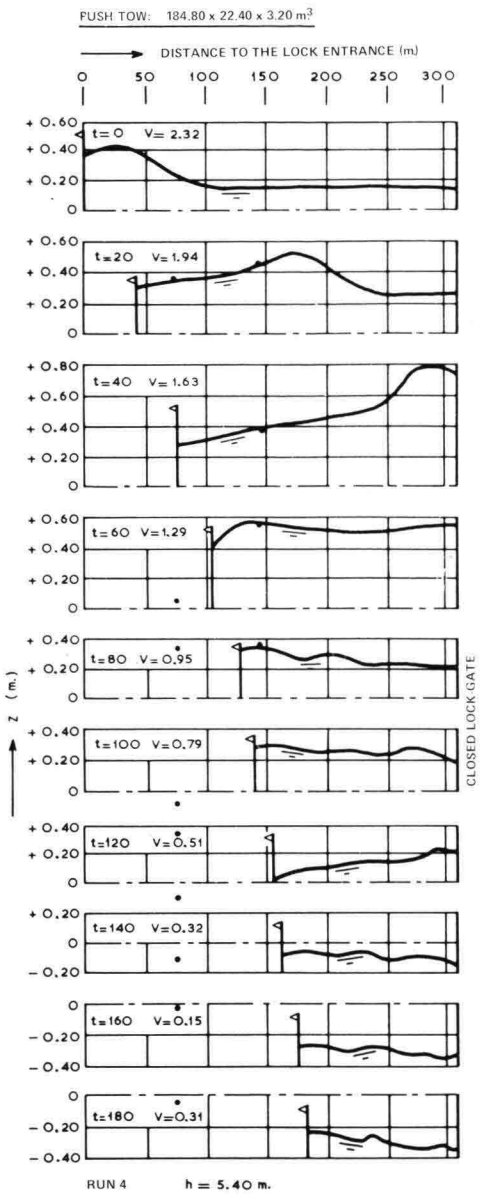

Figure 55. Translatory waves generated by an entering push tow, in the chamber of the Hartel Lock

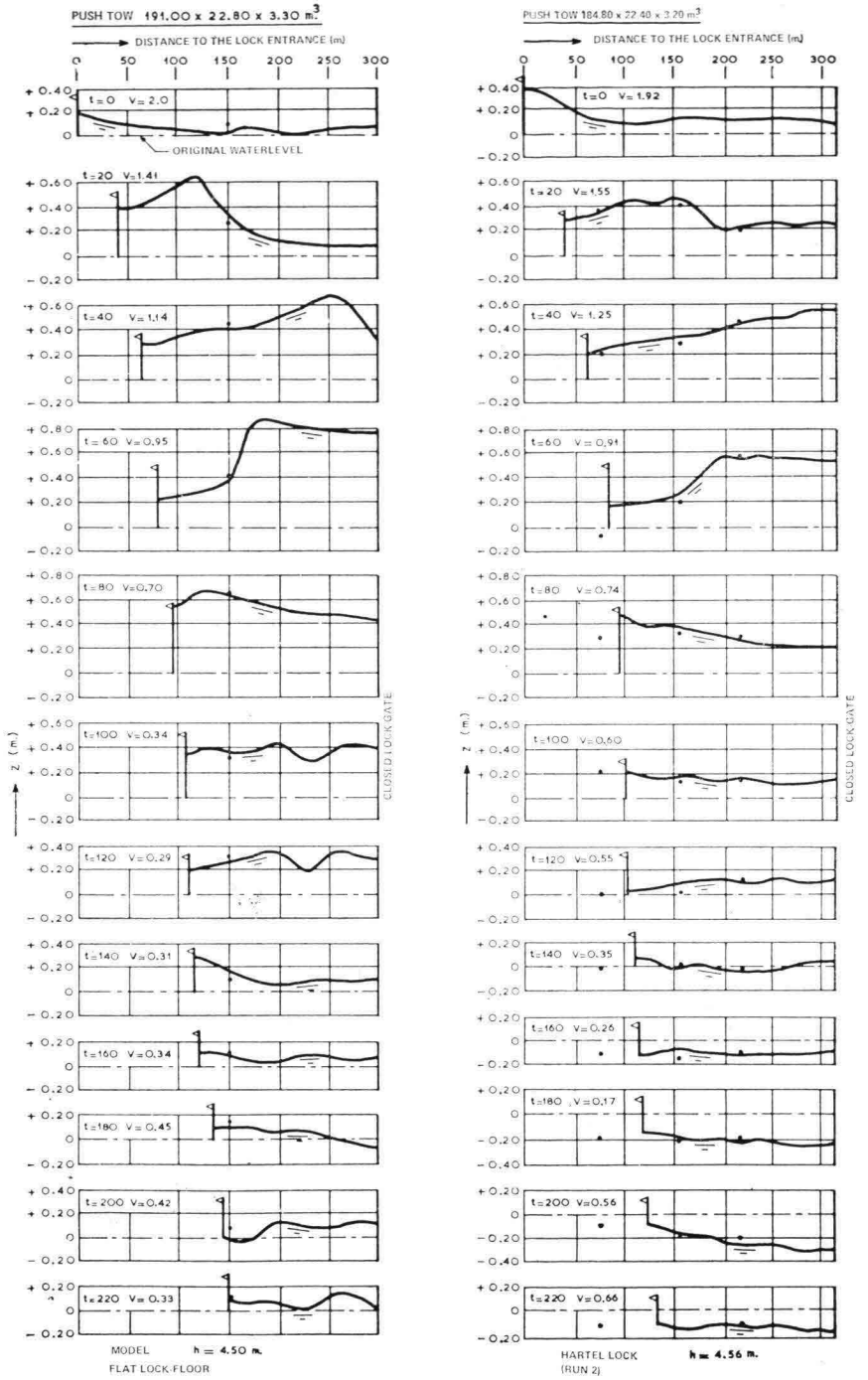

Figure 56. Comparison of the time history of the generated translatory waves in model and prototype

taking it roughly, similar circumstances. The most important differences in conditions are:

- A locally wider cross-section at the closed lock-gate in the Hartel lock,
- Idem, at the open gates near the lock entrance,
- A constant number of propeller-revolutions in the model, against a variable number in the prototype.

To allow for a comparison between the maximum wave heights of the prototype and the model, a correction was made to compensate for the differences in cross-section at the locked gate. In general, this correction is:

$$Z_{max}\,(\text{corr.}) = \tfrac{1}{2} Z_{max}\left(1 + \frac{B_k}{B}\sqrt{\frac{h_k}{h}}\right)$$

in which: B_k = chamber width at the gate-recesses (27 m.)
B = chamber width (24 m.)
h_k = waterdepth at the closed lock-gate
h = waterdepth above the lock floor

The Volkerak lock was compared with a lock model with sills. The correction is:

$$Z_{max}\,(\text{corr.}) = 1.06\, Z_{max}$$

The Hartel lock was compared with a lock model with a flat floor. Here the correction is:

$$Z_{max}\,(\text{corr.}) = \tfrac{1}{2} Z_{max}\left(1 + 1.12\sqrt{\frac{h + 0.50}{h}}\right)$$

In figure 57 the corrected values, stated in table 13.2.2., are compared with the average values from the model.

13.4. Conclusions

1. The progress of the entry corresponds with the observed behaviour of the translatory wave.
2. Experiments have revealed that there is a linear relation between

$$\frac{V_o^2}{gh} \cdot \frac{f/F}{1 - f/F} \text{ and } \frac{Z_{max}}{h}.$$

3. The magnitude of the occurring maximum wave slopes suggests that the longitudinal forces on ships moored in the chamber, will be considerable.
4. The results of the full scale tests show a reasonable similarity to the model findings.

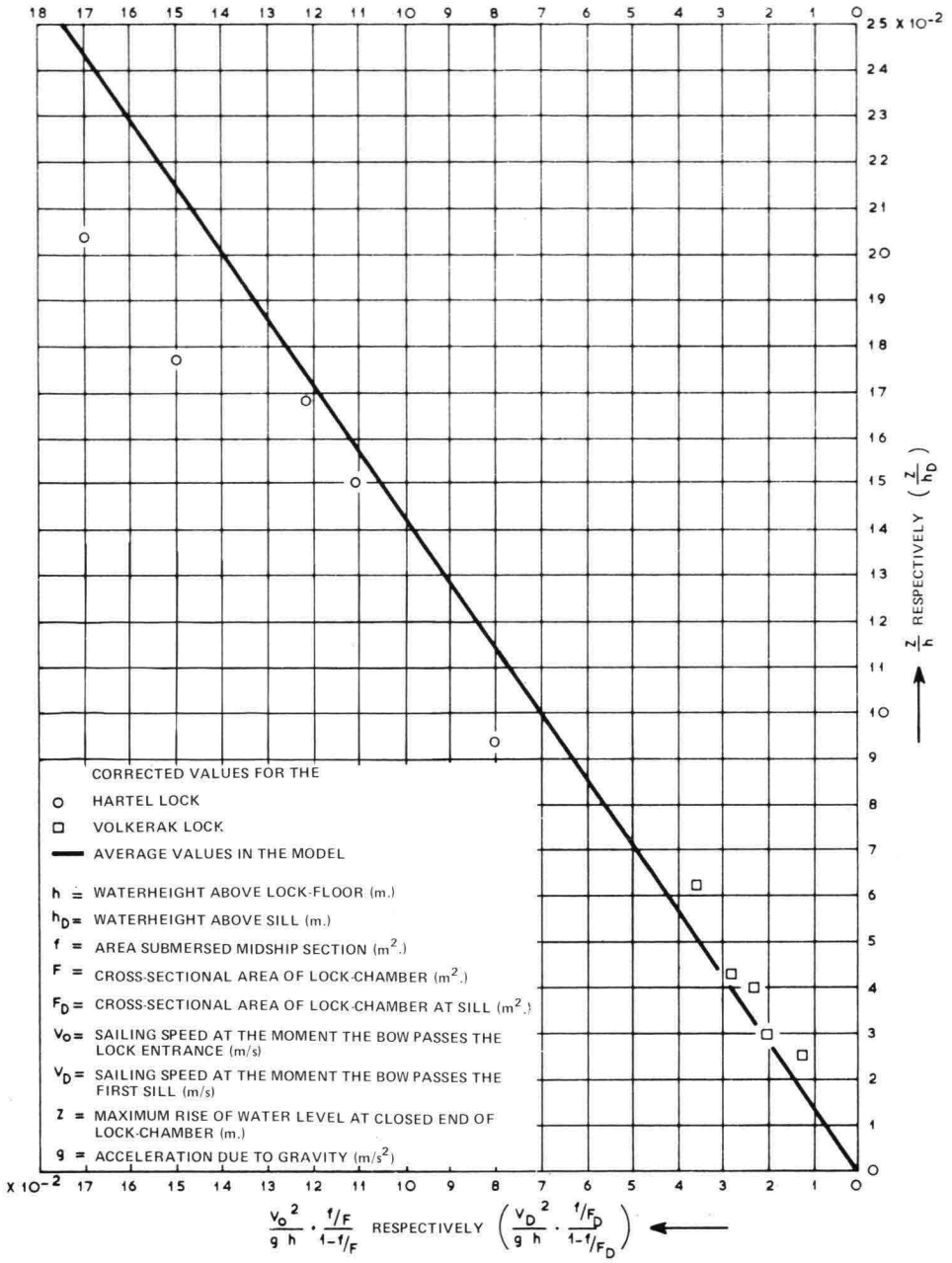

Figure 57. Maximum heights of translatory waves at closed end of lock-chamber caused by entering ships; comparison between model and prototype

14. The safety of ships moored in the chamber during the entry and exit of push tows

14.1. Investigation methods

A push tow entering a lock generates a translatory wave, which runs into the chamber ahead of the ship. Any other ship present in the lock is then influenced by the translatory wave. This causes forces in the hawsers that keep the ship moored. A similar phenomenon also occurs when a push tow of great engine power revs up its propellers in order to leave the lock. A ship moored behind the push tow is then subject to the influence of a translatory wave and the screw race.
Some years ago the Delft Hydraulics Laboratory developed a standard method to measure hawser forces, which is applied when testing the systems of filling and emptying locks. The essential thing about this standard method is the fastening system, which is to prevent any longitudinal movement of the ship. The actual hawser forces will be left out of consideration here, as the longitudinal forces are measured as exerted on the static system, in this case the ship at rest, by the translatory wave. In reality the phenomenon is dynamic because the longitudinal movement of the ship, allowed for by some slack in and elasticity of the hawser, has a major influence on the magnitude of the hawser forces. When using the standard method the criterion is that the longitudinal forces should not exceed $1^0/_{00}$ of the ship's weight for large inland vessels, and between 1.5 and $2^0/_{00}$ for smaller vessels. Practice has shown that the safety of ships in the lock, during filling and emptying the chamber, is sufficiently guaranteed by this criterion, provided two conditions are met as well.

1. The filling and emptying system must be designed in such a way that during a big lift, which causes great forces, the number of changes in the direction of the longitudinal forces is restricted to a minimum.
2. If there is a big lift, the skipper must stand by the hawsers, to let them slip along the bollard during the filling or emptying of the chamber, thus preventing the ship from 'dropping into the hawsers'.

The advantage of an investigation on mooring forces according to the standard method is, that a very great number of variable quantities such as hawser length and diameter, elasticity modulus, slack, the way of belaying the hawser and the interference of the skipper, are eliminated.
But the question remains whether this criterion may also be used in the case of a translatory wave caused by an entering push tow.
Pending the results of the investigation, in figure 58 the longitudinal forces on a

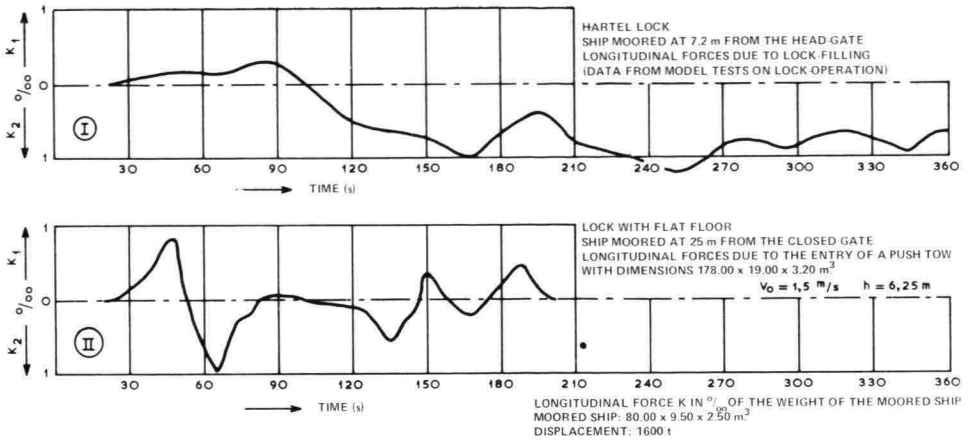

Figure 58. Time history of longitudinal forces acting on a ship moored in the lock chamber. Comparison between the effect of lock-filling (I) and an entering push tow (II)

moored ship occurring during the filling of the Hartel lock, are compared with the longitudinal forces resulting from the entry of a push tow.
In the latter case the pattern of the forces is clearly less favourable because of the much quicker change from maximum positive to maximum negative.
For this reason the following method was applied. The influence of the translatory wave on the moored ship was basically determined by measuring the longitudinal forces, using the standard method. Later a complementary investigation was carried out, in which the actually occurring hawser forces were measured for a limited number of boundary conditions in the model. The criterion by which the results of the standard method can be judged, was deduced from this.

14.2. Execution of the tests

The entries of the various ships were carried out in the same way as during the investigation into the progress of the sailing speed in the lock-chamber (paragraph 12.2.1). Rhine Herne canal ships and a lighter with a displacement of 500 tons were used as moored ships. The positions of these ships are given with the measurement results.
For the exit tests, use was made of a large push tow (191 × 22.8 × 3.3 m^3.) A starting time corresponding to 10 seconds was taken, which means that the propellers were revved up to the desired number of revolutions in 10 seconds (full scale). The number of revolutions is expressed in parts of VK (full speed = max. number of revolutions) or HK (half speed = $\frac{1}{2}$ VK).

The boundary conditions were varied in the same way as during the translatory wave tests.

The measuring arrangement used to measure the longitudinal forces according to the standard method, is schematically indicated in figure 59. The moored ship was fastened to a vertical bar, which could move up and down with the ship, and the weight of which was compensated by a counterweight. In the ship a stiff leaf spring was fixed, which was connected to the bar by a cardanic joint. The bend of the leaf spring, which is a measure for the force on the ship, was electronically measured and continuously recorded. In regard to the occurring forces, distinction was made between K_1, directed at the closed lock-gate and K_2, directed at the lock entrance. The longitudinal forces are acting in the horizontal plane.

The measuring arrangement, applied to record the hawser forces is indicated in figure 60. In the model the hawsers were imitated by thin steel wires of which the elasticity, resulting from the occurring loading and the dead weight can be neglected. The wires were connected with a spring, indicating the elastic extension of the hawser to scale, by means of an arm, tilting in the vertical plane, projected through the longitudinal ship centerline. The spring constant can be varied by attaching the hawser higher or lower to the arm. Photograph 10 shows the moored ship and the hawser force meter used.

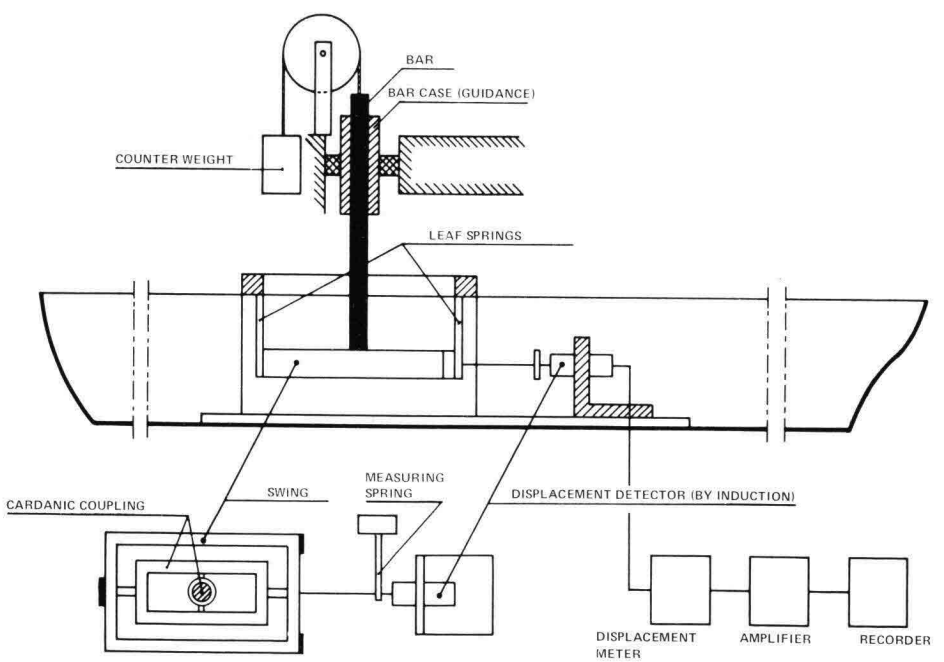

Figure 59. Arrangement for the measuring of longitudinal forces according to the standard method

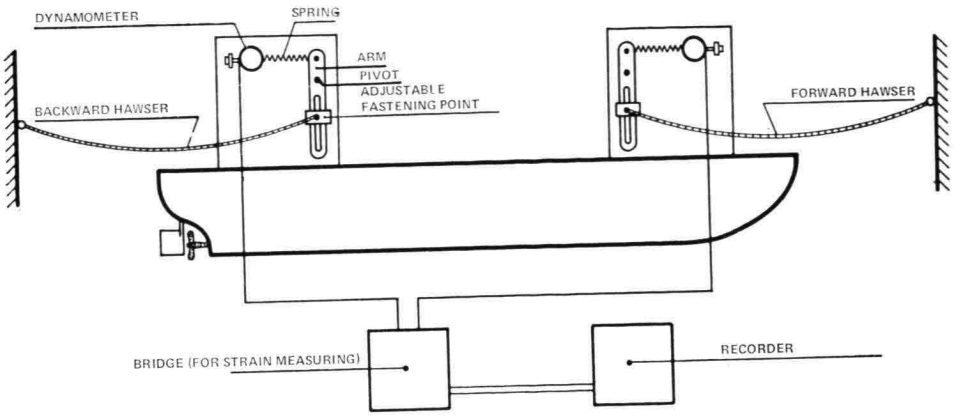

Figure 60. Arrangement for the measuring of hawser forces

In practice it was found that ships with a displacement of about 1600 tons usually have hawsers on board with a diameter of 18, 20 or 22 mm. The data are given below.
Construction: 6 × 15 steel-wire + 7 rope cores.
Elasticity modulus E: 10^{11} N/m^2. (Newton per square meter)

Diameter (mm.)	Material cross-section (10^{-6} m^2.)	Theoretical breaking strength (10^4 N)	Dead weight (N/m^1.)
18	71.0	8.0	7.7
20	85.4	9.7	9.4
22	102.0	11.5	11.2

Table 14.2. Data steel-wire hawsers (prototype dimensions)

The spring constant (C) of the hawser, expressed in meters extension per Newton (N) tensile force is defined as follows:

$$C = \frac{s}{E \cdot F_t}$$

in which: s = hawser length (m.)
F_t = material cross-section (m^2.)
Two values of C were applied:

$$C = 8 \times 10^{-7} \text{ m./N and } 16 \times 10^{-7} \text{ m./N.}$$

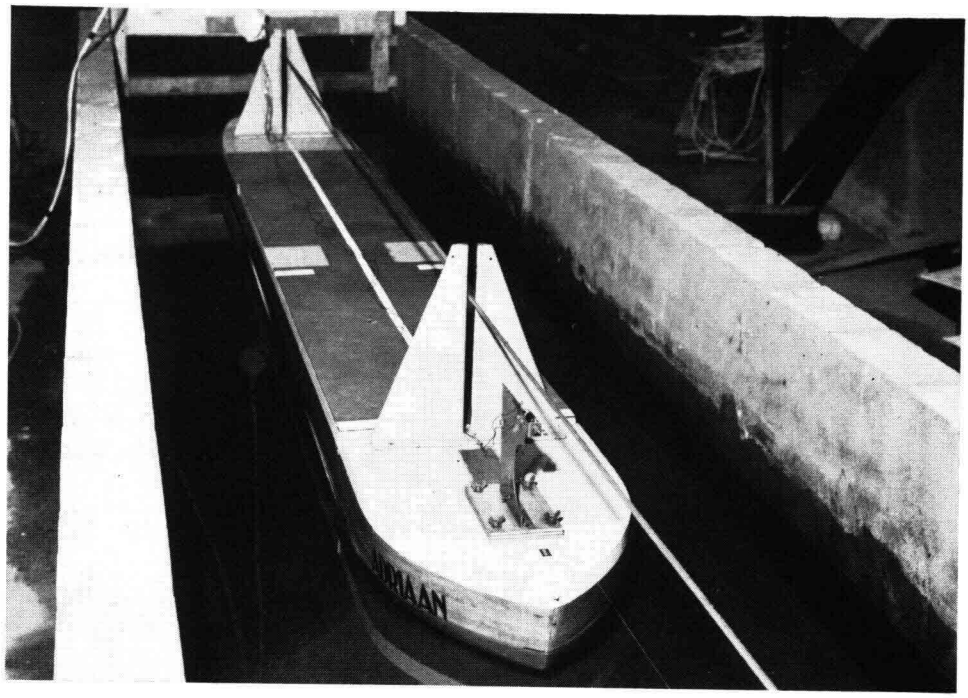

Photograph 10. Tests on hawser forces

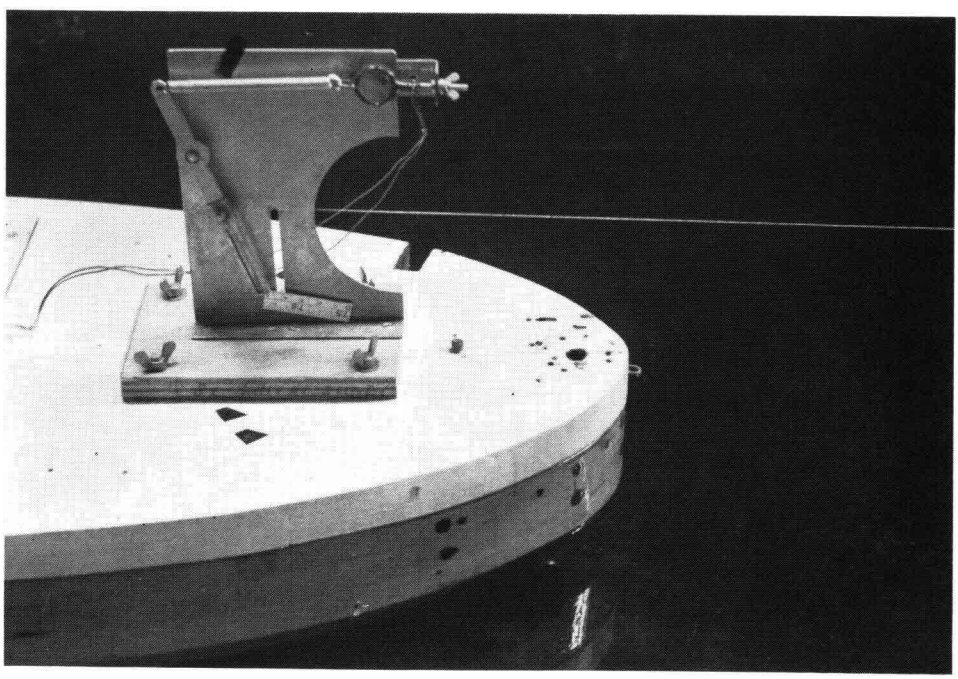

For a hawser of 22 mm. dia. this means lengths of about 8 and 16 meters respectively. The slack in the hawsers was varied. The moored ship could move freely in a longitudinal direction over a distance equal to the total amount of slack (r) in both hawsers, without any force occurring in the hawsers. In the main, three values were applied: r = 0 m., 0.25 m. and 0.50 m.
When measuring the hawser forces a number of schematisations were applied, the most important of which were:

a. Motion of the ship sideways was prevented with the help of a guiding cable (photograph 10),
b. The elasticity modulus was kept constant over the total elasticity area,
c. The hawsers were placed in the vertical plane in the longitudinal ship center line and the fastening points were at the same level. As a result, the forces in the model will relatively be too small.

14.3. Longitudinal forces

In figure 61 a number of longitudinal force diagrams are given. The fact that the maximum values occur just before and after the first reflection of the generated translatory wave, is characteristic of the patterns. The longitudinal force caused by the reflected wave K_2, is in all cases bigger than K_1; also for other boundary conditions.
The maximum values of K_2 are indicated in figure 62, 63 and 64, for various boundary conditions. In figure 62 the maximum longitudinal forces are compared with the maximum wave slopes from paragraph 13.1.4.
The longitudinal forces are always greater than the inclines of the waterlevel measured in a lock chamber in which no ship was moored. It may be expected that the wave slope becomes somewhat steeper if there is a ship in the chamber.
Figure 64 shows that a comparatively greater longitudinal force is exerted on a short ship than on a long one. The reason is that the average wave slope becomes slighter if it is determined over a greater distance.
The longitudinal forces, occurring as a result of the starting of the propellers of a push tow leaving the lock, are given in figure 65. The flow pattern which arises, was photographically established as can be seen on photograph 11.

14.4. Hawser forces

In figure 66 three diagrams of hawser forces are given, which were determined at various degrees of slack in the hawsers. For comparison, a diagram is given of longitudinal forces determined under the same circumstances. The forces in the backward hawser (corresponding to K_1) are small with respect to the forces in the forward hawser (K_v). The movement of the ship is as follows:

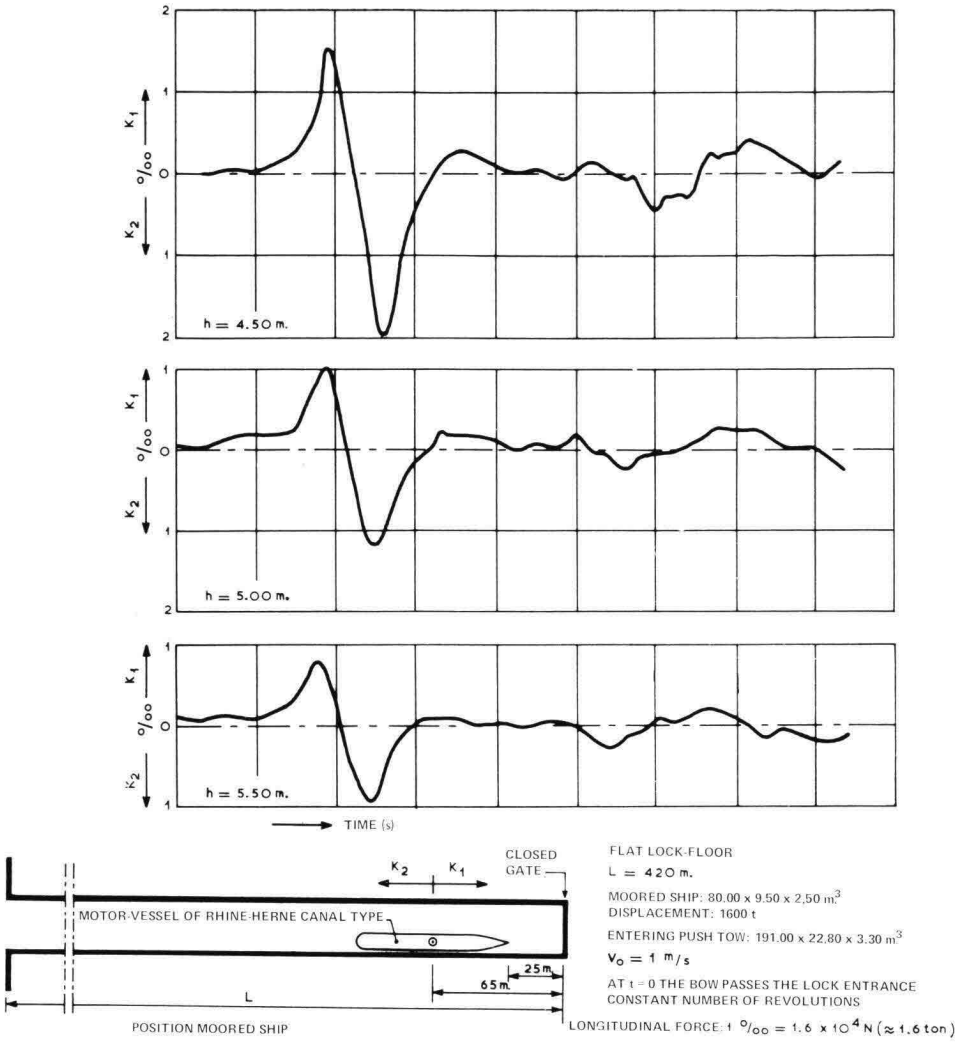

Figure 61. Time history of longitudinal forces

1. Under the influence of the slight initial slope of the translatory wave (figures 48 and 49) the moored ship gradually moves into the direction of the closed lock-gate. At the moment when the steepest part of the wave passes, the backward hawser has already tightened. The hawser force, K_a, is than about equal to the static longitudinal force K_1. In the forward hawser, slack arises. It is equal to the total amount of slack (r) plus the elasticity in the backward hawser,
2. Directly after the reflection of the wave the longitudinal force changes direction and the ship begins to move faster and faster in the direction of the lock entrance.

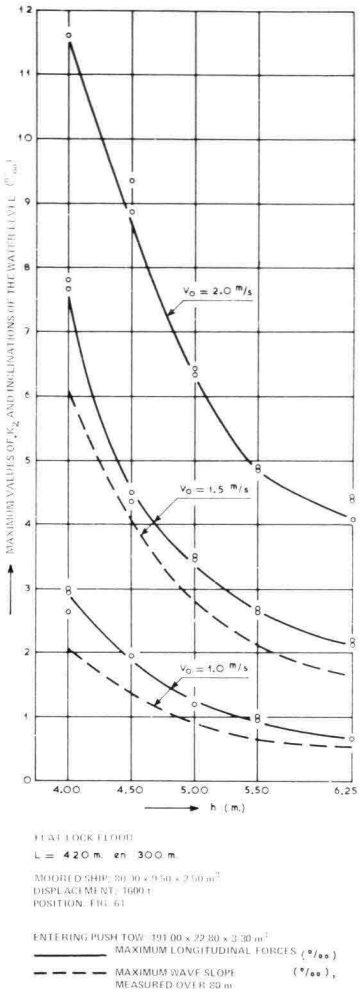

Figure 62. Maximum longitudinal forces and wave slopes

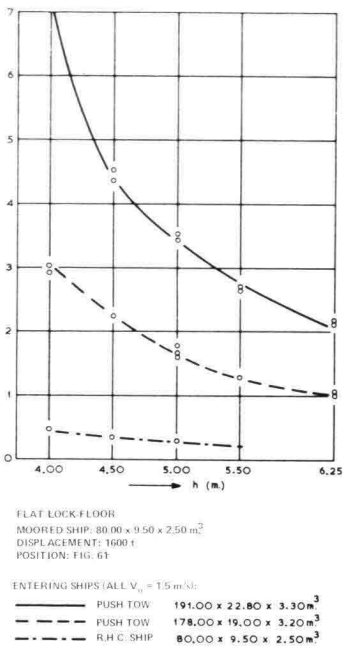

Figure 63. Maximum longitudinal forces (various entering ships)

The ship 'falls' into the forward hawser. Owing to this dynamic effect the size of K_v is a multiple of K_a.

3. Both hawsers become loaded repeatedly during the entry. The occurring forces are much smaller, however, than the maximum value of K_v.

The maximum values occurring under various boundary conditions in the forward hawser, are indicated in the figures 67, 68 and 69. In figure 70 diagrams for hawser forces are given, which were determined during the exit of a push tow. The influence of the starting distance on the hawser forces is clearly perceptible from this.

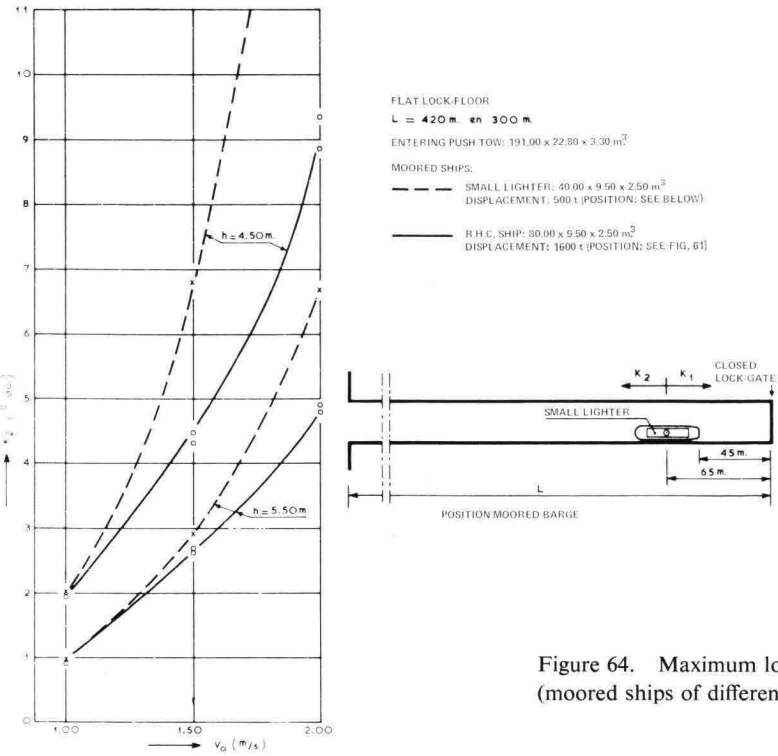

Figure 64. Maximum longitudinal forces (moored ships of different lenghts)

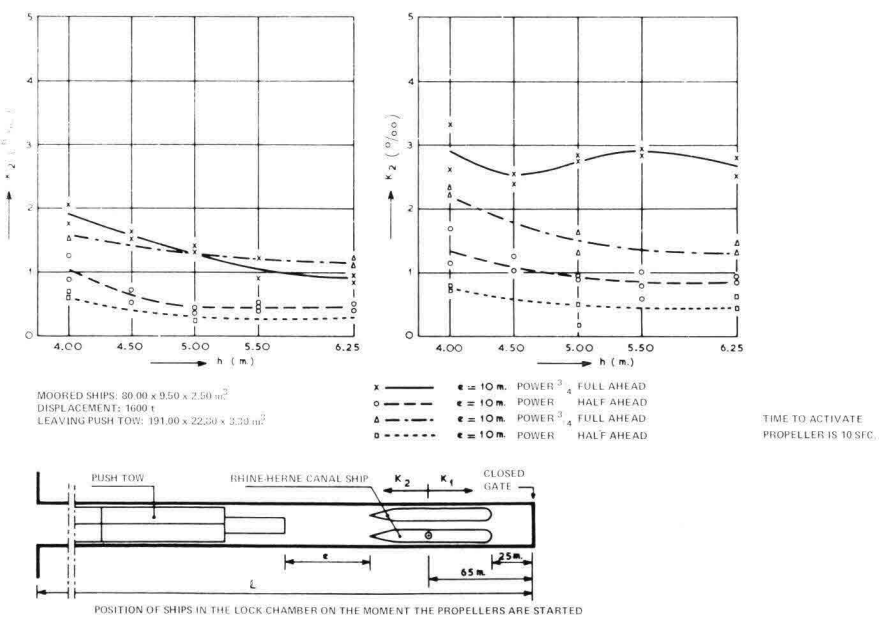

Figure 65. Maximum longitudinal forces (caused by a push tow leaving the lock)

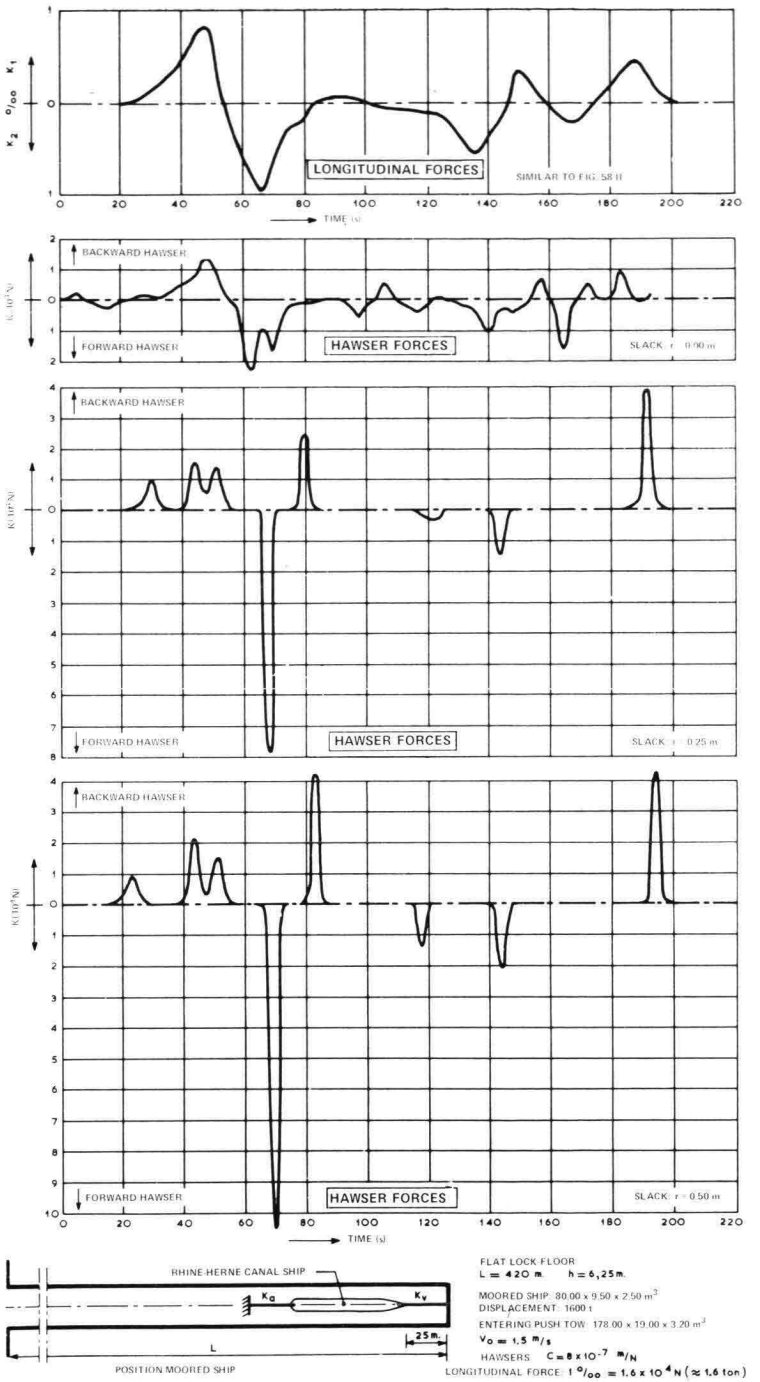

Figure 66. Hawser forces compared with longitudinal forces

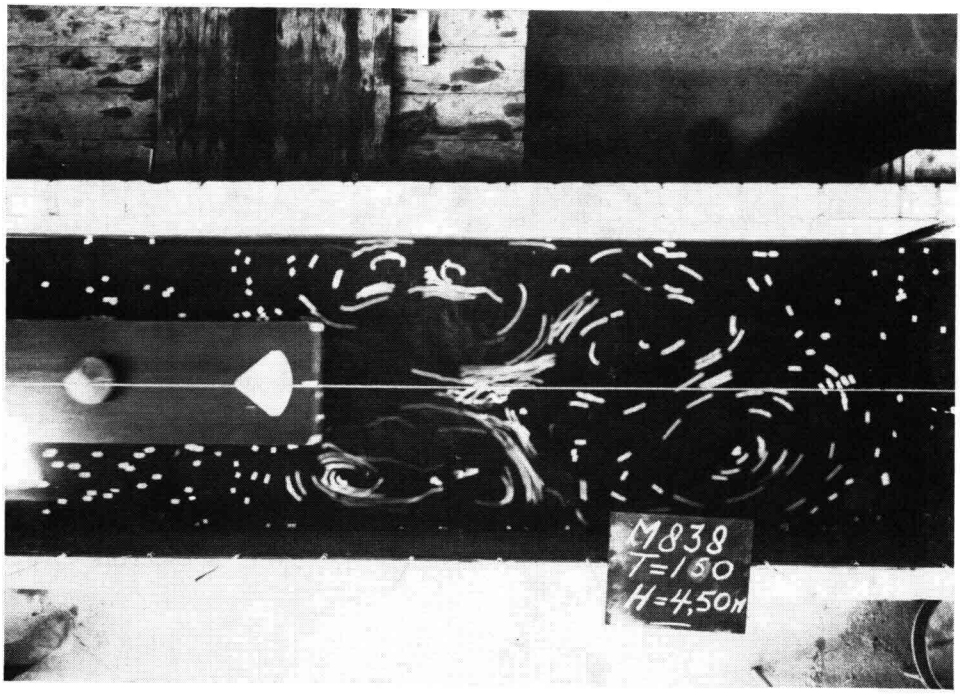

Photograph 11. Flow pattern caused by the propellers of a push tow leaving the lock (model)

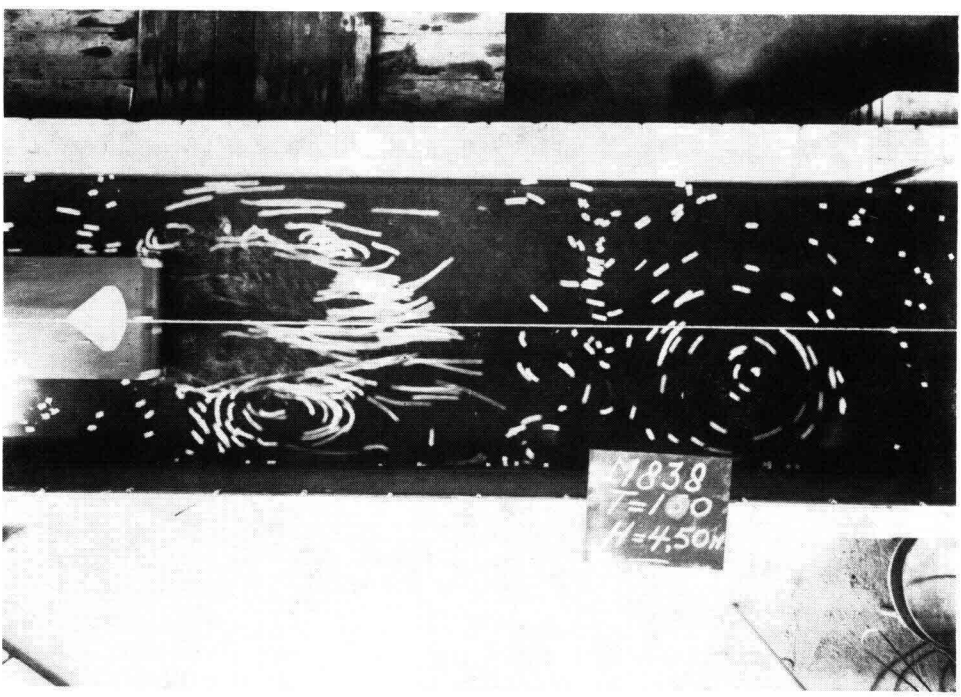

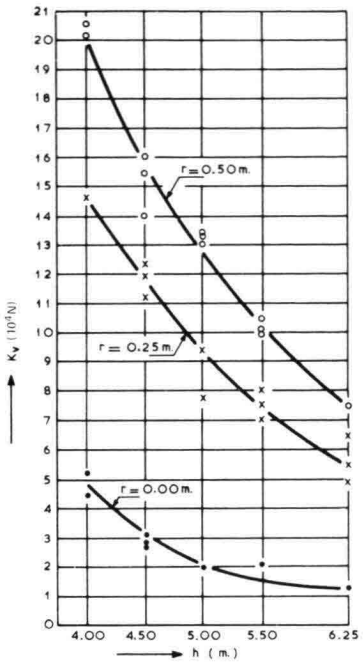

FLAT LOCK-FLOOR
ENTERING PUSH-TOW: 191.00 x 22.80 x 3.30 m^3
V_o = 1.0 m/s
MOORED SHIP: 80.00 x 9.50 x 2.50 m^3
DISPLACEMENT: 1600 t
POSITION: SEE FIG. 66
HAWSERS: $C = 8 \times 10^{-7}$ m/N 10^4N ≈ 1 TON

Figure 67. Maximum hawser forces as a function of slack and waterdepth ('large' push tow)

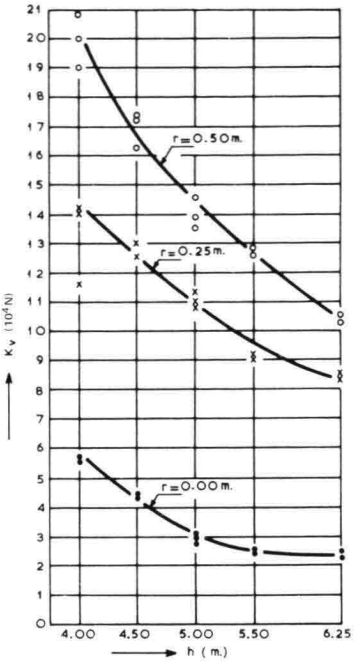

FLAT LOCK-FLOOR
ENTERING PUSH-TOW: 178.00 x 19.00 x 3.20 m^3
V_o = 1.5 m/s
MOORED SHIP: 80.00 x 9.50 x 2.50 m^3
DISPLACEMENT: 1600 t
POSITION: SEE FIG. 66
HAWSERS: $C = 8 \times 10^{-7}$ m/N

Figure 68. Maximum hawser forces as a function of slack and waterdepth ('small' push tow)

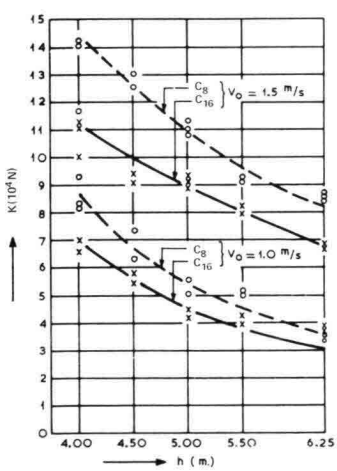

FLAT LOCK-FLOOR
ENTERING PUSH TOW: 178.00 x 19.00 x 3.20 m^3
MOORED SHIP: 80.00 x 9.50 x 2.50 m^3
DISPLACEMENT: 1600 t
POSITION: FIG. 66
HAWSERS: $C_8 = 8 \times 10^{-7}$ m/N en $C_{16} = 16 \times 10^{-7}$ m/N
SLACK: r = 0.25 m.

Figure 69. Comparison of maximum forces in hawsers with various properties

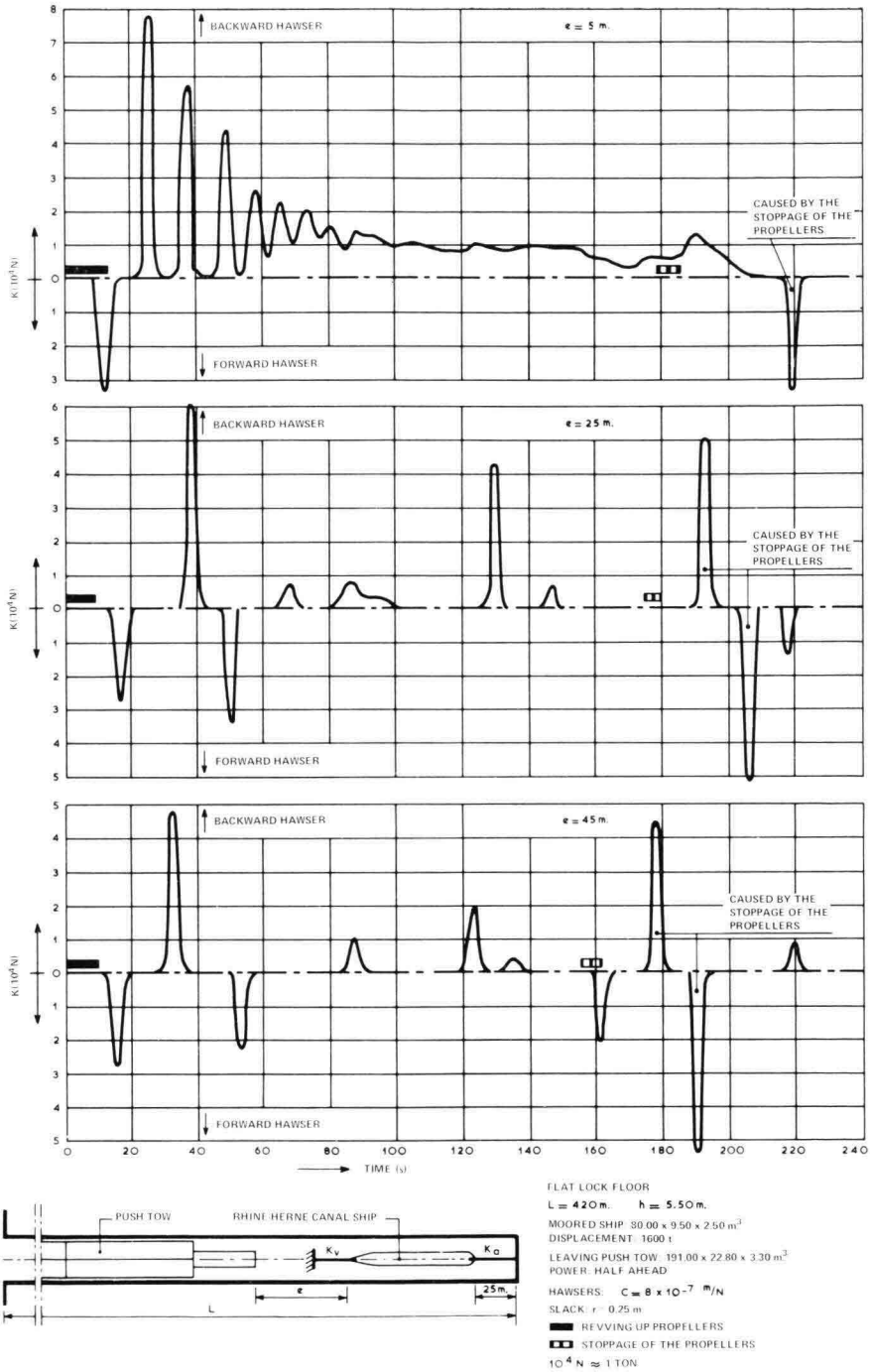

Figure 70. Time history of hawser forces (caused by a leaving push tow)

14.5. Some notes on the test results

Measurement results have revealed that the magnitude of the hawser forces is closely related to the freedom of movement of the moored ship, as a result of slack in the hawsers. From inland navigation practice it is clear that it is hardly ever possible to reduce the slack to nil because the rather stiff hawsers must be tighthened and belaid round the bollard by hand.
Some examples of slack in the hawsers are given in photographs 12 and 13.
In existing locks, observations were made as to the mooring of big inland ships. A survey of these observations is given in table 14.5., which also shows a similar situation from the model. This situation will serve as a standard for the evaluation of the test findings.

Quantity	Prototype	Model (full scale dimensions)
displacement of ship (m^3.)	> 1,000	1,600
ship length (m.)	60 to 100	80
diameter of hawser (mm.)	18 to 24	20
length backward hawser (m.)	8 to 18	6.8
length forward hawser (m.)	4 to 6	6.8
slack r (m.)	0.20 to 0.30	0.25
angle backward hawser with horitzontal (degrees)	5 to 15	0
angle forward hawser with horizontal (degrees)	15 to 30	0

Table 14.5. Standard conditions in the model based on observations in full scale situations

For safety reasons, the maximum allowable hawser force should be less than the theoretical breaking strength. Therefore the maximum allowable hawser force for the standard model situation is fixed at 5×10^4 N ($\approx$ 5 tons). This is a little more than 50% of the theoretical breaking strenth of a hawser with a diameter of 20 mm. and corresponds with a hawser force equal to about $3.1^0/_{00}$ of the ship's weight.
The relation between hawser forces and longitudinal forces, occurring under the same conditions, is given in figure 71. If a slack in the hawsers of $r = 0.25$ m. is considered the standard value, the maximum allowable longitudinal force will be about $0.55/^0/_{00}$ of the ship's weight.
Small ships are equipped with comparatively heavier hawsers than big ships. The longitudinal forces on these small ships are, however, greater in comparison, especially in small waterdepths and with high entry speeds of the push tow, as appears from

figure 64. This is why no distinction is made in safety requirements for small or big ships in the lock-chamber.
Based on the measurement results from the model and the criteria drawn up for it, the relation between the entry speed of fully loaded push tows and the existing water-depths for which the maximum allowable hawser forces are exceeded is indicated in figure 72. Figure 72 also indicates this relation for the theoretical breaking strenghts of hawsers with a diameter of 20 and 22 mm.
The longitudinal forces acting on a moored ship while a push tow leaves the lock are only to a small degree dependent on the waterdepth. The starting distance certainly plays an important part, which also appears from the diagrams of the hawser forces in figure 70. The occurring forces exceed the safety-limit if the propellers of the pusher tug are revved up to a high number of revolutions too quickly.

14.6. Conclusions

1. The progress of the longitudinal forces acting on a moored ship due to entering push tows or other ships, shows characteristic differences from the progress of the longitudinal forces occurring during filling or emptying of the lock-chamber. The hawsers are, moreover, 'attended to' during the filling and emptying process. Therefore different criteria must be applied to either case.
2. From the investigation into the hawser forces in the model it appears that, due to entering push tows, the maximum allowable longitudinal forces acting on a moored ship in the chamber, should not exceed 0.5 to $0.6^0/_{00}$ of the ship's weight.
3. In general, fully loaded push tows should not be allowed to enter a lock if there are already other ships present. Only at large waterdepth and low entry speeds the safety is not endangered.
4. Only when using its propellers carefully, a push tow can leave the lock without endangering the safety of other ships, moored behind it.

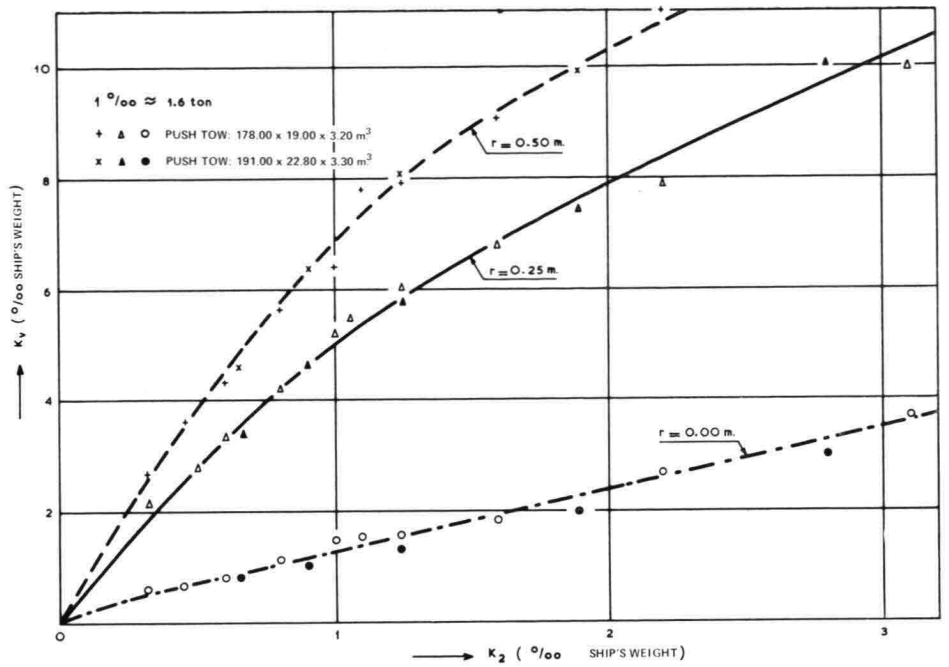

Figure 71. Relation between maximum longitudinal force (K_2) and maximum hawser force (K_V)

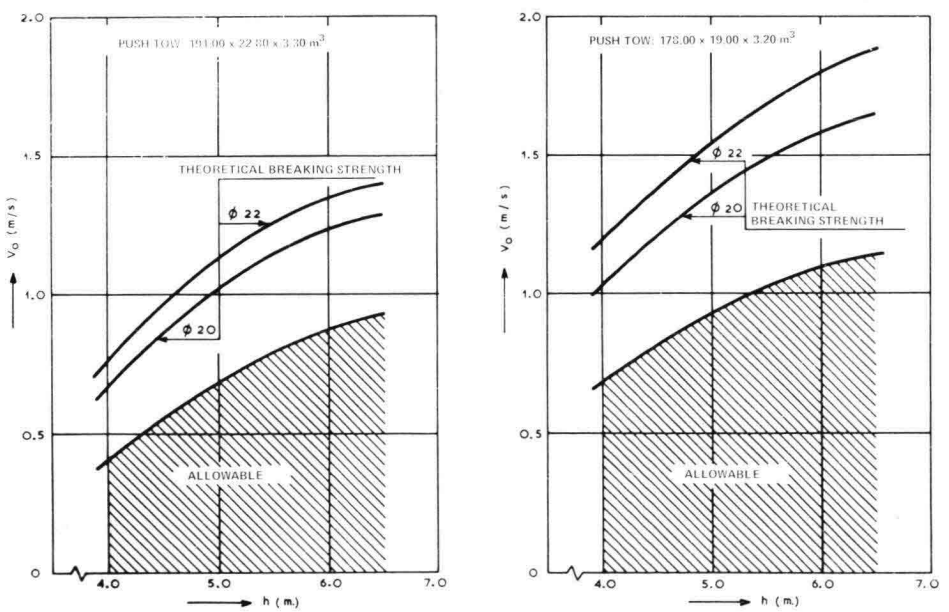

Figure 72. Relation between entry speed (V_0) and waterdepth (h) at which the maximum allowable hawser forces and the theoretical breaking strenghts of the hawsers with diameters ∅ 20 and 22 mm are surpassed

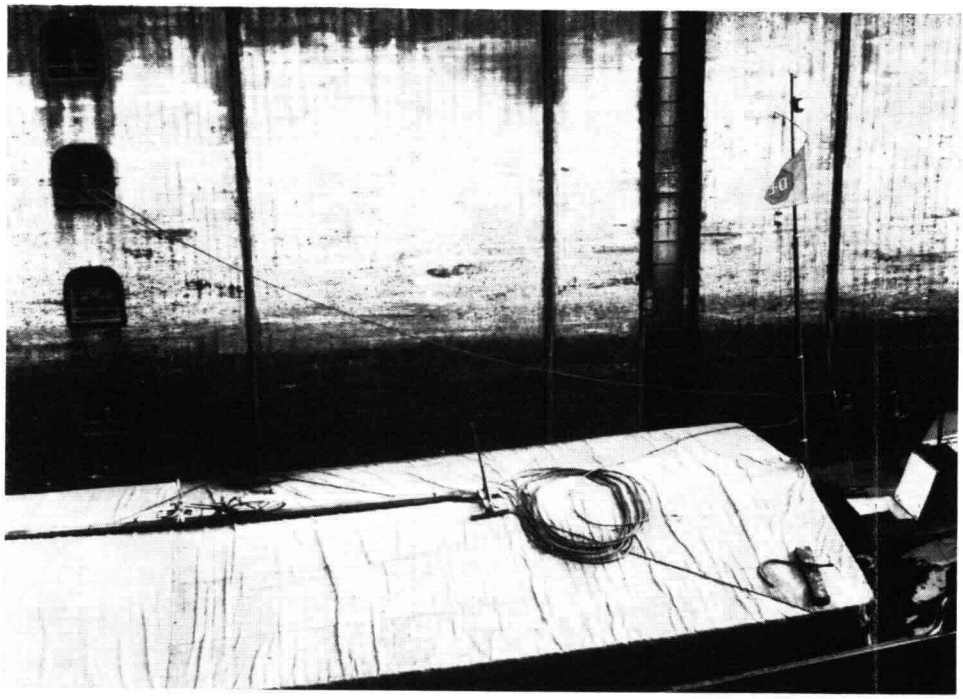

Photograph 12. Slack in the hawsers of moored ships

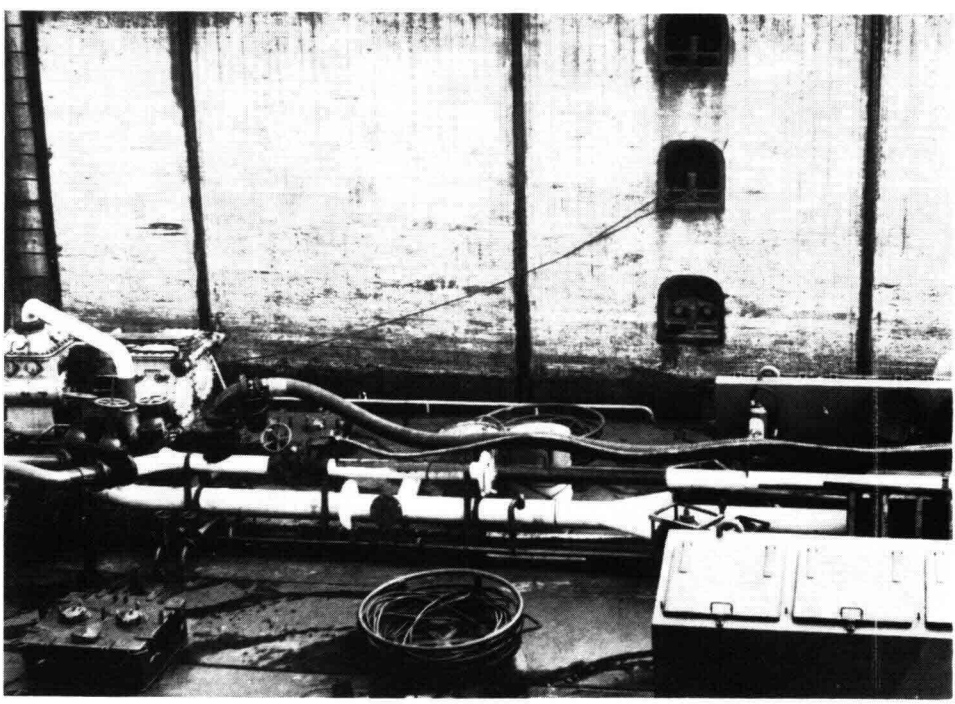

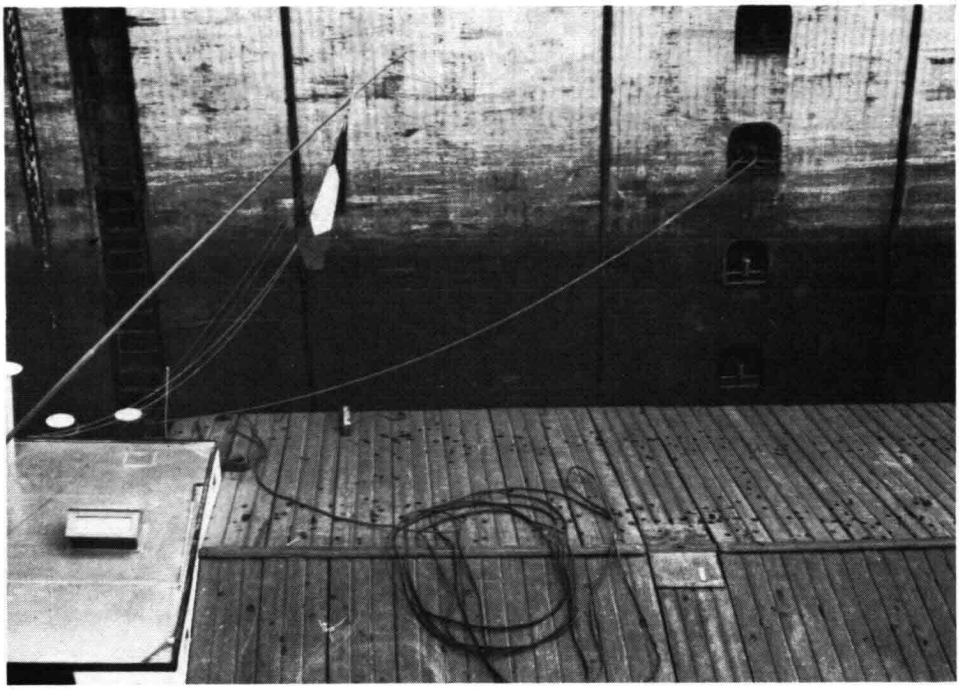

Photograph 13. Freedom of movement of a ship moored in the lock-chamber

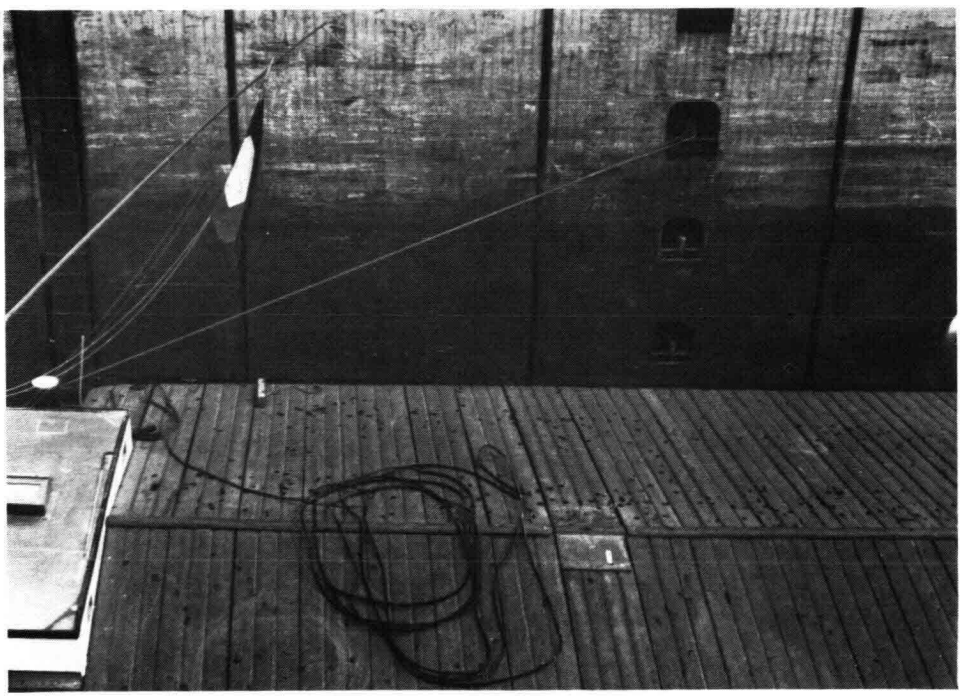

15. Progress of the lock exit

About the progress of the lock exit little of interest is to be said.
After starting its propellers the push tow gains speed rather quickly. As long as the barge formation is in the chamber, the sailing speed remains fairly constant unless the number of propellerrevolutions is changed. Only the relatively small translatory wave, arising when the propeller is quickly revved up, will cause some variation in the sailing speed.
As soon as the barge formation has left the chamber, the sailing speed gradually increases. An example of the progress of the sailing speed is given in figure 73.
The exit times, taken from the starting of the propellers until the moment when the stern of the push boat passes the lock entrance, are given in figure 74. From this it appears that these times strongly increase, especially for large push tows, if the water-depth becomes less than 5.50 m. This limit will shift for bigger drafts.
The exit time will not significantly shorten if the propeller speed or engine-power exceeds the maximum used in the model. This appears from the exit times, attained when the sailing speed during the whole exit would have been equal to the natural limiting speed as defined in paragraph 11.1.

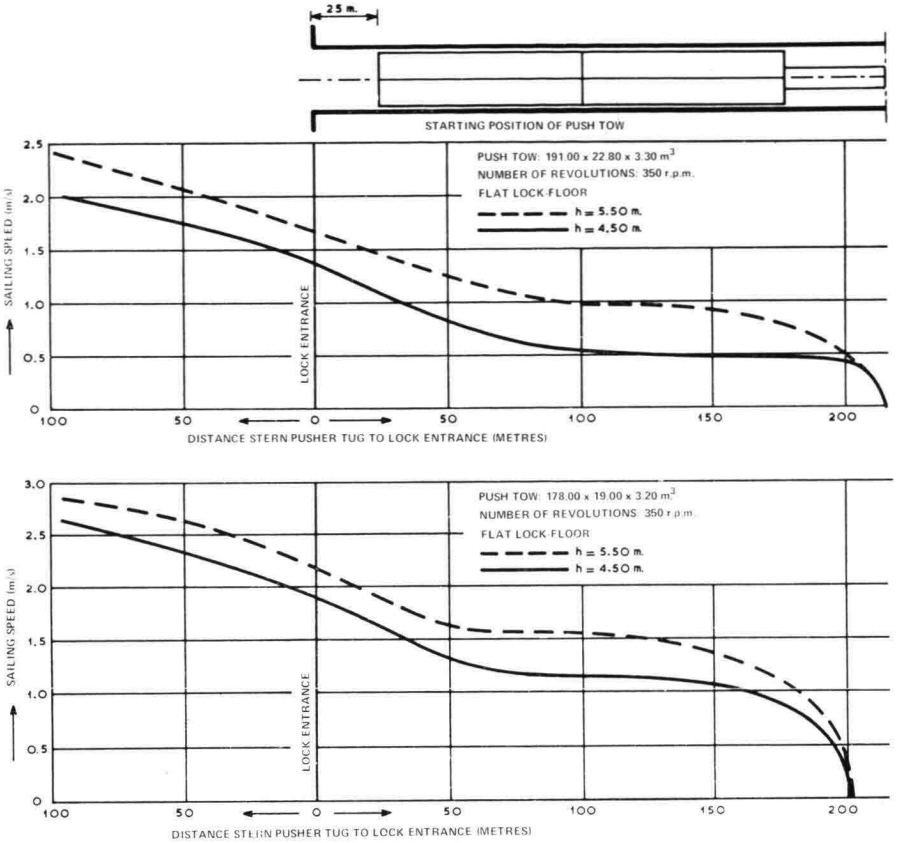

Figure 73. Sailing speed of the push tow in the lock-chamber during exit

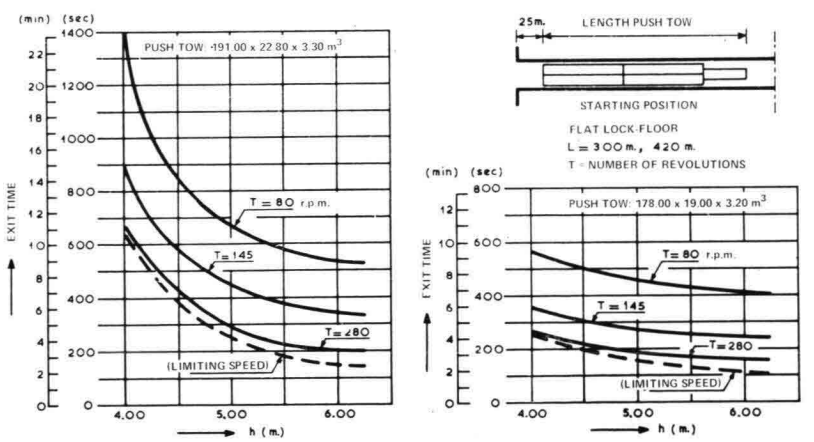

Figure 74. Exit times at various waterdepths and numbers of revolutions

16. Current velocities over the apron

16.1. Model experiments

The lock-entry of push tows or other big ships is accompanied by a strong current over the bottom of the lock approach near the lock entrance. This can be determining for the stability of the apron. Model tests were carried out to gain an insight into the relevant phenomena and to determine the current velocities for various boundary conditions.

The tests were carried out in the indoor-model (figure 7, paragraph 3.2.). With regard to the shape of the lock approach three different situations were investigated (T_1, T_2 and T_3), which are given in figure 75.

The entries performed with a large and with a small push tow were similar to those carried out to investigate the progress of the lock-entry, as described in paragraph 12.2. The sailing speed was varied along with the waterdepths.

The current velocities were measured at a level of 0.62 m. above the bottom with the so-called cup-type current meter, as shown on photograph 9 in paragraph 13.1. The meters which were used and which were set up horizontally, only measure the absolute value of the horizontal velocity component. This measuring instrument has an other restriction, in that it indicates values which are too low in the case of a strong, turbulent current.

Four cup-type current meters were used simultaneously, one of which was always set up at a reference station. The current velocities were continuously recorded.

The stations are indicated with coordinates. Just outside the lock entrance the 'density' of the stations is greatest. The positions of the stations follow from figures 78 and 79.

In the measuring area a rough floor was made from loosely dumped broken stone, the d_{50} of which corresponds with 0.20 m.

16.2. The time history of the current velocity

The time history of the current velocity is indicated in figures 76 and 77 for various stations. During the progress various stages can be distinguished (which is demonstrated by the velocity-registration at point (20.0) from figure 76.

a. The stem of the push tow passes the station. The velocity of the return current, normally occurring around each ship in motion, rises from zero to a maximum value. Then it decreases because the return current under the push barges meets a strong resistance owing to which it turns sideways,

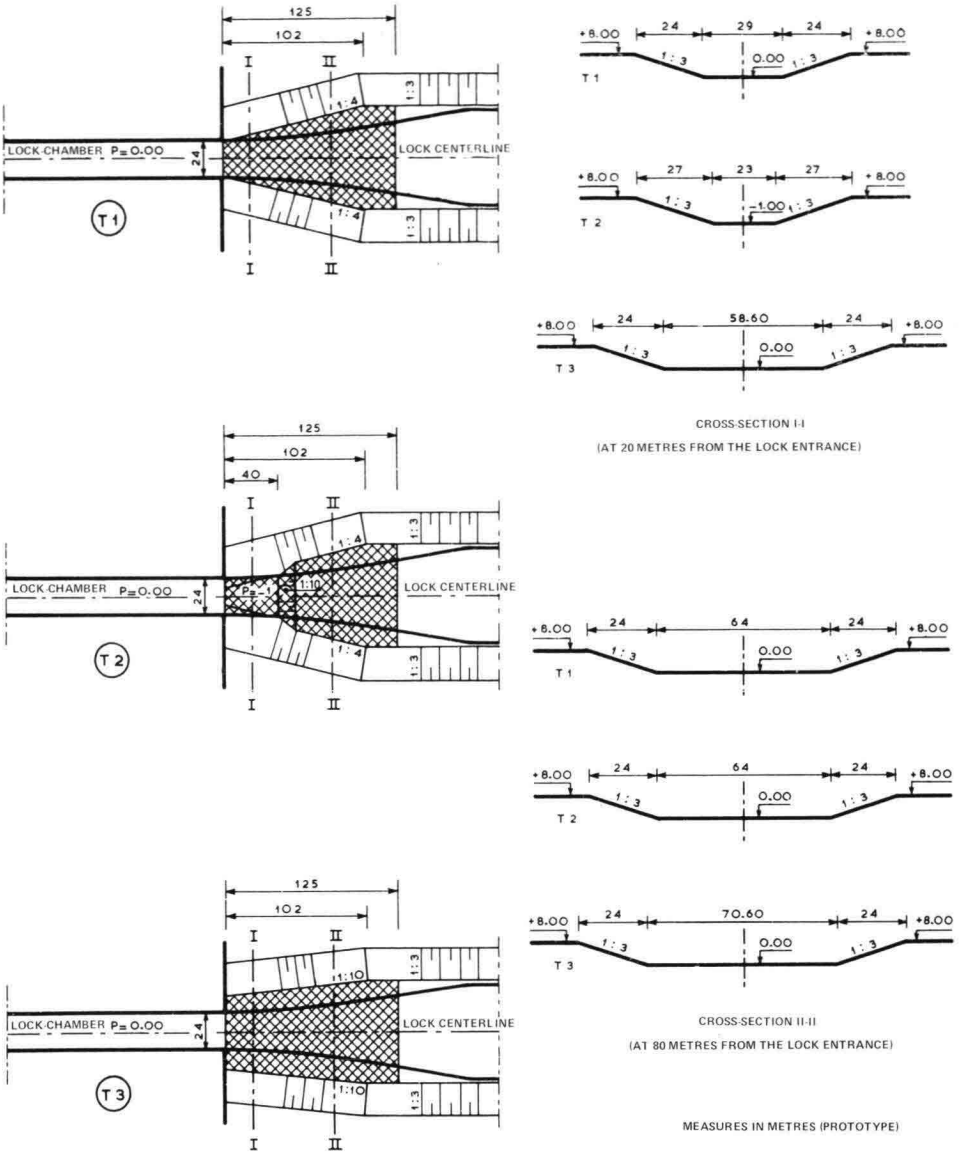

Figure 75. Investigated situations

b. The stem of the push tow passes the lock entrance. As the barges proceed into the lock-chamber, they generate a strong return current, flowing beneath and alongside their hulls, as their sailing speed is comparatively high for conditions in the lock,

c. After reflection against the closed lock-gate, the translatory wave again causes an increase of the return current velocity,
d. The push tow has advanced so far into the chamber that the station is now under the pusher tug. The phenomena are less clearly visible, now. The station is in the suction area of the propellers. Besides, the wake of the barge formation and the translatory wave also play a part,
e. The pusher tug has passed the station and the propeller-current predominates.

In points lying beside the track of the push tow, as e.g. (20.15) the part played by the propeller current is a minor one. The return current becomes less important as the distance from the lock entrance increases.

16.3. Maximum current velocities

The maximum current velocities occurring in situation $T1$ at various waterdepths, are indicated in figure 78. The situations $T1$, $T2$ and $T3$ are compared in figure 79 for a waterdepth of 4.75 m. In both figures only the results of a test-run with a large push tow having a sailing speed of 1.75 m/s, are given. No correction was applied to the propeller current velocity, to allow for the scale effect in the number of propeller-revolutions. This gives a compensation, though an ample one, for the fact that the propeller current is very turbulent, owing to which the current meters applied, indicate values that are too low. When interpreting the measurement results, the fact that, in reality the number of propeller-revolutions is varied at will, must be taken into account.
The maximum return current velocities near the lock entrance are roughly 25 to 35% lower when the large push tow has a sailing speed of 1.25 m/s instead of 1.75 m/s. For the 'small' push tows, allowance must be made for return current velocities that are around 30% lower than is indicated in figures 78 and 79.

16.4. Measurement results from the prototype

As part of the push tow tests in the Volkerak locks, the current velocities were measured above the floor in stations X, Y and Z as indicated in figure 8 (paragraph 4.1). The measuring in station Z failed because the current meter was damaged. In station X no current velocities were measured during the first three entries, due to malfunction.
Owing to the great difference in testing conditions the measurement results are not comparable with those of the model tests. The maximum current velocities in station X and Y are indicated in table 16.4.1. When considering these results it should be borne in mind that station X was at 0.40 m. above the sill, which itself has a height of 1.25 m. Station Y was at 0.40 m. above the apron.

Run No.		1	2	3	4	5	6	7	8	9
h	(m.)	6.91	6.65	6.51	6.83	7.17	7.70	8.63	8.78	8.91
V_o	(m./s.)	1.40	1.90	1.75	1.90	1.01	1.95	2.10	2.05	2.05
current velocity in X	(m./s.)	–	–	–	1.35	0.70	1.10	0.95	0.85	0.75
current velocity in Y	(m./s.)	0.70	0.85	0.80	–	0.65	1.15	0.85	0.60	1.00

Table 16.4.1. Maximum current velocities in stations X and Y during the entry of the push tow 184.80 × 22.40 × 2.50 m³., in the Volkerak lock

In the Hartel lock the current velocities were only measured in one station, Z, of figure 9, which was at 0.50 m. above the floor. The coordinates of that point are (15.12).

Only a rough comparison of the measurement results with those from the model is possible. The time history of the current velocity during runs 1 and 2 is compared in figure 80 with the time history in the model in point (10, 12). The effect of the reflected translatory wave (stage c in paragraph 16.2) is stronger in the model than in the prototype.

This may be partly explained by the difference in shape between the lock in the model and that in the prototype. Also in the prototype the maximum values are somewhat lower than in the model. However, in the latter case the station is also somewhat closer to the lock.

The maximum values measured in station Z (15, 12), are indicated in table 16.4.2

Run No.		1	2	3	4	5
h	(m.)	4.74	4.56	4.82	5.40	5.85
V_o	(m./s.)	1.80	1.92	2.10	2.32	2.05
current velocity in Z	(m./s.)	1.90	2.25	1.95	1.85	1.15

Table 16.4.2. Maximum current velocities in station Z during the entry of the push tow 184.80 × 22.40 × 3.20 m³., into the Hartel lock

16.5. Notes on the results

The model experiments have revealed that the return current is of prevailing importance for the direct surroundings of the lock entrance. The propeller current is prevailing for a greater distance from the lock, but only close to the lock center line.

The apron is most heavily affected by the return current at the corners of the lock-entrance.

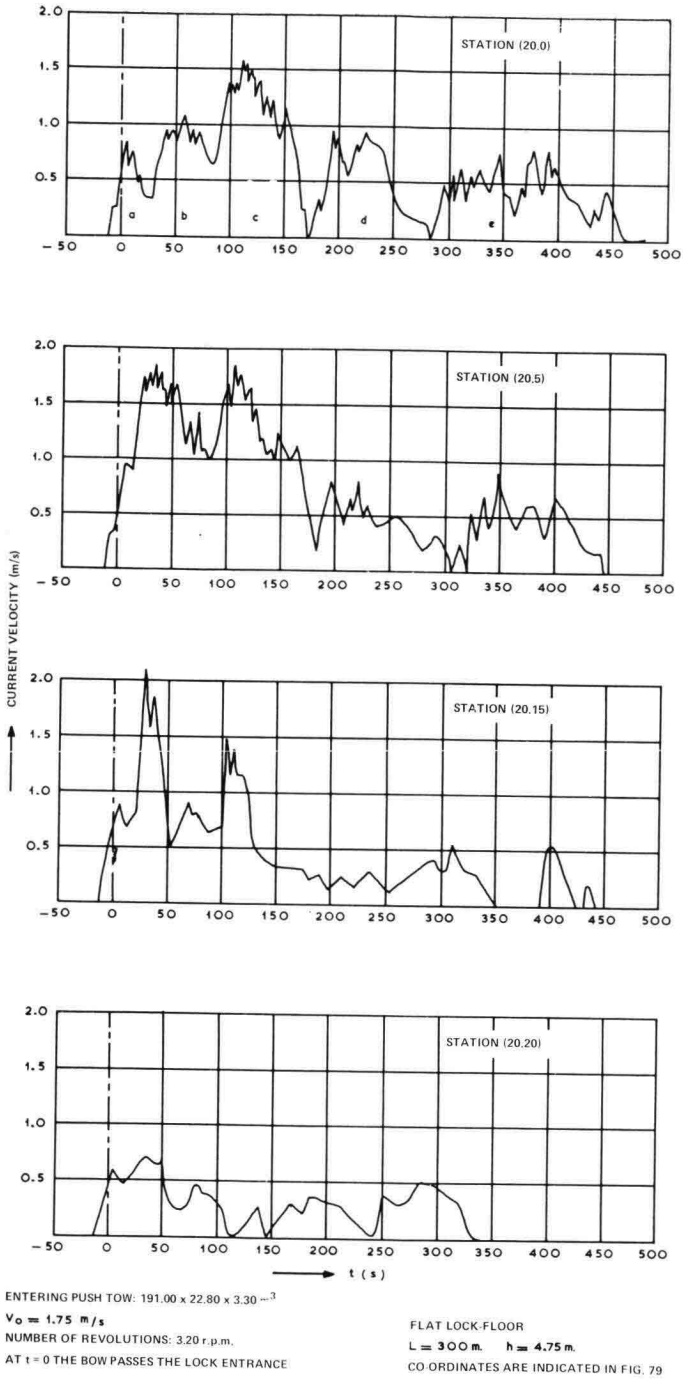

Figure 76. Time history of the current velocity in situation T_3, measured in various stations situated in the same cross-section

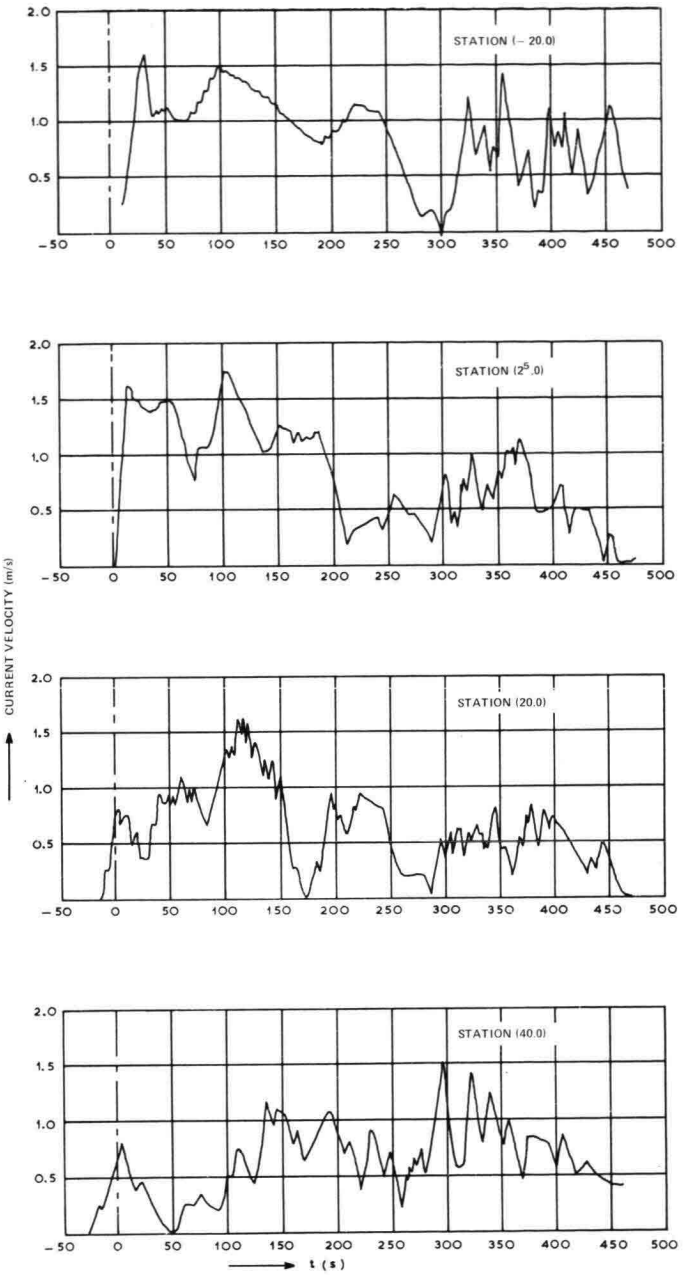

ENTERING PUSH TOW: 191.00 x 22.80 x 3.30 m^3
Vo: 1.75 m/s
NUMBER OF REVOLUTIONS: 230 r.p.m.
At t = 0 THE BOW PASSES THE LOCK ENTRANCE

FLAT LOCK-FLOOR
L = 300 m. h = 4.75 m.
CO-ORDINATES ARE INDICATED IN FIG. 79

Figure 77. Time history of the current velocity in situation T_3, measured in various stations situated on the lock center line

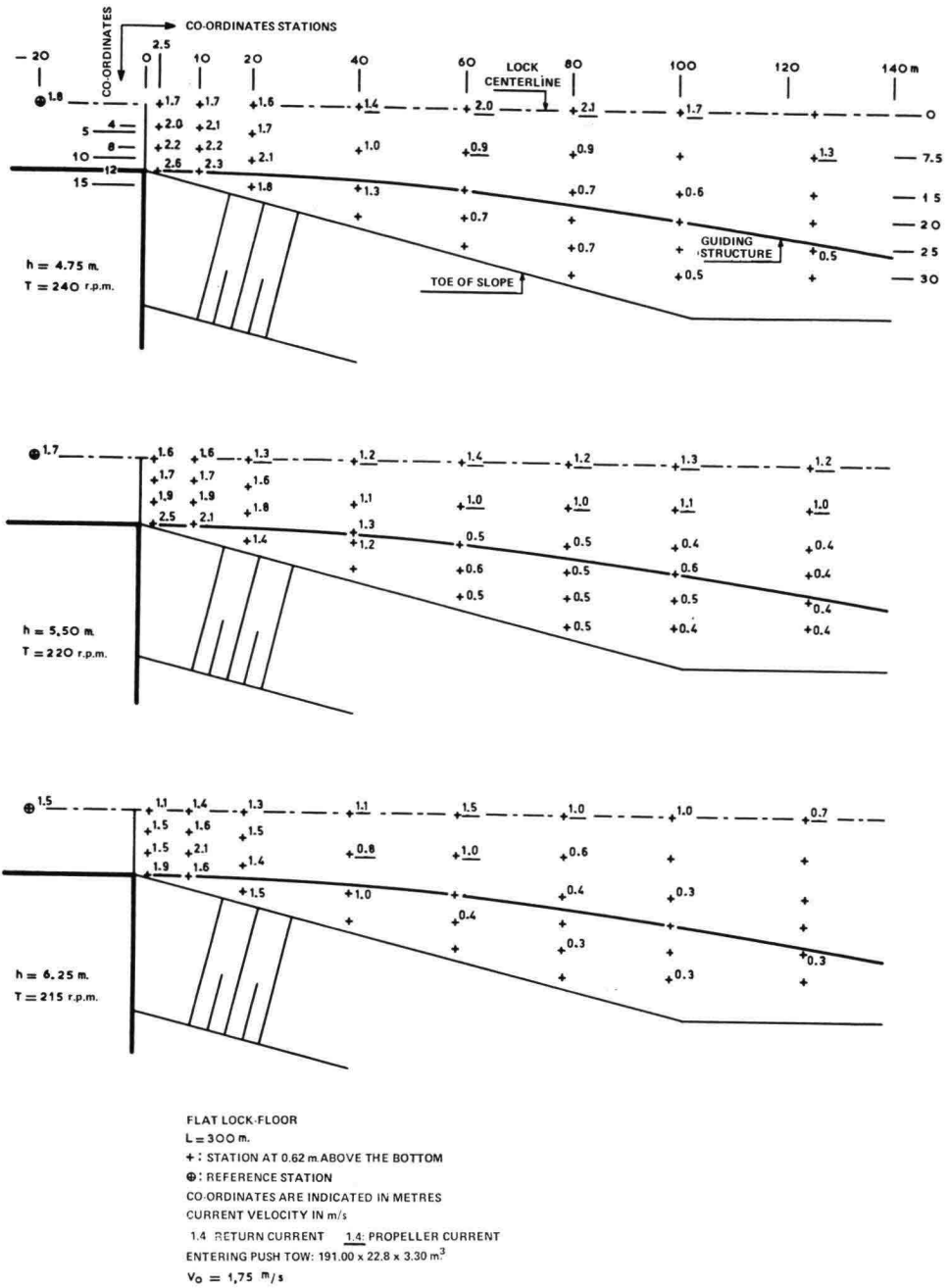

Figure 78. Maximum current velocities above the bottom during entries at various waterdepths in situation T_1

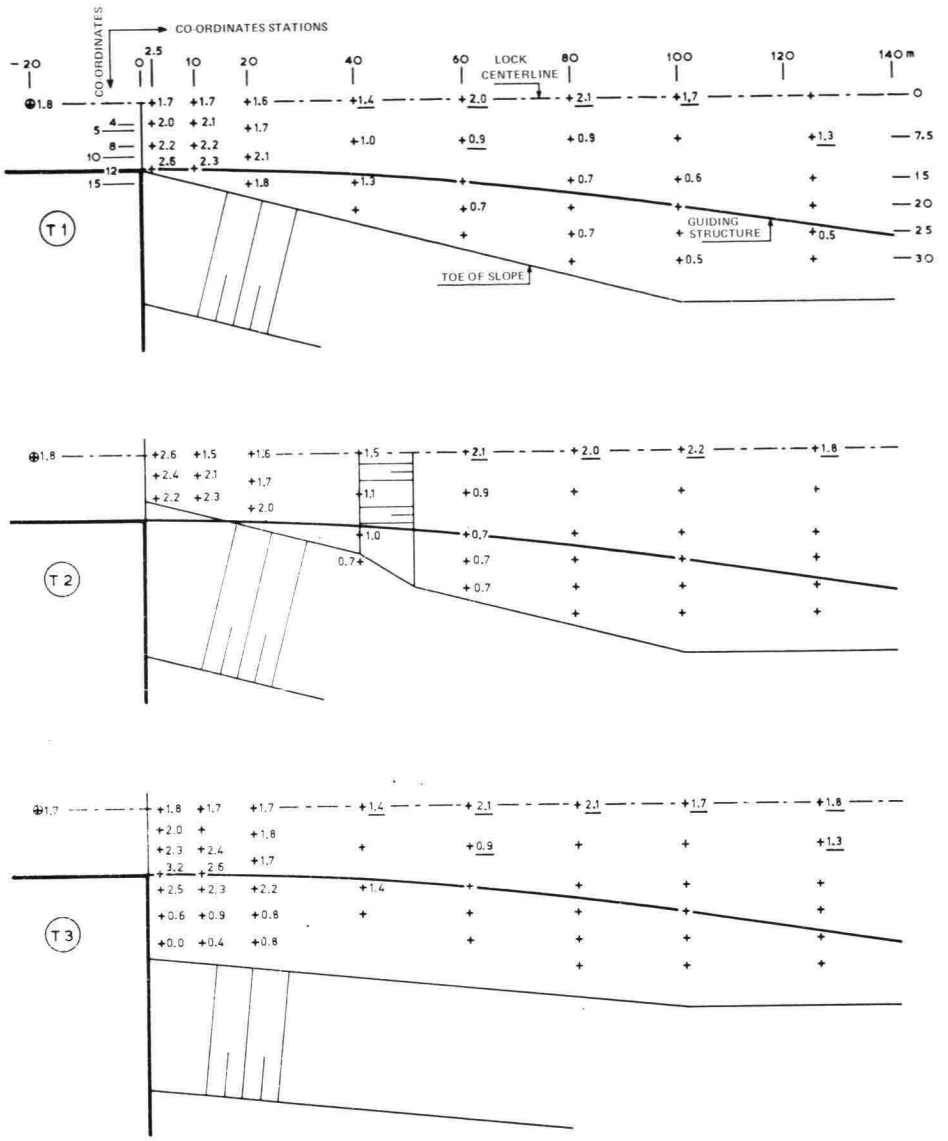

FLAT LOCK-FLOOR
L = 300 m. h = 4.75 m.
+ : STATION AT 0.62 m ABOVE THE BOTTOM
⊕ : REFERENCE STATION
CO-ORDINATES ARE **INDICATED IN METRES**, STATION (20.5): 20 = DISTANCE FROM LOCK ENTRANCE, 5 = DISTANCE FROM LOCK CENTERLINE
CURRENT VELOCITY IN m/s
1.4: RETURN CURRENT 1.4: PROPELLER CURRENT
PUSH TOW: 191.00 x 22.80 x 3.30 m^3
V_o = 1.75 m/s
NUMBER OF REVOLUTIONS = ca 240 r.p.m.

Figure 79. Maximum current velocities above the bottom during entries in various situations

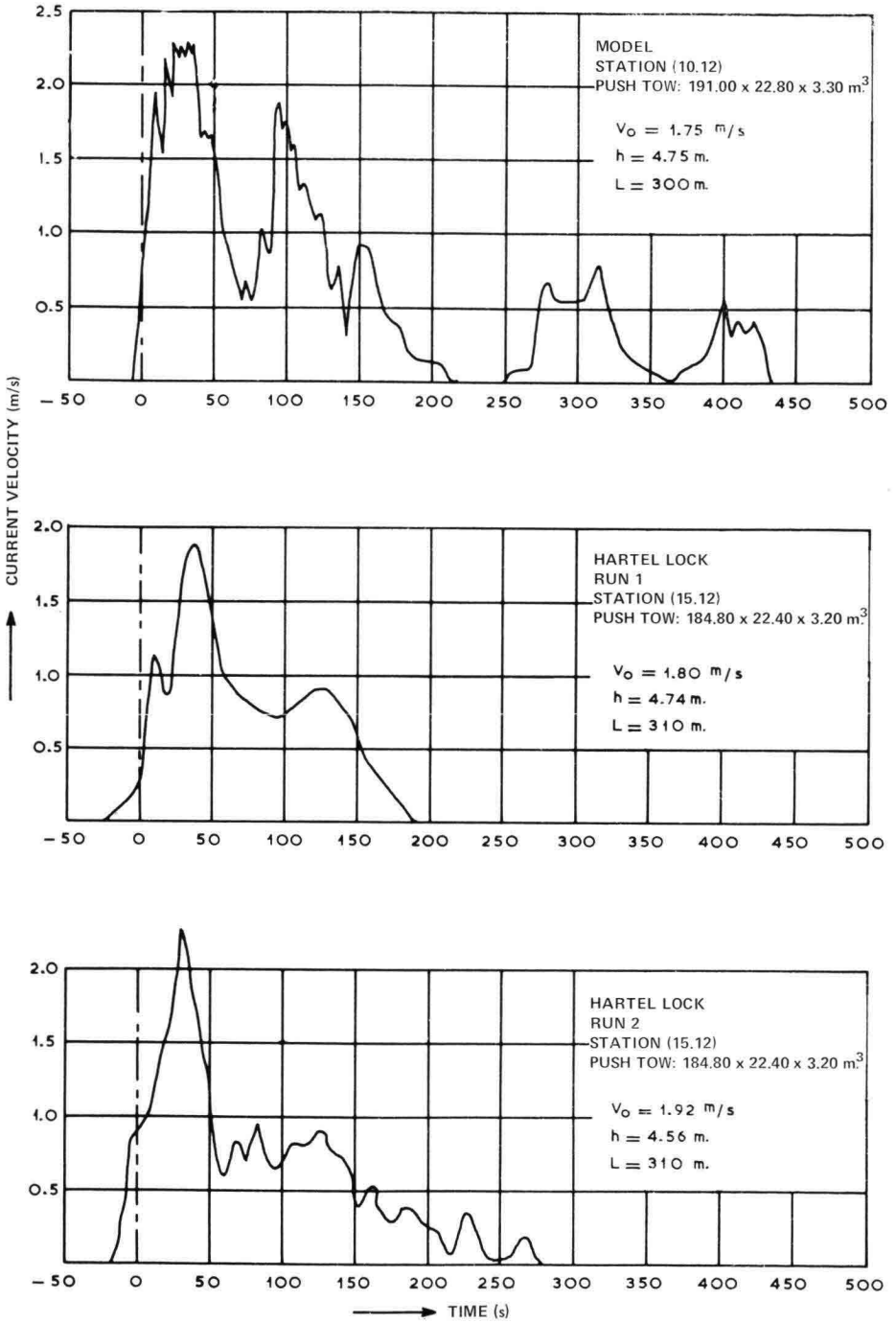

Figure 80. Comparison between the time history of the current velocity in model and prototype

A deepened floor, as in T_2, gives no advantages over T_1. The highest measured current velocities occur in T_3. It is however likely that equally high velocities will occur in T_2, near the corners of the lock entrance. In T_1 it was however not possible to measure on the slope with the current velocity meters available.
Taking the difference in conditions into account, it can be concluded that the time history of the current velocity in the prototype is roughly similar to that in the model. When designing aprons it is advisable to reckon with higher sailing speeds than 1.75 m/s and also with entries of large push tows with a greater draft than 3.30 m. This can be done by increasing the maximum values of the return current velocities as following from figures 78 and 79, by for instance 25%. The apron should have a good constructed termination near the lock axis, to resist the impact of the propeller current. An apron length of about 50 m. will probably be sufficient.

Photograph 14. A push tow enters the Hartel Lock

17. Symbols used in part III

Symbol	
B	width on the undisturbed waterlevel (m.)
C	the constant spring value of the hawser (m/N.)
D	height of the sill above the lock floor (m.)
E	elasticity modulus of the hawser (N/m^2.)
F	area of the wetted cross-section (m^2.)
F_D	area wetted cross-section above the sill (m^2.)
F_t	material cross-section of the hawser (m^2.)
HK	half speed (half of the maximum number of revolutions)
K_1	longitudinal force on moored ship in the direction of the closed lock-gates ($^0/_{00}$ of the ship's weight)
K_2	longitudinal force on moored ship in the direction of the open lock entrance ($^0/_{00}$ of the ship's weight)
K_a	force in the backward hawser (N.)
K_v	force in the forward hawser (N.)
L	length of the lock (between entrance and closed lock-gates) (m.)
T	propeller-speed (r.p.m.)
V	sailing speed (m/s.)
V_D	sailing speed when bow crosses sill (m/s.)
V_o	sailing speed when bow passes lock entrance (m/s.)
V_L	natural limiting speed (m/s.)
V_w	wind velocity in the undistrubed area at a height of 10 m. (m/s.)
VK	full speed (max. number of revolutions)
Z	height of the translatory wave (m.)
e	distance between pusher tug and moored ship (m.)
f	area wetted midship section (m^2.)
g	acceleration of gravity (m/s^2.)
h	waterdepth above the lock floor (m.)
h'	F/B (average waterdepth) (m.)
Δh	drop of the waterlevel (m.)
h_D	waterdepth over the sill (m.)
l	distance over which the slope of the translatory wave was measured. (m.)
r	total amount of slack (total sum of slack in forward and backward hawser) (m.)
s	length of hawser (m.)
t	time (s.)
u	return current velocity (m/s.)

remark: s = second, N = Newton (10^4 N is equal to about 1 ton)

Bibliography

1. XXIth International Navigation Congress, Stockholm 1965 SI - 3 part I by H. VAN OPSTAL.
2. XXIth International Navigation Congress, Stockholm 1965 SI - 3 part II by J. K. IN 'T VELD.
3. Fahrt der Schiffe auf beschränktem Wasser, Schiffbau 1913, S 457, 537, 592, 628 und 731, by H. KREY.
4. XVIIth International Navigation Congress, Lisbon 1949 SI - 2. Report by J. B. SCHIJF.

Unpublished technical reports

Delft Hydraulics Laboratory

5. Duwvaartsluizen, M 838-I, 1964 (guiding structures outside the lock entrance).
6. Duwvaartsluizen, M 838-II, 1965. Botsingsverschijnselen bij asymmetrische invaart van de sluis (impact phenomena during asymmetrical entering manoeuvres).
7. Duwvaartsluizen, M 838-III, 1966. Hoogte van geleidewerken (height of guiding structures).
8. Duwvaartsluizen, M 838-IV, 1966. Translatiegolven, invaarsnelheden, invaartijden, uitvaartijden (translatory waves, entering speeds, duration of lock-entry and exit).
9. Duwvaartsluizen, M 838-V, 1966. Troskrachten (hawser forces acting on ships moored in the lock chamber during entry of a push tow).
10. Duwvaartsluizen, M 838-VI, 1970. Algemene beschouwing over de functies van geleidewerken (general discourse on the functions of guiding structures).
11. Duwvaartsluizen, M 838-VII, 1970. Stroomsnelheden over het stortebed (return and propeller currents over the apron).

Institute for Perception RVO-TNO

12. Optische geleiding door remmingwerken en richtmiddelen, 1964. (optical guidance for push tows entering comparatively narrow locks).
13. Optische geleiding van de Volkeraksluizen, 1967. (optical guidance at the Volkerak locks).

Rijkswaterstaat Deltadienst

14. Nota No. 4-1966. Verslag oriëntatiereis duwvaart Moezel, 1966. (report on a study tour of the canalised Moselle).

15. Nota W-68.701. Volkeraksluizen. Proefvaarten met duweenheid, 1968. (report on prototype measurements).
Public Works of Rotterdam
16. Duwvaartproeven Hartelsluis, 1968. (report on prototype measurements).

In the series of Rijkswaterstaat Communications the following numbers have been published before:

No. 1.* *Tidal Computations in Shallow Water*
Dr. J. J. Dronkers† and Prof. dr. ir. J. C. Schönfeld
Report on Hydrostatic Levelling across the Westerschelde
Ir. A. Waalewijn

No. 2.* *Computation of the Decca Pattern for the Netherlands Delta Works*
Ir. H. Ph. van der Schaaf† and P. Vetterli, Ing. Dipl. E.T.H.

No. 3. *The Aging of Asphaltic Bitumen*
Ir. A. J. P. van der Burgh, J. P. Bouwman and G. M. A. Steffelaar

No. 4. *Mud Distribution and Land Reclamation in the Eastern Wadden Shallows*
Dr. L. F. Kamps†

No. 5. *Modern Construction of Wing-Gates*
Ir. J. C. le Nobel

No. 6. *A Structure Plan for the Southern IJsselmeerpolders*
Board of the Zuyder Zee Works

No. 7. *The Use of Explosives for Clearing Ice*
Ir. J. van der Kley

No. 8. *The Design and Construction of the Van Brienenoord Bridge across the River Nieuwe Maas*
Ir. W. J. van der Eb†

No. 9. *Electronic Computation of Water Levels in Rivers during High Discharges*
Section River Studies, Directie Bovenrivieren of Rijkswaterstaat

No. 10. *The Canalization of the Lower Rhine*
Ir. A. C. de Gaay and Ir. P. Blokland

No. 11. *The Haringvliet Sluices*
Ir. H. A. Ferguson, ir. P. Blokland and Ir. drs. H. Kuiper

No. 12. *The Application of Piecewise Polynomials to Problems of Curve and Surface Approximation*
Dr. Kurt Kubik

No. 13. *Systems for Automatic Computation and Plotting of Position Fixing Patterns*
Ir. H. Ph. van der Schaaf†

No. 14. *The Realization and Function of the Northern Basin of the Delta Project*
Deltadienst of Rijkswaterstaat

No. 15. *Fysical-Engineering Model of Reinforced Concrete Frames in Compression*
Ir. J. Blaauwendraad

* out of print

Photographs:

Delft Hydraulics Laboratory No's 1 . . . 5 and 7 . . . 14
Institute for Perception (RVO-TNO) No. 6

ISBN 90 12 00130 7

223885v-316